6238

NAME OF AUTHOR...... *R. SEGAL*

TITLE OF THESIS. *KINETICS OF LITHIN BINDING*

TO HEMIN AND HEME PROTEINS

UNIVERSITY...... *U. of A. Edmonton*

DEGREE.... *PhD* ....YEAR GRANTED.... *1970*

(Signed)...... *R. Segal*

PERMANENT ADDRESS:

Box 218,

PIETERSBURG N. T.l.

Rep. of S. AFRICA.

DATED...... *25/11* 19 *69*

NL-91

THE UNIVERSITY OF ALBERTA

KINETICS OF LIGAND BINDING

TO HEMIN AND HEME PROTEINS

by

(C) RAYMOND SEGAL

A THESIS

SUBMITTED TO THE FACULTY OF GRADUATE STUDIES

IN PARTIAL FULFILMENT OF THE REQUIREMENTS FOR

THE DEGREE OF DOCTOR OF PHILOSOPHY

DEPARTMENT OF CHEMISTRY

EDMONTON, ALBERTA

SPRING, 1970

UNIVERSITY OF ALBERTA

FACULTY OF GRADUATE STUDIES

.

The undersigned certify that they have read,
and recommend to the Faculty of Graduate Studies
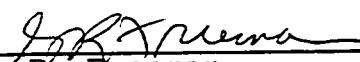for acceptance, a thesis entitled

KINETICS OF LIGAND BINDING
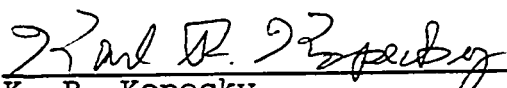
BY HEMIN AND HEME PROTEINS

submitted by RAYMOND SEGAL, in partial fulfilment
of the requirements for the degree of Doctor of
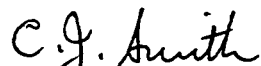Philosophy.

H. B. Dunford, Supervisor

G. R. Freeman

K. R. Kopecky

D. D. Tanner

C. J. Smith

M. Gaucher, External Examiner

Date _Nov. 24, 1969_

ABSTRACT

The kinetics of the reversible binding of cyanide by catalase was studied at 25° and an ionic strength equal to 0.11 over the pH range 5.6 to 9.6 by means of a temperature jump apparatus. Analysis of the pH dependence of the bimolecular rate constants is consistent with the presence of two ionizable groups (heme-linked groups) with pK values of 6.1 and 9.8.

In another study conducted on a stopped flow apparatus results on the kinetics of the binding of fluoride to lactoperoxidase were obtained. The results are consistent with a mechanism in which HF binds to the active site which contains no groups capable of ionization in the pH range of the present study. The specific rate constant for the binding reaction of HF to lactoperoxidase is $9.7(\pm 0.4) \times 10^2$ $M^{-1} sec^{-1}$. The reaction was studied by means of a stopped-flow apparatus at 25° and an ionic strength of 0.11.

The kinetics of the reversible binding of cyanide to ferriprotoporphyrin IX(hemin) was studied at 25° and an ionic strength of 0.11 over the pH range 6.25 to 10, by means of a stopped flow apparatus. Two relaxation times were observed between pH's 6.25 to 8.5. The most reasonable mechanism that will explain the k_{1app} data involves four hemin species in solution with pK values of 6.82, 8.0 and

7.9. Analysis of the k_{2app} data is consistent with the presence of three hemin species with pK values of 7.33 and 8.2.

ACKNOWLEDGMENTS

It is a pleasure to acknowledge the support of Dr. H. B. Dunford, the supervisor of this work.

Discussions with other graduate students are appreciated.

TABLE OF CONTENTS

.

LIST OF TABLES

LIST OF FIGURES

General Introduction

During the period of the author's research, three
separate projects were undertaken which are organized
into three separate chapters in this thesis. Each
chapter is intended to be complete in itself with regard
to an introduction, experimental details and discussion
of the results.

Chapter 1 and chapter 2 deal largely with the
kinetics of the binding of cyanide and fluoride to cata-
lase and lactoperoxidase respectively, and chapter 3, the
kinetics of the binding of cyanide to ferriprotoporphyrin
IX in 44.5 weight % ethanol.

CHAPTER 1

THE KINETICS OF CYANIDE BINDING

BY BOVINE LIVER CATALASE

Introduction

Catalase is an enzyme which catalyses the reaction

$$2H_2O_2 \rightarrow 2H_2O + O_2$$
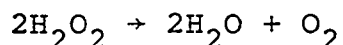
in contrast to the peroxidases such as horseradish
peroxidase and lactoperoxidase which are noted for their
catalyses of oxidation of other substrates in the presence
of hydrogen peroxide. It was demonstrated by Loew[1] in
1901 that the rapid decomposition of H_2O_2 by tissue
extracts was catalysed by one specific enzyme which he
labelled catalase.

Catalase has been found in the great majority of
organisms examined. In mammals the highest concentrations
are found in the liver and erythrocytes, and catalase
obtained from these two sources has been intensively
investigated.

In Table I, taken from Nicholls and Schonbaum[2],
some properties of catalase from various sources are
summarized.

TABLE I

PROPERTIES OF VARIOUS CATALASE-PROTEIN MOIETIES

Origin	Molecular weight	Hemin groups per molecule	Isoelectric point	R.Z.= $\frac{O.D.(406\ mu)}{O.D.(280\ mu)}$
Horse liver	225,000	2.5-3.5	5.4	0.71
Horse blood	225,000-250,000	4	5.5	1.20
Bovine liver	230,000-250,000	2.5-3.5	5.8	—
Human blood	220,000	4	—	—
Micrococcus lyso-deikticus	232,000	4	—	1.18
Rhodopsuedomonas spheroides	232,000	4	—	1.00
Yeast	240,000	4	7	1.08
Plant chloroplasts	450,000	4	7	0.65

In general catalase has four ferriprotoporphyrin IX(hemin) groups per molecule. However, catalases from horse and bovine liver contain less than four hemin groups per molecule, and this is due to some hemin being degraded to bile pigments[3], probably by reactions occurring during attempted purification of the enzyme. Lemberg and Legge[3] have developed a simple spectrophotometric method of analysis for determination of the molar ratio of hemin converted to bile pigment to total hemin. In Table II a comparison is made by them of the spectrophotometric determination of bile pigment compared to the older acetic acid method. Different preparations are given arbitrary designations in the first column of Table II. It can be seen from the second and third columns that the two methods agree quite well.

The hemin nature of catalase was established by Zeile and Hellstrom[4]. Unlike peroxidase[5], metmyoglobin[6] and methemoglobin[7], catalase does not form alkaline derivatives[5]. Neither does dithionite reduce native catalase to ferrous form, and the maintenance of the protein structure seems to depend on the presence of the hemin. Removal of the prosthetic group gives a denatured apoenzyme, but the splitting is similar to that of peroxidase[8,9]. Since the apoenzyme is so unstable the nature of the binding of the hemin to the protein moiety has so far not been determined.

TABLE II

Comparative Methods for the Determination
of the Ratio of Bile Pigment to Total Hemin

Molar ratio: $\dfrac{\text{bile pigment hemin}}{\text{total hemin}}$

Ox liver catalase preparation	Found by acetic acid method[15]	Found by spectro-photometric analysis
F_2	0.31	0.35
D_2c	0.32	0.33
E_1	0.36	0.38
D_1	0.37	0.40
E_2	0.38	0.38
L	0.40	0.42
E_3	0.44	0.44
H_1	0.45	0.43
D_2a	0.45	0.43
D_2b	0.49	0.38

With regard to the type of the ligands binding to the fifth and sixth positions on the hemin Fe(III) ion of catalase, Brill and Williams[10] believe that catalase is a "dicarboxylate or less probably a carboxylate-water complex". This conclusion was reached by a comparative study of the reduction potentials, magnetic moments and spectra of the heme proteins. They believe that myoglobin is an imidazole-water complex. This has been confirmed by X-ray studies[11] which show that the imidazole of a histidine residue and water occupy the fifth and sixth positions of the ferric ion. Therefore, the conclusions of Brill and Williams probably bear a close resemblance to reality with regard to catalase.

A number of ligands bind to catalase, and Figure 1 taken from Keilin and Hartree[5] shows the absorption spectra of catalase (from horse liver) and its cyanide, azide and fluoride complexes at pH 6. From X-ray crystallographic studies on myoglobin complexes[11,12], the ligand is found on the sixth position of the iron, having replaced the water molecule, and most probably the ligands bind to the sixth position on the ferric ion of the hemin of catalase as well. There are five unpaired electrons on each ferric ion for the azide and fluoride complexes of catalase, as for catalase-water, but the ferric ion of the catalase-cyanide complex has only one unpaired electron[2].
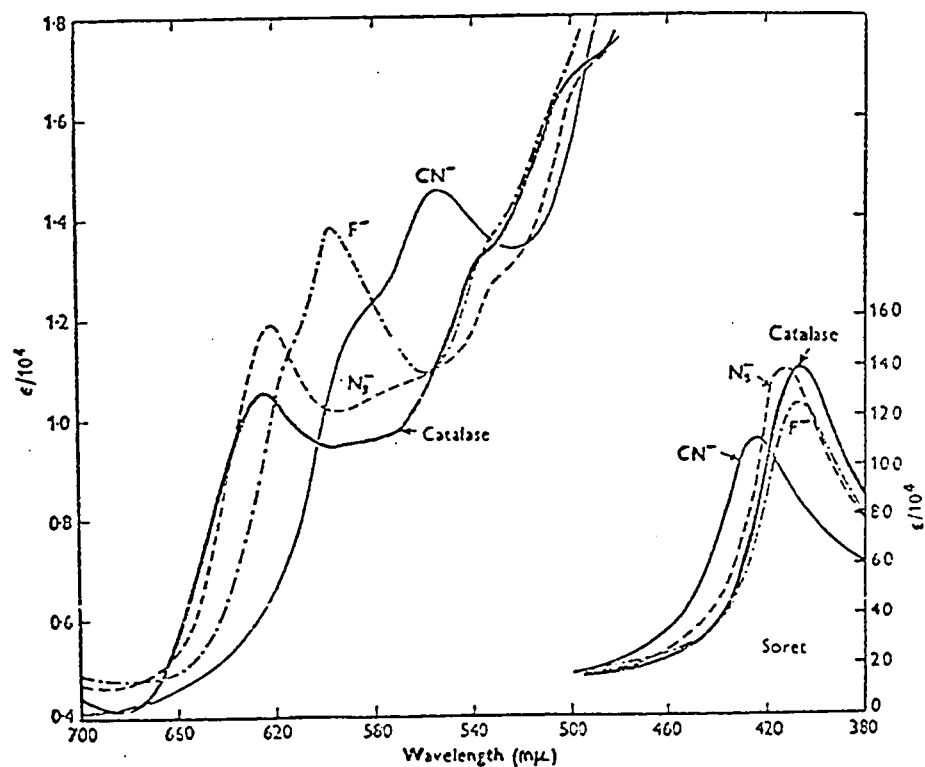
Figure 1. The absolute absorption spectra (molar absorptivity <u>vs</u>. wavelength) of liver catalase and its complexes with cyanide, azide and fluoride[5].

Chance[13] studied the reaction of catalase with a number of ligands, and the dissociation constants are given in Table III.

TABLE III

Dissociation Constants for Complexes of Human
Blood Catalase with a Number of Different Ligands, Based
Upon Free-Acid (HA) Concentration

Ligand	$K_{Diss} = \dfrac{[Cat^*][HA]}{[CatHA]}$ (M)
CH_3COOH	9×10^{-3}
HF	4×10^{-5}
HCOOH	6×10^{-6}
HCN	7×10^{-6}
HN_3	3×10^{-6}

Figure 2[2] shows the variation of equilibrium constants with pH for catalase complexes. In each case the reaction follows the equation:

$$CatH_2O + HA \underset{k_{-1}}{\overset{k_1}{\rightleftharpoons}} CatHA + H_2O \qquad (1)$$
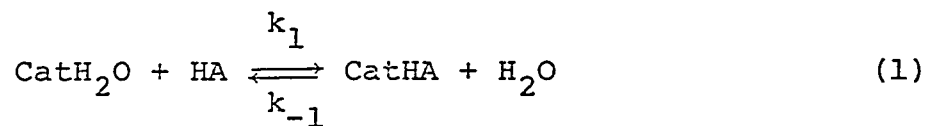
For most of the ligands studied, the equilibrium constants are proportional to the amount of undissociated acid present.

*Cat is an abbreviation for catalase.
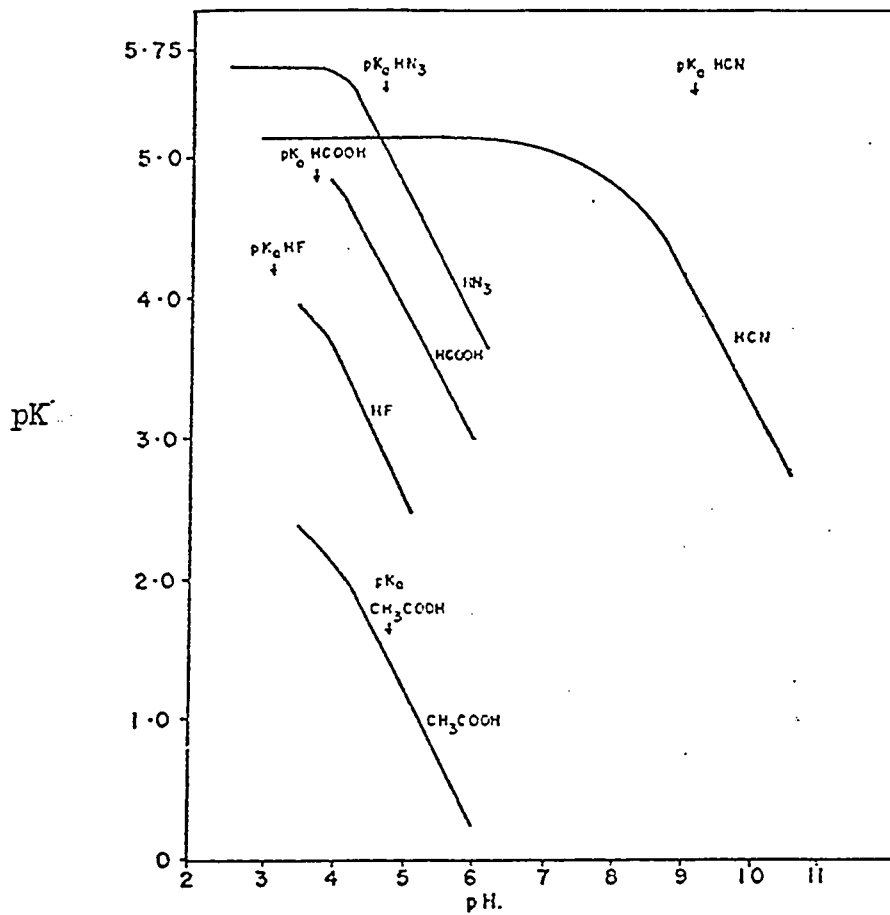
Figure 2. The effect of pH upon the dissociation constants of catalase complexes[2].

Although the reaction with cyanide approximately follows eq 1, a decrease in the affinity of blood catalase for cyanide occurs at pH 8.5 that cannot be attributed wholly to the acid dissociation of HCN[13].

Over the range from 7 to 98% saturation of catalase with cyanide at pH 7, there was no change of the dissociation constant of the catalase-cyanide complex in excess of experimental error, and thus no detectable hemin-hemin interaction[14].

Chance[14] studied the reaction kinetics of the formation and dissociation of the catalase-cyanide complex spectrophotometrically by the rapid flow technique, and obtained a value for k_1 (eq 1) of 9.0×10^5 M^{-1} sec^{-1} at pH 6.5 and for k_{-1}, 3.2 sec^{-1} at pH 7.0 and 2.9 sec^{-1} at pH 4.6.

In view of the study by Chance of the HCN binding to catalase, it was considered reasonable that a similar study of the binding of cyanide to catalase over a wide pH range, might yield some information on the environment of the hemin moiety, and by studying the problem with a temperature jump apparatus, further information may have become available for reaction velocities outside the stopped-flow range.

Experimental

Catalase was isolated from bovine liver by the method of Shirakawa[16,17]. Although several liver preparations were carried out only about 10 mgms of catalase were obtained with an R.Z of 0.915 (the 406mµ/276mµ absorbancy ratio). However, large quantities of liver catalase with R.Z numbers ranging between 0.2 and 0.8 were obtained. Liver catalase with an R.Z of 0.87 was also obtained from Boehringer - Mannheim Corp., N.Y. Catalase concentrations were determined from absorbance measurements at 406mµ using a molar absorptivity[17] of $3.24 \times 10^{+5}$ M^{-1} cm^{-1}.

Doubly distilled water was used to prepare all solutions. Inorganic chemicals of reagent grade were used without further purification. Fresh potassium cyanide solutions were made up for each day's experiments. Sodium cyanide was not used as sodium ions interfere with pH measurements at high pH[21]. A Beckman expanded-scale pH meter in conjunction with a Beckman 39183 combination electrode was used for pH measurements. Both a Beckman DU spectrophotometer and Cary 14 Recording Spectrophotometer were used for routine absorption measurements.

The temperature jump apparatus was built in this laboratory and has been described elsewhere[18]. The discharge from a 0.1 uF capacitor charged to 22kV was used to cause a temperature jump of about 6°C. The reaction cell was maintained at 19° so that temperature of

the kinetic experiments was approximately 25°C. For each

temperature jump experiment, 10 ml of a solution was used

that contained 0.1M KNO_3 (to conduct the discharge current),

6.00×10^{-7} M catalase, 1×10^{-6} M to 5.4×10^{-5} M potassium

cyanide, and a buffer of ionic strength 0.01. The total

ionic strength was 0.11. The buffers and pH ranges covered

were: phosphate 5.6 - 8.0, Tris 8.5 - 8.85, and glycinate

at 9.6. Temperature jump experiments at a given pH were

conducted on five to six solutions covering a range of

cyanide concentrations of about 50. The relaxation to

the new equilibrium after temperature perturbation was ob-

served spectrophotometrically at 430mµ and the results

displayed on an oscilloscope. Photographs of the oscillo-

scope traces were taken and values of the voltage at a

given time were read from them using a photographic en-

larger. In general at least three experiments were per-

formed on any one solution and the average of the relax-

ation time constants was taken. Differences between

amplified photomultiplier voltages displayed on the oscillo-

scope are directly proportional to differences in the

intensity of light transmitted by the reaction solution.

These in turn, because of the small overall change

(ca 1-3%) in transmitted light intensity during reaction,

are good approximations of absorbance differences. Con-

sequently plots of $\ln(V_\infty - Vt)$ vs time were used to

determine the relaxation time constants, τ, which ranged

between 19 and 115 msec.

Values of K dissociation, as defined on page 17, were determined at a few pH values spectrophotometrically at 25°, by titrating a saturated catalase-cyanide solution into a catalase solution. This obviated all dilution effects.

The concentration of protoporphyrin IX on the protein moiety was determined after conversion to pyridine hemochromogen by spectrophotometric measurement at 557 mμ[19], using a molar extinction coefficient of 3.4 x 10^4 M^{-1} cm^{-1}.

The ratio of bile pigment hemin to total hemin was measured spectrophotometrically after conversion of hemin and degraded products to CO-pyridine hemochromogen[15]. The ratio of bile pigment to total hemin can be calculated from the formula:

$$(A_{630}/A_{570} - 0.047) \, / \, (0.55 \times A_{630}/A_{570} + 0.96) \qquad (1)$$

where A = absorbance. The absorbance at 630 mμ is due to the presence of bile pigment.

The molecular weight of catalase of R.Z = 0.915 was determined by using the Archibald method at 5200 r.p.m. at 20° on a Beckman Model E Analytical Ultracentrifuge at pH 7.0 and 0.02 molar phosphate buffer, and the catalase concentration was 3.5 mgms/cc. The partial specific volume of catalase was assumed to be 0.730[20]. We thank Dr. C. M. Kay and Mr. M. Aarbau for this analysis.

The optical rotatory dispersion of catalase with an RZ of 0.915 and 0.87 was measured on a Jasco model ORD/UV-5 recording spectrometer at room temperature, at pH 7.0, in 0.02 molar phosphate buffer. The absorbance of catalase was kept less than two in the wavelength regions of interest, to eliminate rotatory artifacts[29]. The values of specific rotation were calculated using the molar concentrations determined spectrophotometrically and a value of 240,000 for the molecular weight of catalase[17].

Results

There are no shifts in the liver catalase spectrum over the pH range 5.6 to 9.7. Below pH 5.5 liver catalase rapidly precipitates and above pH 10 there is a spectral shift to shorter wavelengths characteristic of hematin dissociation[22]. The Soret maximum of the catalase-cyanide complex occurs at 426 mμ with a molar absorptivity of 2.64×10^5 M^{-1} cm^{-1}.

The optical rotatory dispersion curves for catalase of R.Z = 0.915 and R.Z = 0.87 are shown in Figures 3 and 4 plotted as specific rotation vs wavelength. Figure 4 shows a single peak Cotton effect in the Soret region near 400 mμ and the curve in Figure 3 shows a minimum at 233 mμ. The specific rotations for catalase are negative at all wavelengths from 220 to 500 mμ. The Cotton effect in the ultraviolet region indicates the presence of α-helix[23,24], and as a quantitative measure of the amplitude of this trough, the reduced mean residue rotation $[R']_{233}$ has been used. The values of $[R']_{233}$ for catalase of R.Z = 0.915 and R.Z = 0.87 were calculated from the formula:

$$[R']_{233} = \frac{3M_R [\alpha']_{233}}{100(n_{233}^2 + 2)} \tag{2}$$

where the refractive index for water, n_{233} was taken as 1.39.
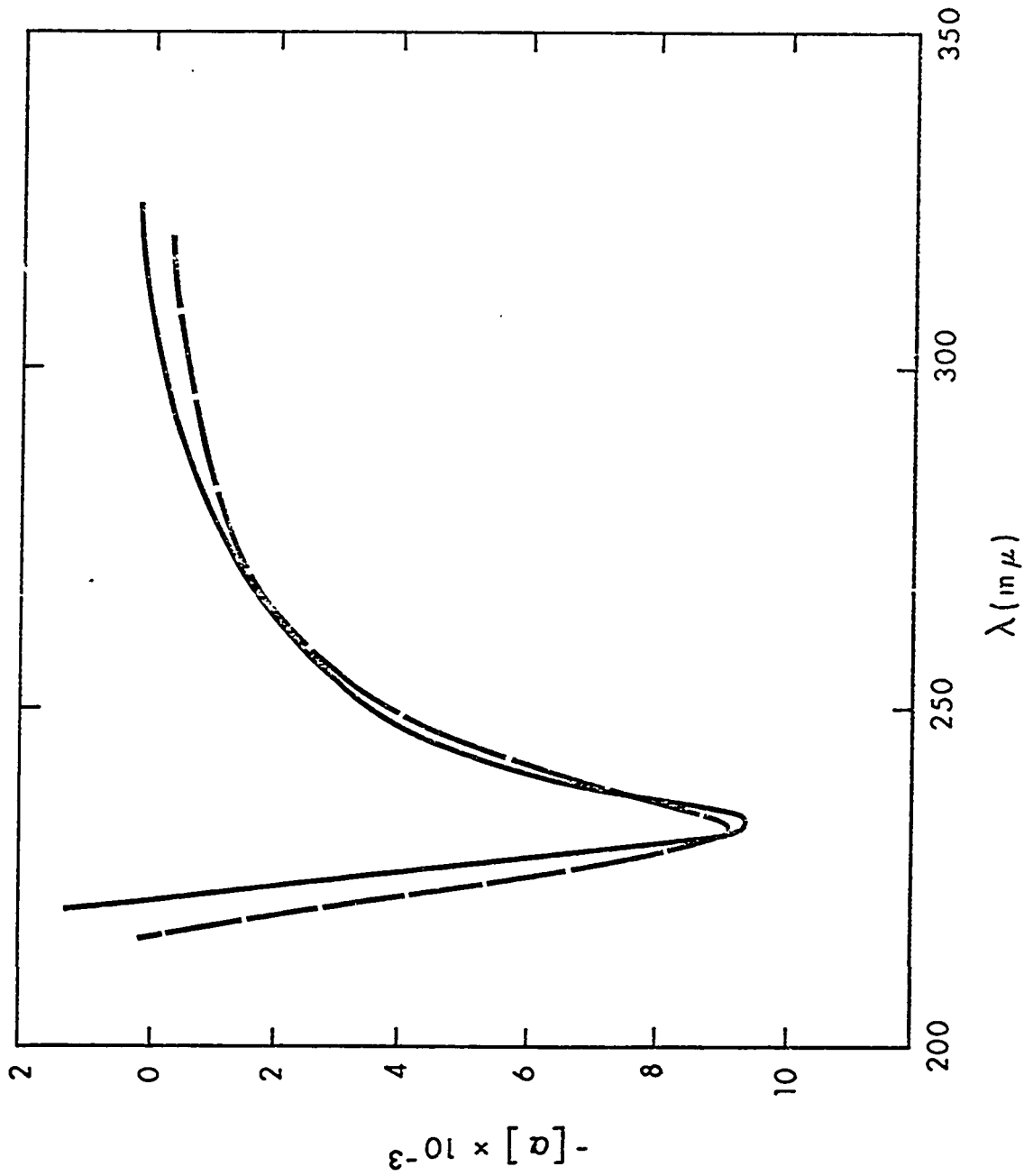
Figure 3. ORD curves in the UV region of liver catalase of R.Z = 0.915 (———) and the Boehringer - Mannheim preparation of R.Z = 0.87 (- - -)
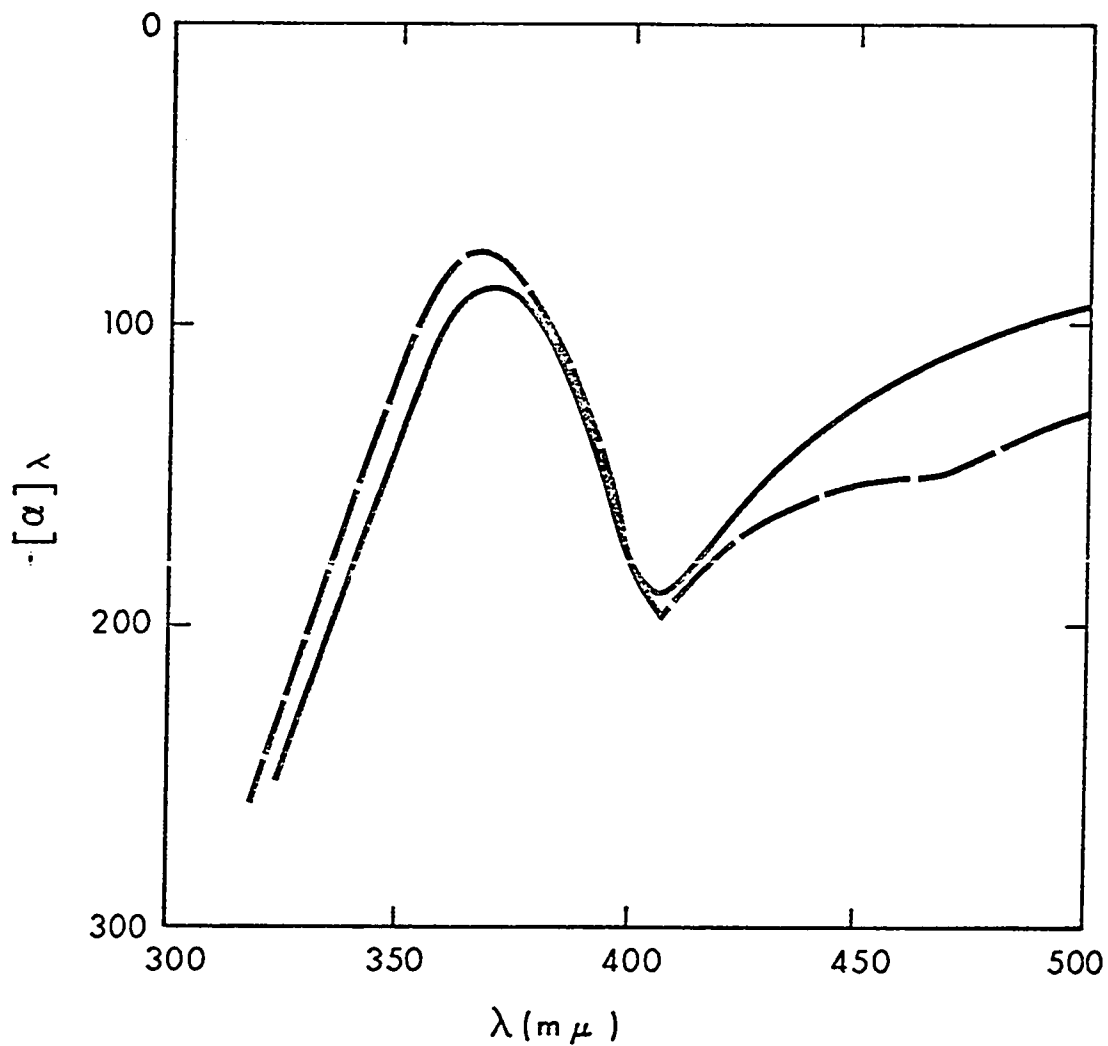
Figure 4. ORD curves in the visible region of liver
catalase of R.Z = 0.915 (———) and the Boehringer -
Mannheim preparation of R.Z = 0.87 (- - -)

The sedimentation velocity patterns of liver catalase of R.Z = 0.915 are shown in Figure 5. The reduced pyridine-hemochromogen spectra of pure hemin and catalase of R.Z's = 0.915 and 0.87 are displayed in Figure 6. The spectra of the two catalases were corrected to coincide with the hemin spectrum at 557 mμ. Figure 7 contains the reduced CO-pyridine hemochromogen spectra of pure hemin and catalase of R.Z's = 0.915 and 0.87. The spectra of the two catalases were once again corrected to coincide with the hemin spectrum at 570 mμ. The bile pigment / total hemin ratios for both catalases are 0.24.

The equilibrium and kinetic behavior of the catalase-cyanide system at a given pH is consistent with the following equation:

$$\text{Cat} + \text{CN} \underset{k_{-1app}}{\overset{k_{1app}}{\rightleftarrows}} \text{CatCN} \qquad (2)$$

The titration curves of liver catalase (with a variety of R.Z's) with total cyanide, are shown in Figure 8. All of these curves showed single inflection points, the $\log[\text{CN}]_0$ values of which were considered equivalent to the pK values of the dissociation constants.

$$K_{Diss} = \frac{[\overline{\text{Cat}}][\text{Total CN}]}{[\overline{\text{CatCN}}]} \qquad (3)$$
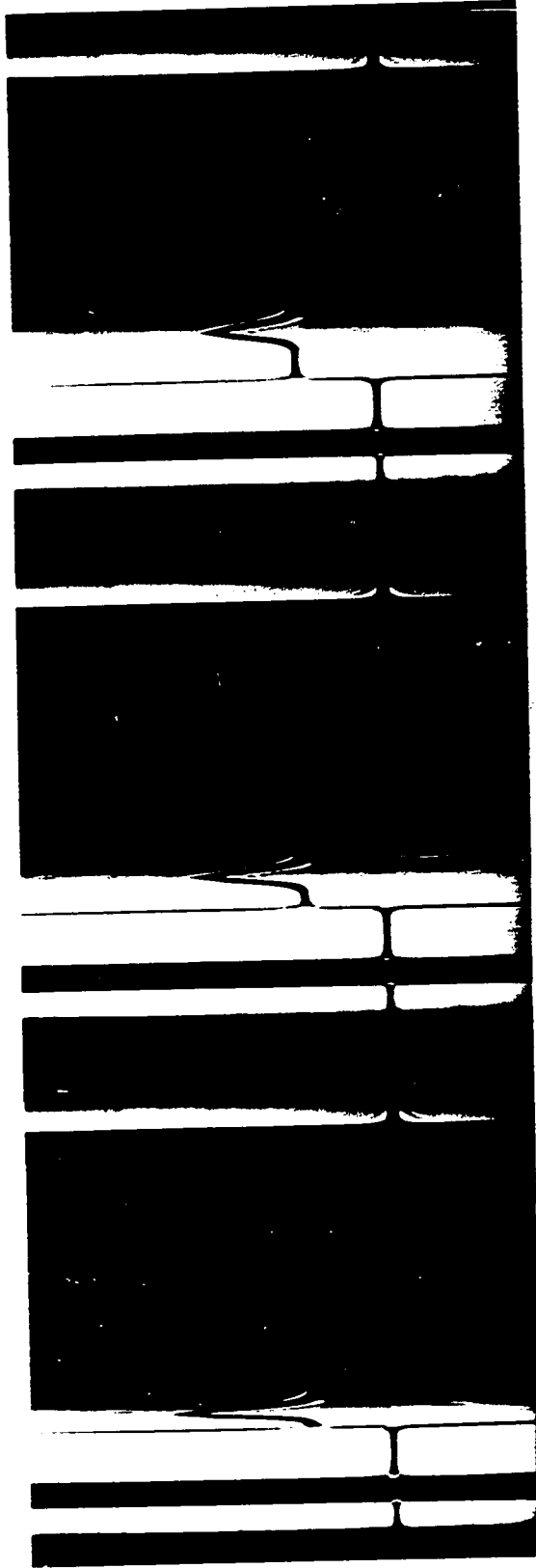
Figure 5. Sedimentation velocity patterns of liver catalase of R.Z = 0.915 at 20° in 0.02 M phosphate buffer (pH 7). Protein concentration : 3.5 mg/cc; bar angle 65°. Photographs were taken at 4 minute intervals after reaching a speed of 60,000 r.p.m.
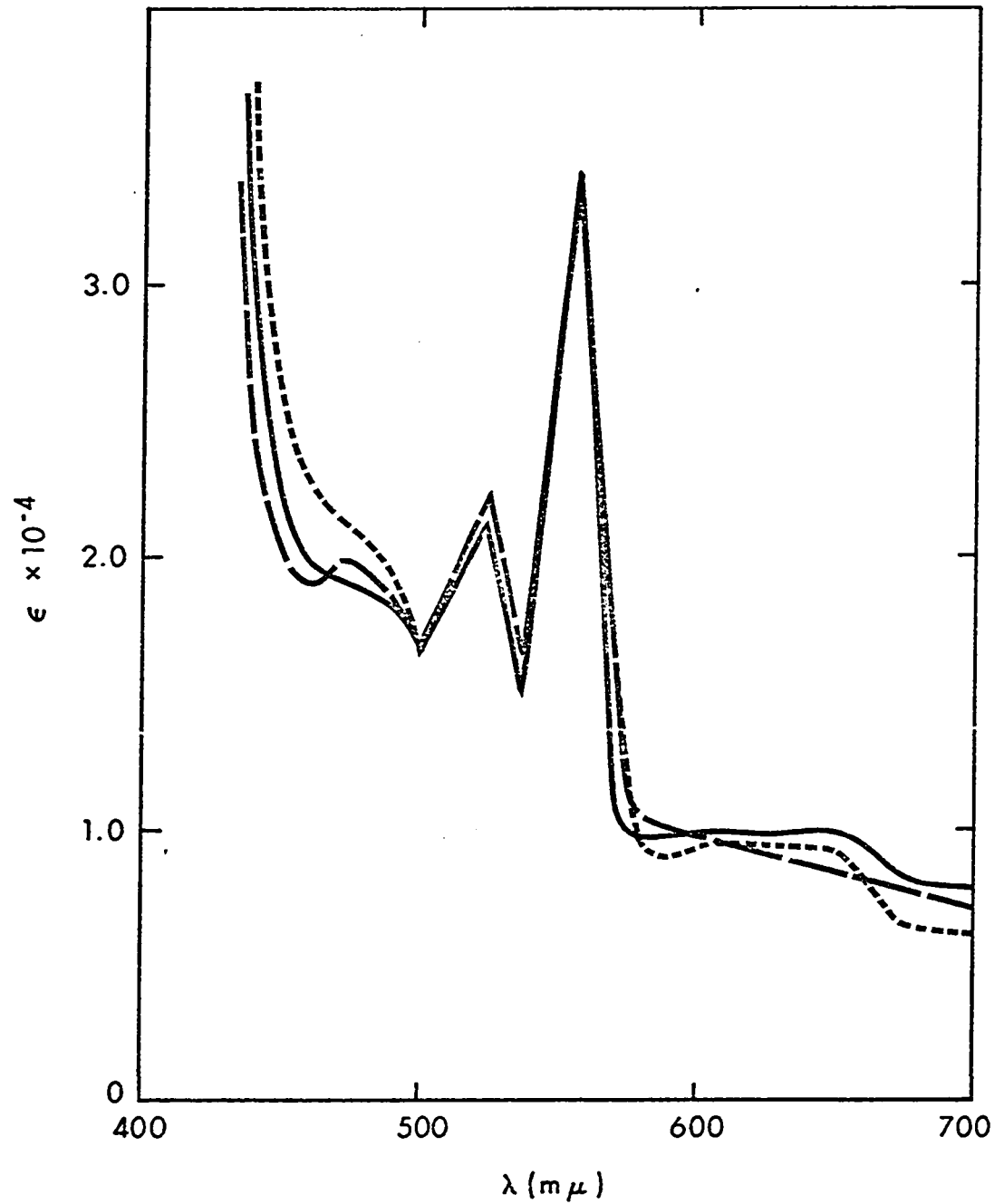
Figure 6. The reduced pyridine-hemochromogen spectra of pure hemin (————), liver catalase of R.Z = 0.915 (————) and Boehringer – Mannheim preparation of R.Z = 0.87 (————)
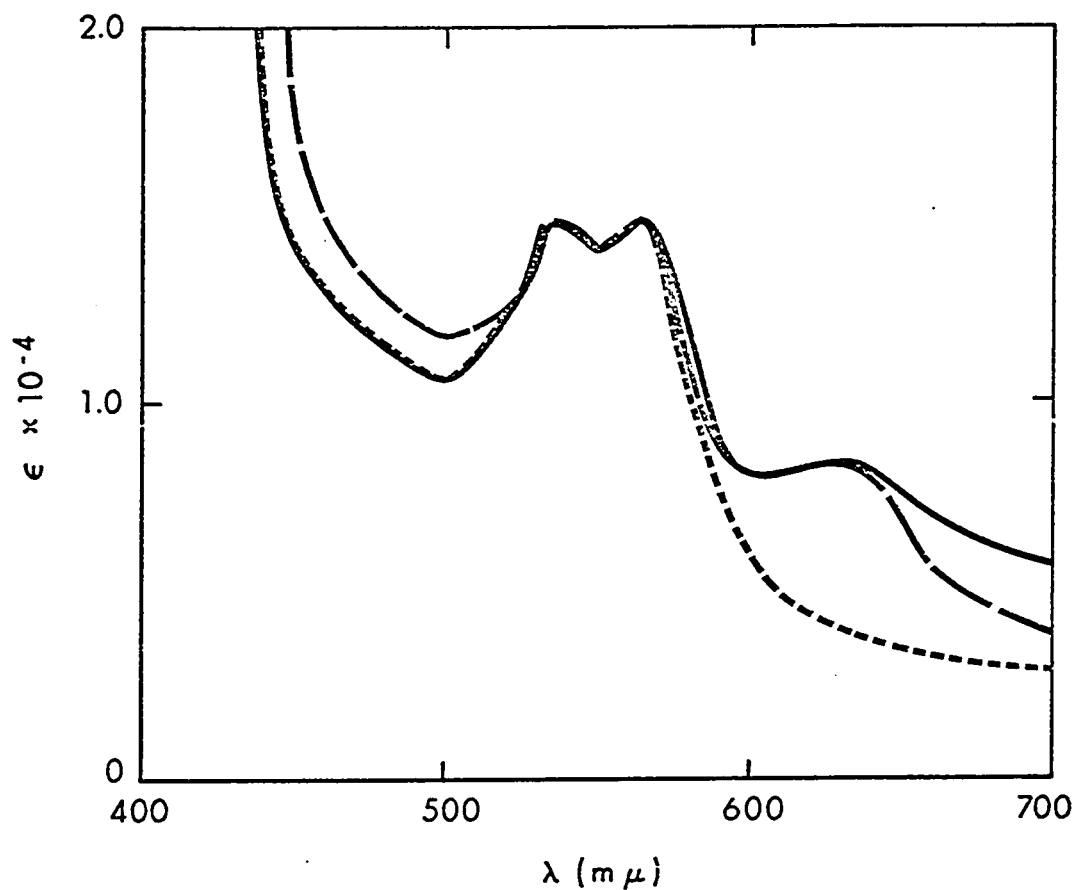
Figure 7. The reduced CO-pyridine hemochromogen spectra of pure hemin (----), liver catalase of R.Z = 0.915 (————) and Boehringer - Mannheim preparation of 0.87 (— — —)
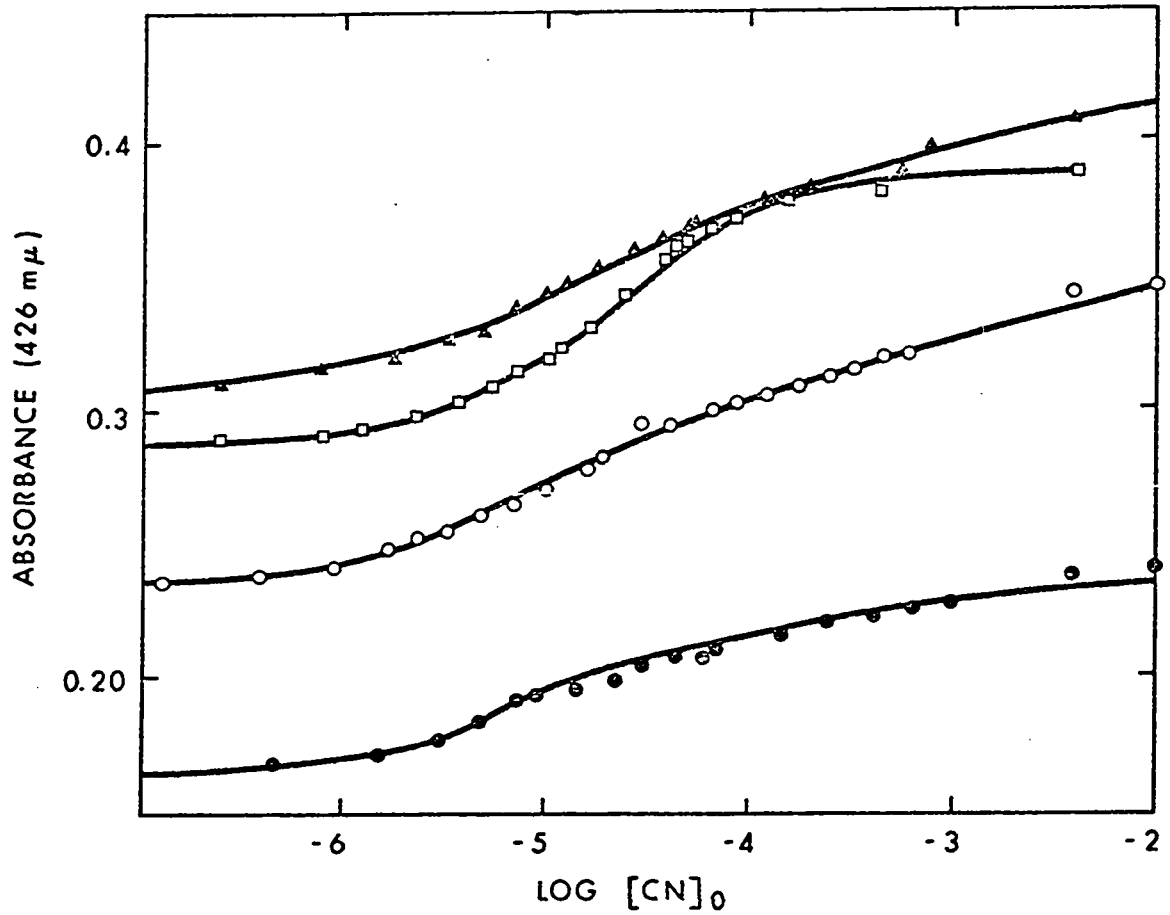
Figure 8. Titration curves of various liver catalases with cyanide, of R.Z = 0.286, pH 6.8 (▲-▲-▲), R.Z = 0.65, pH 8.8 (□-□-□), R.Z = 0.915, pH 6.95 (o-o-o) and R.Z = 0.87, pH 7 (●-●-●).

The superscript bars indicate equilibrium concentrations. Since cyanide was present in large excess, its total concentration can be regarded as equal to the equilibrium concentration of unbound cyanide. The values of K_{Diss} are listed in Table IV.

In all temperature jump experiments only one relaxation time was observed. The kinetic behavior is consistent with equation 2, for which the reciprocal of the time constant, τ, describing the relaxation to equilibrium for a system near equilibrium is given by the following equation[25]:

$$\frac{1}{\tau} = k_{1app}([\overline{Cat}] + [\overline{CN}]) + k_{-1app} \tag{4}$$

The values of $[\overline{Cat}]$ and $[\overline{CN}]$ are the equilibrium values of free catalase and cyanide. However, since the concentration of total cyanide $[CN]_0$, was generally much greater than that of catalase, the sum $([\overline{Cat}] + [\overline{CN}])$ can be approximated by $[CN]_0$. Therefore, the values of k_{1app} and k_{-1app} were obtained from the slope and intercept of a plot of $\frac{1}{\tau}$ vs $[CN]_0$. Examples of plots of $\frac{1}{\tau}$ vs $[CN]_0$ are shown in Figure 9. The values of k_{1app} and k_{-1app} obtained in this manner are listed in Table V. This Table also contains the apparent dissociation equilibrium constants from kinetic data as well as from spectrophotometric measurement. A plot of k_{1app} vs pH, which is a curve with a maximum at pH 7.5, is shown in Figure 10. Because of the errors inherent in the temperature-jump technique it

is believed that the k_{1app} and k_{-1app} values are probably accurate to within 15%.

TABLE IV

Dissociation Constants for Cyanide Binding to
Several Catalase Preparations from Bovine Liver at 25°

R.Z	pH	Dissociation Constants (M)
0.915	6.85	2.50×10^{-6}
	6.95	3.97×10^{-6}
	9.60	6.25×10^{-5}
0.870	6.79	7.80×10^{-6}
	7.00	7.90×10^{-6}
0.832	7.10	7.90×10^{-6}
0.650	7.25	7.80×10^{-6}
	8.80	3.46×10^{-5}
	9.00	2.33×10^{-5}
0.400	6.70	7.90×10^{-6}
0.286	6.80	6.26×10^{-6}
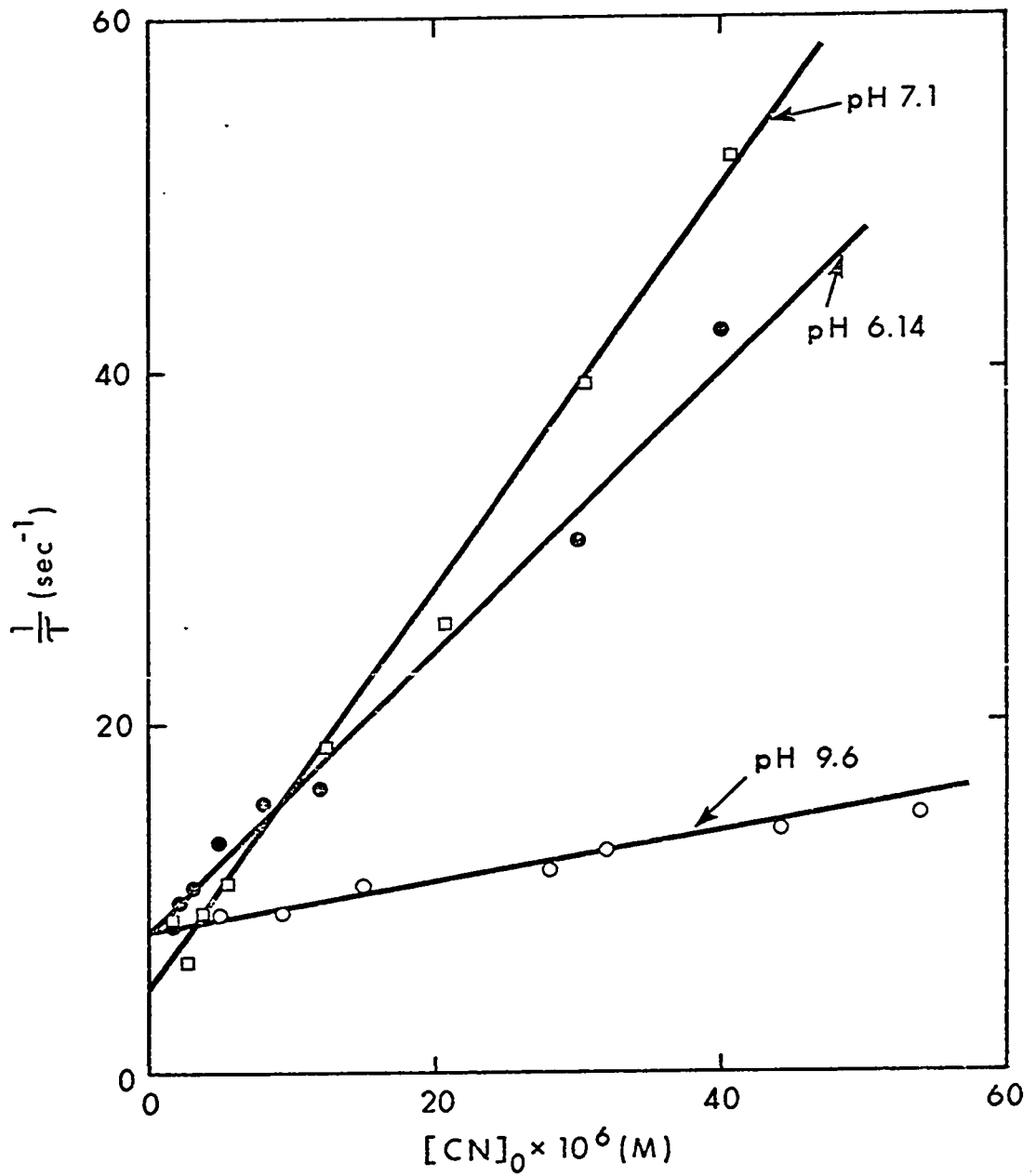
Figure 9. Plots of reciprocal relaxation times, vs total cyanide concentrations, at various pH's, for the binding of cyanide by liver catalase.

TABLE V

Rate and Equilibrium Constants for the
Binding of Cyanide by Catalase from Bovine Liver at 25°

| pH | Experimental apparent rate constants | | $K_{Diss} = \dfrac{[\overline{Cat}][\overline{CN}]}{[\overline{CatCN}]}$ | |
	k_{1app} ($M^{-1} sec^{-1}$)	k_{-1app} (sec^{-1})	From kinetic data	Spectro-photometric[†] determinations
5.70	2.76×10^5	6.60	2.39×10^{-5}	
6.14	7.15×10^5	9.00	1.26×10^{-5}	
6.79				7.80×10^{-6}[b]
6.83	1.17×10^6	4.00	3.40×10^{-6}	
6.83*	1.15×10^6	2.00	1.70×10^{-6}	
6.85				2.50×10^{-6}[a]
6.95	1.00×10^6	3.50	3.50×10^{-6}	3.97×10^{-6}[a]
7.10	1.11×10^6	5.25	4.72×10^{-6}	7.90×10^{-6}[b]
7.92	7.85×10^5	4.50	5.75×10^{-6}	
8.50	5.77×10^5	5.80	1.01×10^{-5}	
8.80				3.46×10^{-5}[c]
8.85	5.65×10^5	6.00	1.05×10^{-5}	
9.60	1.31×10^5	8.15	6.25×10^{-5}	6.25×10^{-5}[a]

*All the kinetic experiments were done on Boehringer-Mann-heim liver catalase preparations with an R.Z = 0.87, except at this pH which had an R.Z of 0.915.

[†]For the Spectrophotometric determinations of K_{Diss} the R.Z's of liver catalase used at these pH's were: a, 0.915, b, 0.87 and c, 0.65.
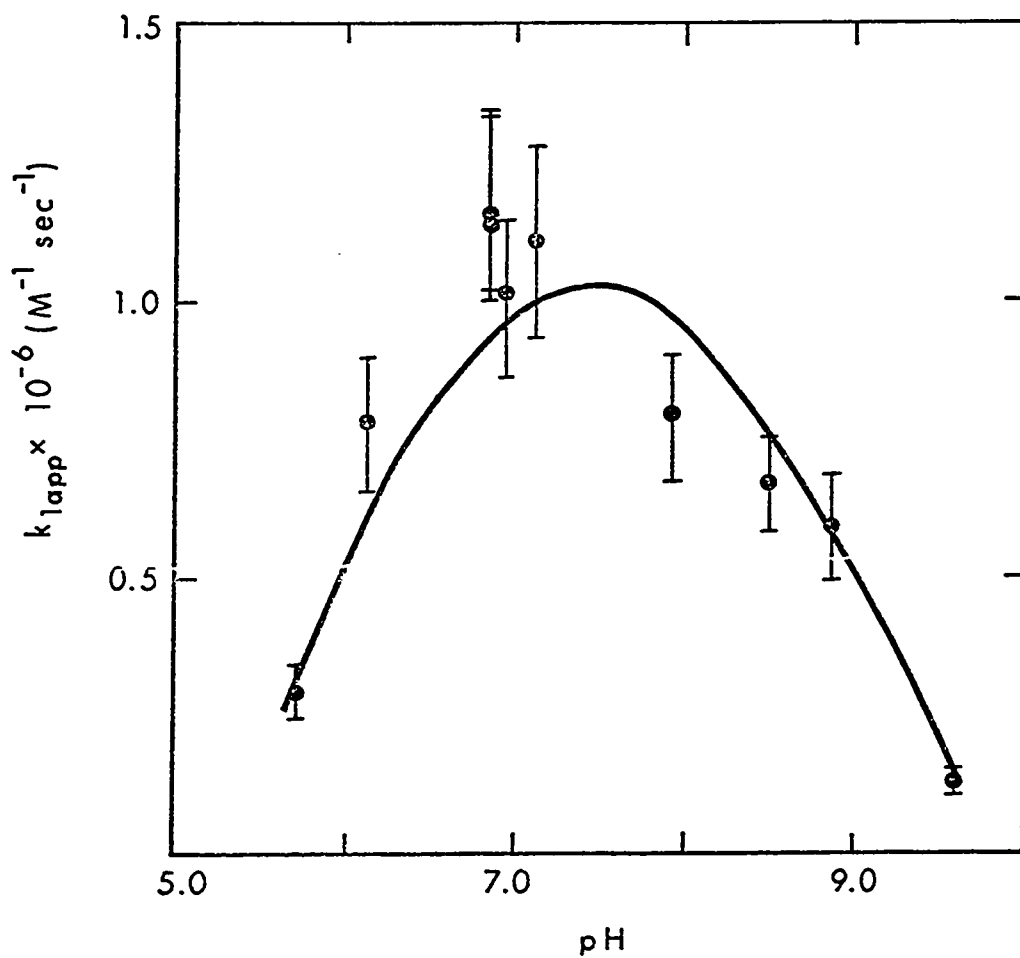
Figure 10. Plot of k_{1app} vs pH for the binding of cyanide
to catalase with error limits of ± 15% shown for the
k_{1app} values. The solid line is calculated using the
best-fit parameters of equation 5.

Discussion

The results from the ORD spectra indicate that both liver catalase preparations are in their native or helical conformation. The absolute value of $[R']_{233} = -10,500$ (± 500) for both catalases is greater by about 15% than the value obtained by Yang and Samejima[26] of -9000. This does not mean that their catalase preparation was less helical or more denatured, but probably reflects the uncertainty in obtaining absolute values for degree of helicity[23,24]. The presence of a single peak Cotton effect in the Soret region near 400 mμ is shown in Figure 4. The results of Yang and Samejima appear to show the presence of two peaks, which is believed by these authors to be due to normal experimental errors.

The molecular weight of catalase of R.Z = 0.915, as determined by the Archibald technique at 20° to be 231,945, agrees reasonably well with previously reported values of 248,000[20], 225,000[27] and 240,000[17]. From Figure 5 it can be seen that the preparation has only a single symmetrical peak. The $S^{\circ}_{20,w}$ value of 11.4 S, for our liver catalase of R.Z = 0.915 is identical to that of Samejima and Yang[17]. The ORD spectra show that the Boehringer-Mannheim preparation of R.Z = 0.87 is not denatured, and it can be reasonably assumed that it is similar to liver catalase of R.Z = 0.915.

The reduced pyridine-hemochromogen spectra and CO-

pyridine hemochromogen spectra indicate that there are
fewer than three hemin groups per protein molecule, and
at least 24% bile pigment for both of the catalase prepa-
rations which we used.   Thus the catalase preparations
are essentially degraded and the presence of bile pigment
makes the preparations heterogeneous.   Most liver catalase
preparations are partly degraded[28].

Most of the titration curves of liver catalase vs
$\log[CN]_0$ as shown in Figure 8 appear asymmetrical at about
pH 7, but at high pH the curves tended to be symmetrical
which may indicate the presence of at least one ionizable
group affecting the equilibrium constants.   However, since
only one relaxation time was observed kinetically, and as
seen in Tables IV and V that the dissociation constants
obtained kinetically compare favorably to those obtained
from the inflection points of the titration curves, no
further attempt was made to analyze the titration data for
disparate dissociation constants.   From these Tables it
can be seen that the pK's of the various catalase-cyanide
preparations show some pH dependency, increasing at lower
and higher pH.   Chance[13,14] found no effect of pH on K_{DISS}
between pH 3 and 7 for both human and horse catalase from
erythrocytes, obtaining a value of 7×10^{-6} and 4×10^{-6} M
respectively.   However, for human blood catalase there are
deviations above pH 8.5 which are not attributable to
dissociation of HCN.   Table IV shows that the pK values at

about pH 7 for catalase of R.Z = 0.915 are within experimental error to that obtained by Chance for horse blood catalase, but the pK of catalase lower than R.Z = 0.915 have values about twice that of horse catalase. Chance demonstrated that there were no observable interactions between the four hemin groups of catalase. However, one may speculate that the higher pK values obtained for the binding of cyanide to degraded catalases may indicate a certain degree of interactions. Unfortunately the presence of bile pigment complicates matters, and further the degraded protein may have exposed hitherto buried ionizable groups which can now affect the binding constants and protein stability. This is noteworthy as liver catalase preparations rapidly precipitate below pH 5.5, whilst catalase from blood erythrocytes do not.

Although only a relatively small number of kinetic determinations at various pH's were carried out, it was still possible to obtain a reasonable mechanism for the binding of cyanide to liver catalase.

If catalase had no ionizable groups involved in cyanide-complex formation then k_{1app} should have limiting values at low and high pH and the k_{1app} values at intermediate pH should lie between these extremes. Obviously this is not the case and a mechanism capable of explaining the rate data must involve at least one ionizable group.

The next simplest possibility is mechanism I, involving two species of catalase reacting with CN^- and HCN.

$$\text{HP} + \begin{cases} CN^- \xrightarrow{k_1} \\ HCN \xrightarrow{k_2} \end{cases} HP(CN)$$

$$K_1 \updownarrow$$

$$P + \begin{cases} CN^- \xrightarrow{k_3} \\ HCN \xrightarrow{k_4} \end{cases} P(CN) \qquad\qquad (I)$$
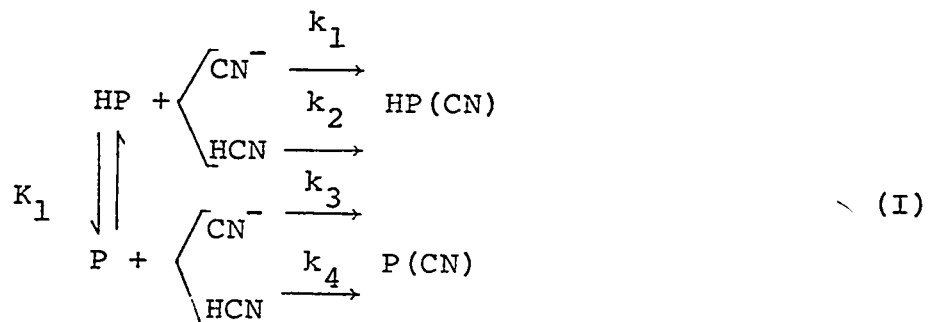
Protons involved in ionization equilibria have been omitted from this reaction as have charges on the enzyme species as they are unknown. The form in which cyanide is bound in the complex is unknown, and the dissociation reaction paths have not been indicated since here only association rate data are of interest. The equation for k_{1app} in terms of this mechanism is:

$$k_{1app} = \frac{k_1 + \dfrac{k_2[H^+]}{K_L} + \dfrac{k_3K_1}{[H^+]} + \dfrac{k_4K_1}{K_L}}{1 + \dfrac{K_1}{[H^+]} + \dfrac{[H^+]}{K_L} + \dfrac{K_1}{K_L}} \qquad\qquad (5)$$

where K_L is the dissociation constant of HCN corrected for ionic strength of 0.11. With the aid of a nonlinear least-squares program[30] eq 5 can be used to yield the best-fit values for the rate constants, k_1 to k_4 and for the dissociation constant K_1 from an analysis of the k_{1app} data. The k_{1app} data could not be fitted within experimental error

using eq 5. Consequently a mechanism capable of explaining the observed forward rate data must involve more than one ionizable group in the active site of the enzyme.

The simplest mechanism that will explain the data satisfactorily involves two such groups and in its general form can be written as mechanism II.

$$
\begin{array}{ccl}
H_2P & + & \begin{cases} CN^- \xrightarrow{k_5} \\ HCN \xrightarrow{k_6} \end{cases} H_2P(CN) \\[1em]
K_2 \updownarrow & & \\[0.5em]
HP & + & \begin{cases} CN^- \xrightarrow{k_7} \\ HCN \xrightarrow{k_8} \end{cases} HP(CN) \\[1em]
K_3 \updownarrow & & \\[0.5em]
P & + & \begin{cases} CN^- \xrightarrow{k_9} \\ HCN \xrightarrow{k_{10}} \end{cases} P(CN)
\end{array}
\qquad (II)
$$
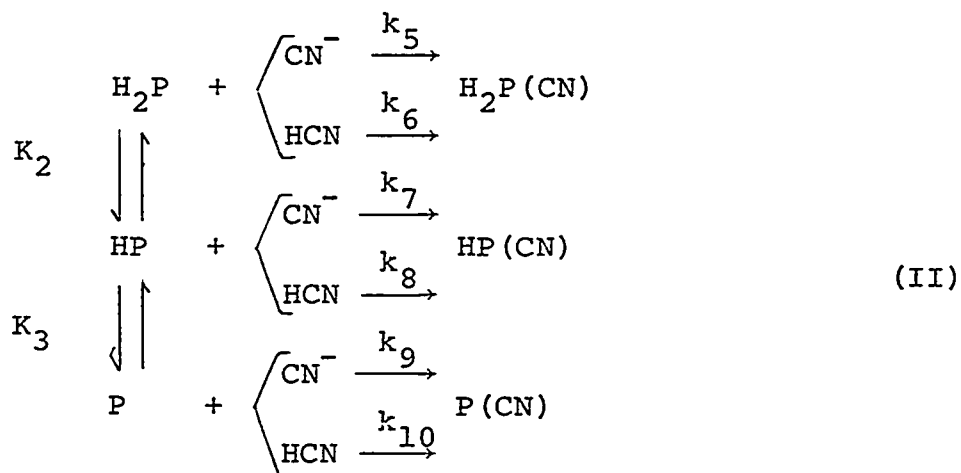
From this it can be shown that

$$
k_{1app} = \frac{k_5 + \dfrac{k_7 K_2}{[H^+]} + \dfrac{k_9 K_2 K_3}{[H^+]^2}}{\left(1 + \dfrac{K_2}{[H^+]} + \dfrac{K_2 K_3}{[H^+]^2}\right)\left(1 + \dfrac{[H^+]}{K_L}\right)}
$$

$$
+ \frac{k_6 + \dfrac{k_8 K_2}{[H^+]} + \dfrac{k_{10} K_2 K_3}{[H^+]^2}}{\left(1 + \dfrac{K_2}{[H^+]} + \dfrac{K_1 K_2}{[H^+]^2}\right)\left(1 + \dfrac{K_L}{[H^+]}\right)}
\qquad (6)
$$

There also exist two simplified forms of mechanism II
(mechanisms IIa - IIb) which will reproduce the forward
rate data and which predict exactly the same values of
k_{1app} at any given pH:

$$
\begin{array}{c}
H_2P + CN^- \xrightarrow{k_5} H_2P(CN) \\
K_2 \updownarrow \\
HP \\
K_3 \updownarrow \\
P
\end{array}
\qquad (IIa)
$$

$$
\begin{array}{c}
H_2P \\
K_2 \updownarrow \\
HP + HCN \xrightarrow{k_8} HP(CN) \\
K_3 \updownarrow \\
P
\end{array}
\qquad (IIb)
$$
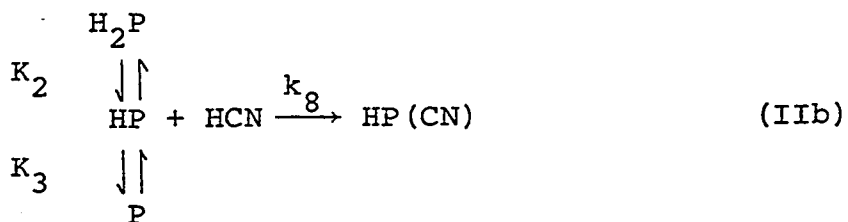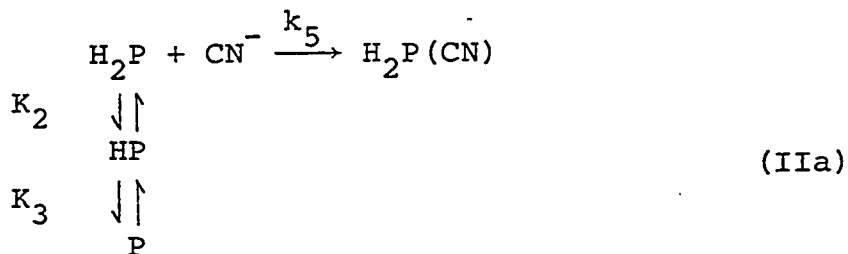
The best fit values for the rate and equilibrium constants
for both simplified mechanisms obtained using the nonlinear
least-squares program are listed in Table VI. The existance
of two simplified versions of mechanism II giving equivalent
fits to the data is due to the inability of the kinetic
method to distinguish between reaction paths such as:

$$H_2P + CN^- \xrightarrow{k_5}$$

and

$$HP + HCN \xrightarrow{k_8}$$
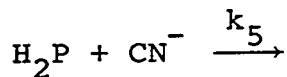
in which the total number of ionizable protons on the two reactants is the same but the positions of their attachment are different. The fit of the k_{1app} values predicted by eq 4 to the experimental data using any of the two sets of constants in Table VI is shown in Figure 10 where the solid line gives the predicted values of k_{1app}. The pK values for these ionizable groups are 6.1 and 9.8. No attempt was made to analyse the reverse rate data because of the random nature of the experimental points.

It must be emphasized that the kinetic mechanism obtained here presents merely a reasonable possibility with respect to the few experimental points obtained. It also presents the kinetic behavior of a catalase system with a large amount of bile pigment present and it is thus necessary to do a comparative study with intact catalase, and with liver catalase free from bile pigment before any conclusive statements can be made regarding the kinetic behavior of catalase.

TABLE VI

Rate and Equilibrium Constants
of Simplified Forms of Mechanism II

Constant	$\underline{a}$	$\underline{b}$
k_5	$(8.6\pm1.9) \times 10^8\ M^{-1}sec^{-1}$	
k_8		$(1.1\pm0.1) \times 10^6\ M^{-1}sec^{-1}$
K_2	$(8.3\pm2.3) \times 10^{-7}\ M$	$(8.3\pm2.3) \times 10^{-7}\ M$
K_3	$(1.6\pm0.9) \times 10^{-10}\ M$	$(1.6\pm0.9) \times 10^{-10}\ M$

LITERATURE CITED

1. Loew, O., U.S. Dep. Agri. Wash. Report No. 68, 1 (1901).

2. Nichols, P., and Schonbaum, G.R., "The Enzymes", Boyer, D.P., Lardy, H., Myrback, K., Eds., Academic Press, New York and London, 1963, Vol. 8, page 147.

3. Lemberg, R., and Legge, J. W., Biochem. J. (London) 37, 117 (1943).

4. Zeile, K., and Hellstrom, H., Z. Physiol. Chem. 192, 171 (1930).

5. Keilin, D., and Hartree, E. F., Biochem. J. 49, 88 (1951).

6. George, P., and Hanania, G., Biochem. J. 52, 517 (1952).

7. George, P., and Hanania, G., Biochem. J. 55, 236 (1953).

8. Yonetani, T., J. Biol. Chem. 242, 5008 (1967).

9. Lewis, U.J., J. Biol. Chem. 206, 109 (1954).

10. Brill, A. S., and Williams, R. J. P., Biochem. J. 78, 246 (1961).

11. Stryer, L., Kendrew, J. C., and Watson, H. C., J. Mol. Biol. 8, 96 (1964).

12. Watson, H. C., and Chance, B., in "Hemes and Hemoproteins". Chance, B., Easterbrook, R. W., and Yonetani, T., Eds., Acad. Press, N.Y., 1966, page 149.

13. Chance, B., J. Biol. Chem. 194, 483 (1952).

14. Chance, B., J. Biol. Chem. 179, 1299 (1949).

15. Lemberg, R., Lockwood, W. H., and Legge, J. W.,
    Biochem. J. 35, 363 (1941b).

16. Shirakawa, M., J. Agr. Chem. Soc. Japan, 23, 361
    (1950).

17. Samejima, T., Yang, J. T., J. Biol. Chem. 238, 3256
    (1963).

18. Hasinoff, B. B., Dunford, H. B., Horne, D. G.,
    Can. J. Chem. 47, 3225 (1969).

19. Paul, K. G., Theorell, H., and Akeson, A., Acta
    Chemica Scand. 7, 1284 (1953).

20. Sumner, J. B., and Grolen, H., J. Biol. Chem. 125,
    33 (1938).

21. Strobel, H. A., "Chemical Instrumentation" Addison-
    Wesley, Reading, Mass., 1960, page 461.

22. Stern, G. K., J. Gen. Physiol. 20, 631 (1937).

23. Simmons, N. S., Cohen, C., Szent-Gyorgyi, A. G.,
    Wetlaufer, D. B., and Blout, E. R., J. Am. Chem. Soc.,
    83, 4766 (1961).

24. Blout, E. R., Schmier, I., and Simmons, N. S., J. Am.
    Chem. Soc. 84, 3193 (1962).

25. Eigen, M., and de Maeyer, L., in Techniques in Organic
    Chemistry, Part II, Vol. VIII, Weissburger, A., Ed.,
    2nd ed, New York, N.Y., Interscience, p 902. (1963).

26. Yang, J. T., and Samejima, T., J. Biol. Chem. 238,
    3262 (1963).

27. Sumner, J. B., Dounce, A. L., and Frampton, V. L.,
    J. Biol. Chem. 136, 343 (1940).

28. Bonnichsen, R. K., Acta Chem. Scand. 2, 561 (1948).

29. Urnes, P., and Doty, P., Advan. Prot. Chem. 16, 401
    (1961).

30. IBM SHARE Library (1964) Program SDA 3094, modified
    for use on a University of Alberta IBM 360 computer.

CHAPTER 2

THE KINETICS OF FLUORIDE BINDING BY LACTOPEROXIDASE

Introduction

There have been numerous studies of ligand binding by hemoproteins. These studies have thrown considerable light on the nature of the heme-linked groups*. The enzyme bovine lactoperoxidase is now readily available in a highly purified form, but there have been no recent reports of the kinetics of its interaction with ligands[1,2]. Lactoperoxidase is a protein with unique properties. The heme is linked by covalent bonds to the protein[3]. Also the protein-heme ratio is higher than that of other known peroxidases. A study of the kinetics of the interaction of lactoperoxidase with a variety of ligands has been undertaken. We report here the results of a kinetic study of fluoride binding to lactoperoxidase at 25° between pH values of 3.8 and 5.4.

* We define a heme-linked group as an ionizable group in the enzyme which affects ligand binding.

Experimental

Kinetic measurements were made by following transmittance changes at 25.0 ± 0.1° using a stopped-flow apparatus[4]. Absorbance measurements to determine LP concentrations and LP-F complex equilibrium constants were made on a Beckman D.U. spectrophotometer*. A Beckman expanded-scale pH meter was used for all pH measurements. Lactoperoxidase of R.Z equal to 0.74 was isolated by the method of Morrison and Hultquist[5] and precipitated with ammonium sulfate for storage. Stock solutions of LP were prepared by dialysis against 0.01 M phosphate buffer at pH 7.4.

Reagent grade NaF (Fisher) was used without further purification. The wavelength used for all stopped-flow

---

*Abbreviations used: LP or P, ferric lactoperoxidase; R.Z, purity number; μ ionic strength; F and PF, all species of fluoride and complex, respectively; $(P)_0$ and $(F)_0$, initial concentrations of all forms of peroxidase and fluoride; $(\overline{P})$, $(\overline{PF})$ and $(\overline{F})$, equilibrium concentrations of all forms of peroxidase, complex, and fluoride; K_L, dissociation constant of ligand; k_{lapp} and k_{-lapp}, apparent second-order binding rate constant and apparent first-order dissociation rate constant; k'_{lapp} is equal to $k_{lapp} (F)_0$; K_{Diss}, apparent dissociation constant of peroxidase-fluoride complex; HRP, ferric horseradish peroxidase.

measurements was 408mμ, where the largest change in absorbance occurred upon complex formation. Solutions of LP and F were made at the desired pH with buffer of ionic strength μ equal to 0.01 and sufficient KNO_3 so that the total μ was always constant at 0.11. The concentrations of LP and F at each pH were such that the absorbance of the LP solution after mixing with F would always be within 0.25 to 0.5 which includes the region of minimum error due to instrumental uncertainty. The final total concentrations of LP and F after mixing were 3.43×10^{-6} M and 0.025 M. Sodium acetate was used to buffer the solutions over the pH range of the kinetic measurements. The possibility of buffer complexing with LP was checked by examining the spectrum of LP in the presence and in the absence of buffer.

Results

The absorption maximum in the Soret region of the LP spectrum shifts from 412 to 410 mμ upon complex formation with fluoride, with a corresponding change[6] in molar absorptivity from 1.14×10^5 to 1.27×10^5 M^{-1} cm^{-1}. Kinetic and equilibrium data were obtained over the pH range 3.8 – 5.4. Between pH 5.4 and 7 the extent of complex formation was too small for accurate measurements and no complexing was observed above pH 7. When the pH was changed suddenly from 7 to 3.6 a slow precipitation of the protein was observed; at pH 3.8 the precipitation did not commence for at

least 1 h. The precipitation could be prevented by dialysis of a neutral solution against acid buffers. No evidence of buffer complexing was obtained.

Differences between output photomultiplier voltages are proportional to differences in light intensity transmitted by the reaction solution. Therefore, ordinate values obtained from enlargements of the oscilloscope trace photographs are proportional to transmittances. Relative transmittance values were converted to concentrations by means of auxiliary transmittance measurements at 408 mµ on solutions of lactoperoxidase and lactoperoxidase-fluoride equilibrium mixtures, which were idential to initial and final reaction mixtures in the comparable stopped-flow experiments[4].

The general form of the rate equation for the reaction is:

$$P + F \underset{k_{-1app}}{\overset{k_{1app}}{\rightleftharpoons}} PF \qquad (1)$$
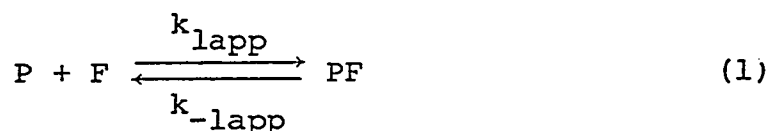
but since the concentration of F was of the order of 10^4 times greater than the concentration of protein, the forward reaction obeyed pseudo-first-order kinetics. We shall therefore, substitute a pseudo-first-order constant k'_{1app} for $k_{1app}(F)_0$ in the differential rate equation for this reaction:

$$\frac{d(PF)}{dt} = k'_{1app}(P) - k_{-1app}(PF) \qquad (2)$$

Equation 2 was analyzed in differential form with the approximation of d(PF)dt by $\Delta(PF)/\Delta t$. Using the chord approximation along with the average concentration of PF complex within each interval, $(PF)_{av}$, eq 2 becomes:

$$\frac{\Delta(PF)}{\Delta t} = k'_{1app}[(P)_0 - (PF)_{av}] - k_{-1app}(PF)_{av} \qquad (3)$$

Values of k'_{1app} and k_{-1app} were obtained from eq 3 by use of a nonlinear least-squares computer program[7] in which 15-20 points from each experiment trace were used. Because the reaction was driven to completion in order to obtain maximum signal changes, the k_{-1app} data cannot be regarded as reliable. Equation 2 can be integrated to give

$$\ln \frac{(P)_0 - (\overline{P})}{(P) - (\overline{P})} = (k'_{1app} + k_{-1app})t \qquad (4)$$

A plot of the left side of eq 4 versus time yields a straight line of slope $(k'_{1app} + k_{-1app})$ and zero intercept as in Figure 1. The experimental constants k'_{1app} and k_{-1app} obtained from eq 3 and $(k'_{1app} + k_{-1app})$ from eq 4 are presented as a function of pH in Table 1. Values of K_{Diss} were obtained by spectrophotometric titration[8]. The results obtained at five pH values over the range 3.8 -5.4 were constant within the range $K_{Diss} = (3 \pm 2) \times 10^{-4}$ M with no trend apparent.

Discussion

The pK of HF ionization at zero μ is 3.1_7[9] and after correction to $\mu = 0.11$ it becomes 2.9_1[10]. Only HF and F^- have been considered as possible binding species[11]. The simplest mechanism involves the binding of the predominant fluoride species F^- by LP which has no heme-linked groups. The mechanism can be represented as follows:

$$P + F^- \underset{k_{-1}}{\overset{k_1}{\rightleftharpoons}} PF \qquad K_L \Big\updownarrow \qquad \text{HF} \tag{I}$$
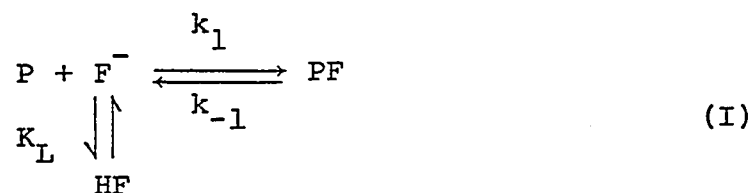
Charges on the peroxidase species are not shown since they are not known. According to this mechanism, the pH dependence of k_{1app} is given by

$$k_{1app} = \frac{k_1}{1 + (H^+)/K_L} \tag{5}$$

Since $(H^+)/K_L$ is small compared to one, mechanism I represented by eq 5 predicts that within experimental error there would be no pH dependence of the values of k_{1app}. It can therefore be eliminated by simple inspection of Figure 2 in which $\log_{10}k_{1app}$ is plotted versus pH.

A second mechanism can be postulated in which the neutral ligand only is binding. It may be written as

$$P + HF \underset{k_{-2}}{\overset{k_2}{\rightleftharpoons}} PHF$$

$$K_L \updownarrow \qquad \qquad \updownarrow K_C$$

$$F^- \qquad \qquad PF \qquad \qquad \text{(II)}$$
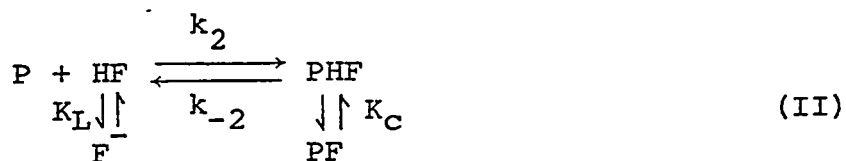
where PHF and PF are distinct species related through the acid dissociation constant K_C.

The corresponding equation for the pH dependence of k_{lapp} is

$$k_{lapp} = \frac{k_2}{1 + K_L/(H^+)} \qquad (6)$$

A plot of $k_{lapp}(1 + K_L/(H^+))$ versus pH should give a straight line with a slope of zero and intercept equal to k_2. From the results of Figure 3, a constant value of k_2 equal to $(9.7 \pm 0.4) \times 10^2 \ M^{-1}s^{-1}$ is obtained. Thus the experimental results can be accounted for simply by the second mechanism.

The values of k'_{lapp} obtained from eq 3 are generally within experimental error of the corresponding $(k'_{lapp} + k_{-lapp})$ data from eq 4. Subtraction of the former from the latter in principle should yield k_{-lapp} values which, however, represent the small difference between two large quantities, and the resultant k_{-lapp} values often have the wrong sign. Since the K_{Diss} data obtained by spectrophotometric titration appear pH independent within the considerable experimental error over the pH range 3.8-5.6 and since

K_{Diss} should equal k_{-1app}/k_{1app}, it follows that the k_{-1app} and k_{1app} data should exhibit a similar pH dependence. Although the k_{-1app} data obtained directly from eq 3 (Table I) show considerable scatter, there appears to be a trend of k_{-1app} becoming larger at lower pH. From mechanism II and eq 2 it can be shown that $k_{-1app}(PF)_{total} = k_{-2}(PHF)$. If the value of pK_c falls within the pH range of the present study, then (PHF) would be increased at lower pH with a corresponding increase in the values of k_{-1app}. Mechanism II therefore is adequate for the pH range of the present study.

Earlier investigators were not able to detect fluoride binding by lactoperoxidase.[2] This might have been due to their preparation of lactoperoxidase since these workers (Theorell and Paul) were unable to establish a reproducible method for the isolation of the enzyme.

The magnitudes of the k_{1app} data obtained from LP + F are in contrast to those for HRP + F. Similarly, the binding postulated in the second mechanism is quite different than the simplest mechanism which will account quantitatively for the binding-rate data of F by HRP[4]. In the latter case the experimental results were consistent with fluoride-ion binding to ferric iron in the presence of two heme-linked groups with pK values of 4.3 and 6.1. One possibility for the differences observed may be in the

different porphyrin structures of the two peroxidases[12].

TABLE I

Kinetic data on the binding of fluoride by lactoperoxidase

pH	$*k'_{1app} + k_{-1app}(s^{-1})$	$^{\dagger}k'_{1app}(s^{-1})$	$^{\dagger}k_{-1app}(s^{-1})$
3.80	2.7 ± 0.3	2.9 ± 0.3	$(1._5\pm1) \times 10^{-1}$
3.84	3.0 ± 0.3	2.7 ± 0.3	$(1._5\pm1) \times 10^{-1}$
4.02	2.0 ± 0.2	2.0 ± 0.2	$(4\pm3) \times 10^{-2}$
4.04	1.5 ± 0.2	1.7 ± 0.2	$(1\pm0._7) \times 10^{-1}$
4.07	1.7 ± 0.2	1.8 ± 0.2	$(2\pm1._5) \times 10^{-1}$
4.12	1.4 ± 0.1	1.5 ± 0.2	$(1._5\pm1) \times 10^{-2}$
4.35	$(7.8\pm0.8) \times 10^{-1}$	$(9.0\pm0.9) \times 10^{-1}$	$(6\pm5) \times 10^{-2}$
4.44	$(6.9\pm0.7) \times 10^{-1}$	$(7.4\pm0.7) \times 10^{-1}$	$(5\pm3) \times 10^{-2}$
4.52	$(5.1\pm0.5) \times 10^{-1}$	$(6.4\pm0.6) \times 10^{-1}$	$(1\pm0._7) \times 10^{-1}$
4.74	$(3.2\pm0.3) \times 10^{-1}$	$(3.7\pm0.4) \times 10^{-1}$	$(5\pm3) \times 10^{-2}$
4.83	$(2.9\pm0.3) \times 10^{-1}$	$(3.2\pm0.3) \times 10^{-1}$	$(2\pm1._5) \times 10^{-2}$
4.93	$(2.2\pm0.2) \times 10^{-1}$	$(2.2\pm0.2) \times 10^{-1}$	$(2\pm1) \times 10^{-2}$
5.24	$(1.3\pm0.1) \times 10^{-1}$	$(1.3\pm0.1) \times 10^{-1}$	$-$
5.25	$(1.0\pm0.1) \times 10^{-1}$	$(1.1\pm0.1) \times 10^{-1}$	$(9\pm6) \times 10^{-3}$
5.38	$(8.1\pm0.8) \times 10^{-2}$	$(8.7\pm0.9) \times 10^{-2}$	$(8\pm5) \times 10^{-3}$

* From eq 4.

† From eq 3.

NOTE: The values of k_{1app} in $M^{-1}s^{-1}$ are given by $k_{1app} = k'_{1app}/(F)_0$ where $(F)_0 = 0.025$ M. Errors quoted are standard deviations.
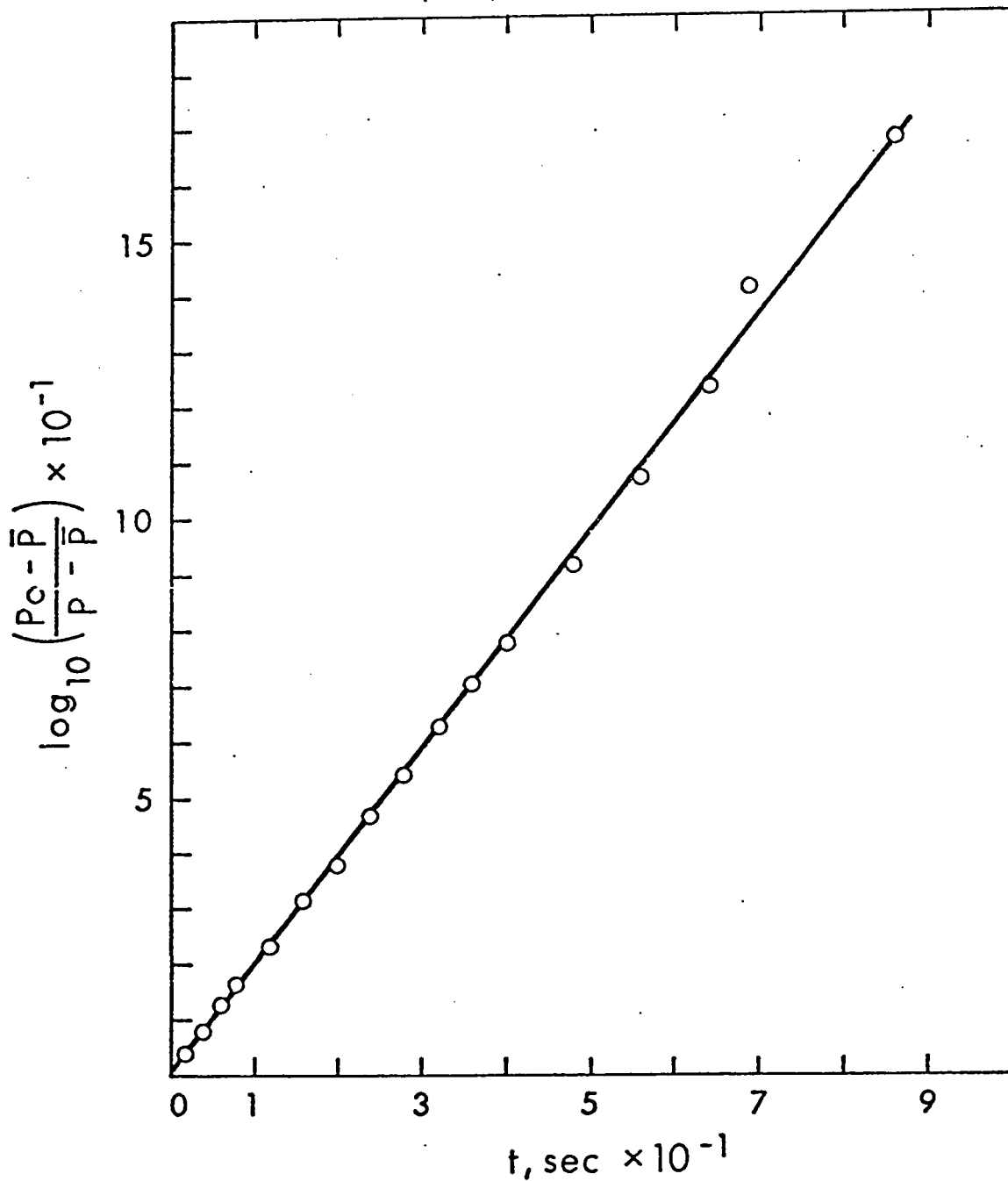
Figure 1. Pseudo-first-order plot for the reaction of LP with F at pH 4.02. The left side of eq 4 is plotted vs time and the slope is equal to $(k'_{1app} + k_{-1app})$ s^{-1}.
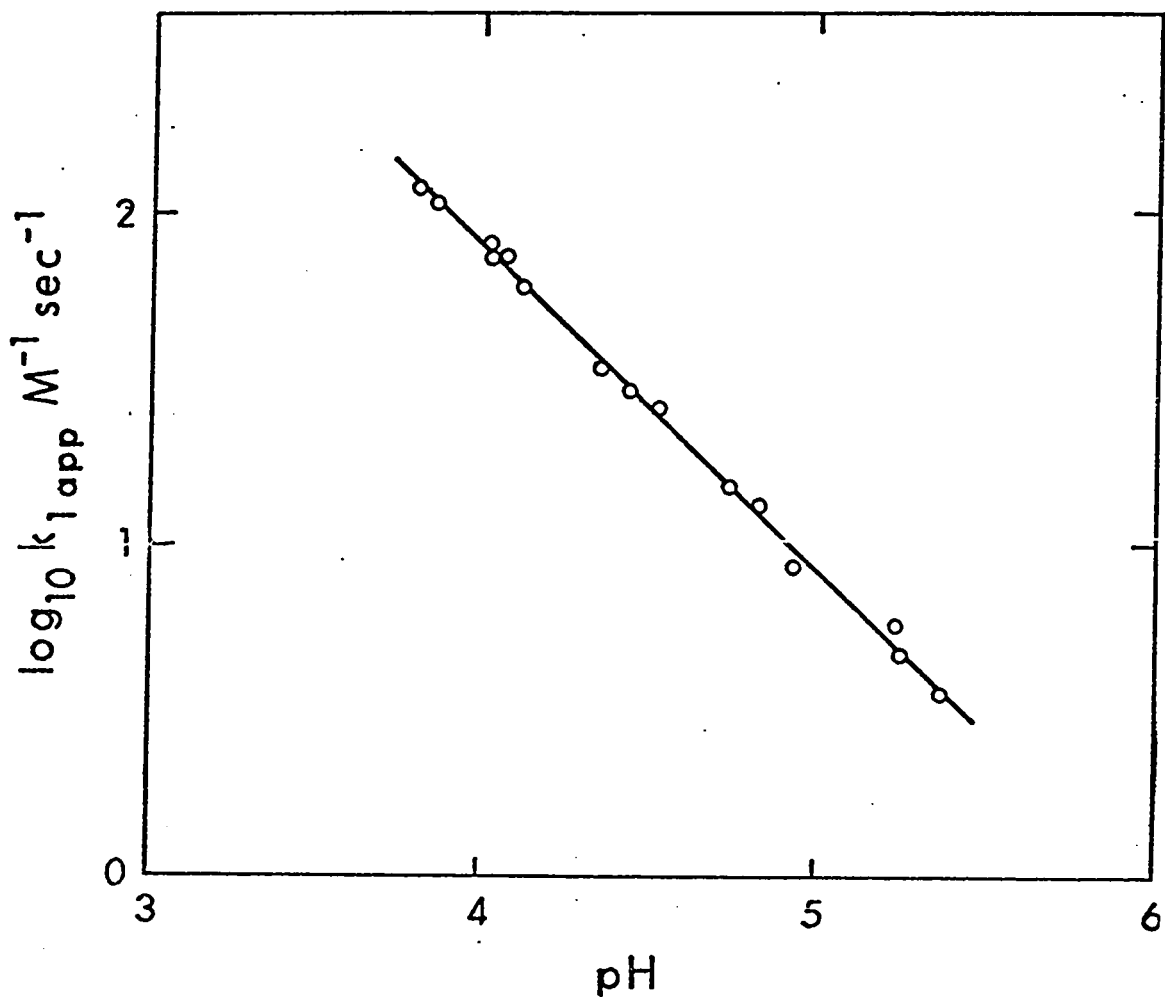
Figure 2. Plot of $\log_{10}k_{1app}$ vs pH for binding of F by LP. The circles are experimental points, and the solid line is calculated from $\log_{10}k_{1app} = \log_{10}[k_2/(1 + K_L/(H^+))]$ with $k_2 = (9.7 \pm 0.4) \times 10^2$ M^{-1} s^{-1}.
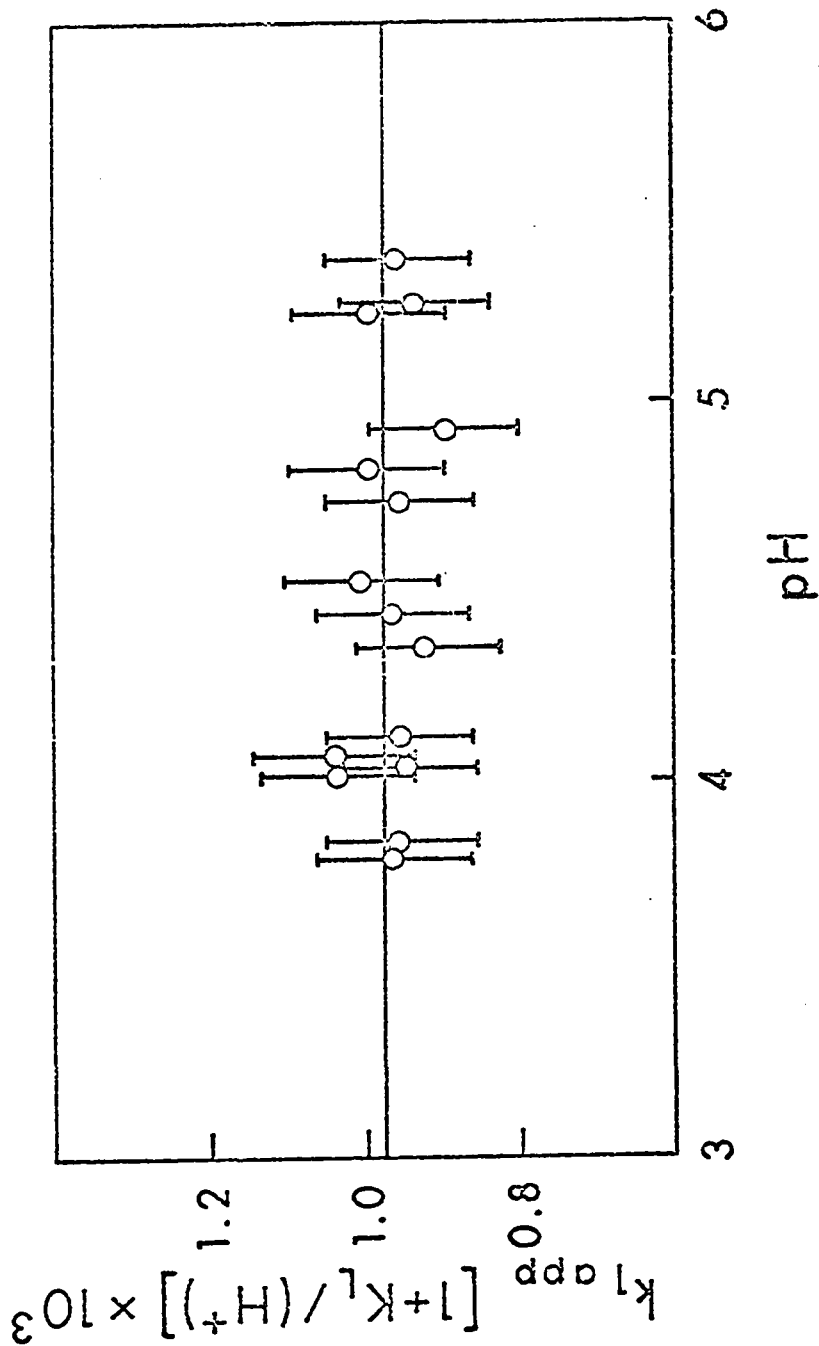
Figure 3. Plot of $k_{1app}(1 + K_L/(H^+))$ vs pH where $K_L = 1.14 \times 10^{-3}$ M. The line of zero slope is consistent with mechanism II. From the intercept, $k = (9.7 \pm 0.4) \times 10^2 \text{ M}^{-1} \text{ s}^{-1}$.

LITERATURE CITED

1. Chance, B., Science, 109, 204 (1949).

2. Theorell, H., and Paul, K. G., Arkiv. Kemi. Minerol. Geol. 18A, 12 (1944).

3. Hultquist, D. E., and Morrison, M. J., Biol. Chem. 238, 2843 (1963).

4. Ellis, W. D., and Dunford, H. B., Biochemistry, 7, 2054 (1968).

5. Morrison, M., and Hultquist, D. E. J., Biol. Chem. 238 2847 (1963).

6. Morrison, M., Hamilton, H. B., and Stotz, E., J. Biol. Chem. 228, 767 (1957).

7. IBM Share Library, Program SDA 3094, modified for use on the University of Alberta IBM 360 computer.

8. Goldsack, D. E., Eberlein, W. S., and Alberty, R. A., J. Biol. Chem. 241, 2653 (1966).

9. Broehne, H. H., and De Vries, T., J. Am. Chem. Soc. 69, 1644 (1947).

10. Davies, C. W., J. Chem. Soc. 2093 (1938).

11. Dunford, H. B., and Alberty, R. A., Biochemistry, 6, 447 (1967).

12. Morrison, M., Rombauts, W. A., and Schroeder, W. A., in "Hemes and Hemoproteins". Chance, B., Estabrook, R. W., and Yonetani, T., Eds., Academic Press, Inc., N.Y. 1966 p 345.

CHAPTER 3

THE KINETICS OF THE BINDING OF

CYANIDE TO FERRIPROTOPORPHYRIN IX

Introduction

The structure of ferriprotoporphyrin IX is shown in
Figure 1. The porphyrin ring provides a tetradentate li-
gand in which the space available for a coordinated metal
ion is 3.7 A[1]. The ring system is not planar but slightly
concave towards the iron atom's sixth coordination position.
The hemin iron occupies a position at least 0.3 A from the
porphyrin plane in all hemin derivatives so far studied[2].
Two of the side chains on the porphyrin structure are pro-
pionic acid groups, which, upon ionization, will contri-
bute two negative charges to the total charge on the ferri-
protoporphyrin IX structure. When the porphyrin ring
binds to four of the six positions on the ferric ion, two
protons dissociate from the pyrrole nitrogen atoms, leaving
a unit residual positive charge. The remaining fifth and
sixth positions of the ferric ion are occupied by solvent
molecules, forming octahedral complexes. The ferric por-
phyrin complex is called hematin when a hydroxyl ion is
associated with it, and hemin when the counter ion is a
halide or an acidic anion. Hematin has a net formal charge
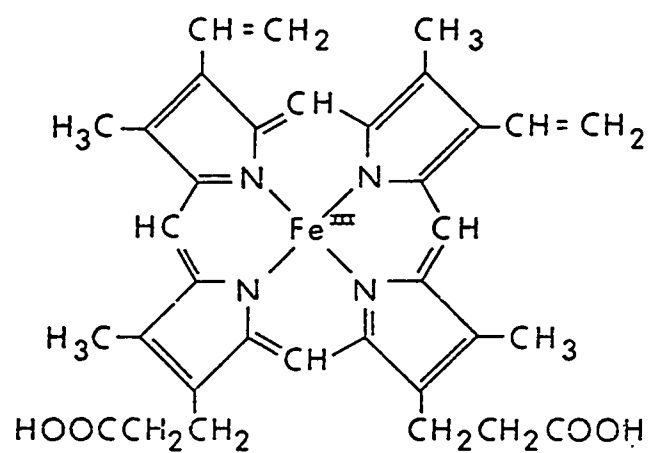
Figure 1.   Ferriprotoporphyrin IX

of -2, whereas hemin, coordinated with neutral solvent
molecules, has an overall formal charge of +1 or -1, de-
pending upon whether the propionic acid residues are
ionized.

Ferriprotoporphyrin IX is the prosthetic group of a
number of hemoproteins, such as catalase, hemoglobin and
horseradish peroxidase.

In alkaline solution hematin tends to dimerize[3,4].
Lemberg and Legge[5] believe that the dimerization in alka-
line aqueous solution is due to electrostatic attraction
between the negative charge of the propionic acid group
of one hematin molecule with the residual positive charge
of the ferric ion of another. Hogness[3] showed that cyanide
ions were able to dissociate the dimers stoichiometrically.
Maehly and Akeson[6] compared hematin-cyanide complexes in
aqueous and in 50% ethanol solutions, at pH 9.2, and the
only spectral change observed was a slight spectral shift
of the Soret band from 425 to 427 mμ, but the intensities
of the bands in 50% ethanol increased by about 13%. At
pH 9.2 they obtained a dissociation constant of 1.6×10^{-3}
for the binding of CN^- to hemin in 50% ethanol and 25 mM
borate buffer. They showed that the extinction coefficient
at 385 mμ changed from 5.3×10^4 M^{-1} cm^{-1} in aqueous solu-
tion to 8.1×10^4 M^{-1} cm^{-1} in 50% ethanol. Dilution of
the alcohol-hemin solution with aqueous buffer yielded a
typical aqueous-hemin spectrum proving the reversibility

of the reaction. It was further shown that the extinction coefficient of hemin solutions in 50% ethanol was independent of hemin concentration from 0.5 to 5.0 x 10^{-6} M at pH 10.0, and from 0.32 to 6.4 x 10^{-6} M at pH 7, Beer's law being obeyed within these limits. From magnetic susceptibility studies Maehly and Akeson found that in both acid and alkali ethanol solutions, hemin had approximately five unpaired electrons.

Hasinoff et al[7] studied the kinetics of imidazole binding to hemin in 44.5 weight percent ethanol with a temperature jump apparatus. In all their experiments only one relaxation was observed. The lack of any spectroscopically observable intermediate led them to apply the steady state treatment in the evaluation of the rate data.

The following study was prompted in the hope that a study of the binding of a different ligand, namely cyanide, to hemin, over a wide pH range, would add further insight into the mechanism of hemin-ligand binding.

Experimental

Hemin of White Label grade (Eastman Organic Chemicals) and all other inorganic chemicals of reagent grade were used without further purification.

The solvent, 44.5 weight percent ethanol, was prepared from doubly distilled water and reagent grade 95% ethanol. A stock hemin solution was prepared by dissolving hemin in 0.1M NaOH and diluting until the stock was 1.0×10^{-3} M in hemin and 1.0×10^{-2}M NaOH. This stock was stored in a refrigerator, from which fresh preparations were made up every few days. Fresh potassium cyanide solutions were made up for each day's experiments.

By using the method of Bates[8] it was possible to establish an operational pH scale. A glass electrode (Beckman Long Thin Probe Combination #38183) was stored in a solution of composition, pH and ionic strength similar to that used in the experiments and was standardized with triethanol-ammonium chloride-triethanolamine buffer of pH 7.05. A Beckman expanded-scale pH meter in conjunction with this electrode was used for pH measurements.

The kinetic measurements were made on a stopped-flow apparatus[9] constructed in this laboratory and thermostated at 25°.

Solutions of hemin and cyanide were each made to the desired pH using buffer of ionic strength equal to 0.01 and sufficient potassium nitrate so that the total ionic

strength was 0.11. The buffer systems employed were: phosphate between pH's 6 and 8, and borate between pH's 8 and 10.

The concentration of hemin between pH's 6 and 8.4 was 1.6×10^{-6} M, and between pH's 8.5 to 10 was 3.2×10^{-6} M. The maximum cyanide concentration used for each kinetic experiment was such that the maximum difference in absorbance at 426 mμ between hemin and the hemin-cyanide complex was never more than 0.05. This meant that the voltage displacement observed on the oscilloscope can be taken to be proportional to absorbance, with a maximum error of 5%[10].

All of the kinetic experiments were observed spectrophotometrically at 426 mμ with the results displayed on an oscilloscope. Photographs of the oscilloscope traces were taken and values of the voltages at a given time were read from them using a photographic enlarger. In general at least three experiments were performed on any one solution and the average of the relaxation time constants, τ, (see page 76) was taken. For each series of experiments at a given pH generally about six different cyanide concentrations were used, which varied by about a factor of six.

Dissociation constants for the binding of cyanide to hemin were determined spectrophotometrically at 400 and 426 mμ with a Beckman spectrophotometer at 25°. This was done by titrating a saturated hemin-cyanide solution

into a hemin solution, all at an ionic strength of 0.11 μ (as described for kinetic experiments) and so avoiding dilution effects. The influence of pH on hemin in 44.5 weight percent ethanol was obtained by titrating a solution of 2.8 x 10^{-6} M hemin with 0.1M HNO_3 and 0.1M KOH. The change in pH was monitored at 400 mμ and 25°. The ionic strength was 0.11 made up with KNO_3. To maintain some buffering effect over the entire pH region, the following buffers were used: acetate between pH 3 - 6, phosphate between pH 6 - 8, and borate between pH 8 - 11. Their concentrations were 4 x 10^{-4} M.

The dissociation constant of HCN in 44.5 weight percent ethanol was obtained by titrating a solution of 5 x 10^{-3} M potassium cyanide with 0.4 M HCl at 25°. The ionic strength was made up to 0.11 with KNO_3.

Titration curves of hemin-cyanide complexes as a function of pH in 44.5% weight ethanol were obtained by titrating these solutions with 0.5 M potassium hydroxide or 1.0 M nitric acid and the respective pH changes were monitored at 400 mμ at 25°. Concentrated solutions of KOH and HNO_3 were used so that when very small quantities were titrated, substantial pH changes occurred but with very small dilution effect so that absorbance is essentially unchanged. In the four titration experiments the concentration of hemin was 1.6 x 10^{-6} M and the cyanide in each was 1.0 x 10^{-4} M, 1 x 10^{-3} M, 1 x 10^{-2} M and 0.14 M respectively. The total ionic strength was kept constant

at 0.11 made up where necessary with potassium nitrate.
An exception were the results obtained at cyanide concentration of 0.14 M. All the experimental solutions contained 2×10^{-4} M acetate buffer for some buffering at low pH.
The potassium cyanide buffered sufficiently at high pH.

Results

At constant pH solutions of hemin in 44.5 weight percent ethanol were found to obey Beer's law as shown in Figure 2 for pH 7. This provides evidence that hemin is in the monomeric form[6].

Hasinoff[7] has shown that there are no significant spectral changes of hemin from pH 8 to 3.6 M NaOH. However, from pH 8 to 4.5 significant spectral changes were observed at 400 mμ where the maximum of the Soret band occurs. The pH titration curve of hemin is shown in Figure 3 with an inflection point at about 6.7 which is in excellent agreement with a previous determination by Hasinoff[7].

The pH titration curve of HCN in 44.5 weight percent ethanol is shown in Figure 4. The pK obtained from the inflection point is 9.5.

When cyanide is added to hemin solutions, large changes in the spectrum occur. Between pH's 6.25 and 8, as shown in Figure 5 for pH 6.7, there are no isosbestic points, indicating the presence of three or more absorbing species such as hemin, monocyano - and dicyano hemin. At pH's higher than pH 8 there is a well defined isosbestic point at 412 mμ as shown in Figure 6 for pH 9.5. This indicates the presence of only two absorbing species in solution (see below) such as free hemin and dicyano hemin. Between pH's 6.5 and 10, the Soret maximum of the hemin-cyanide
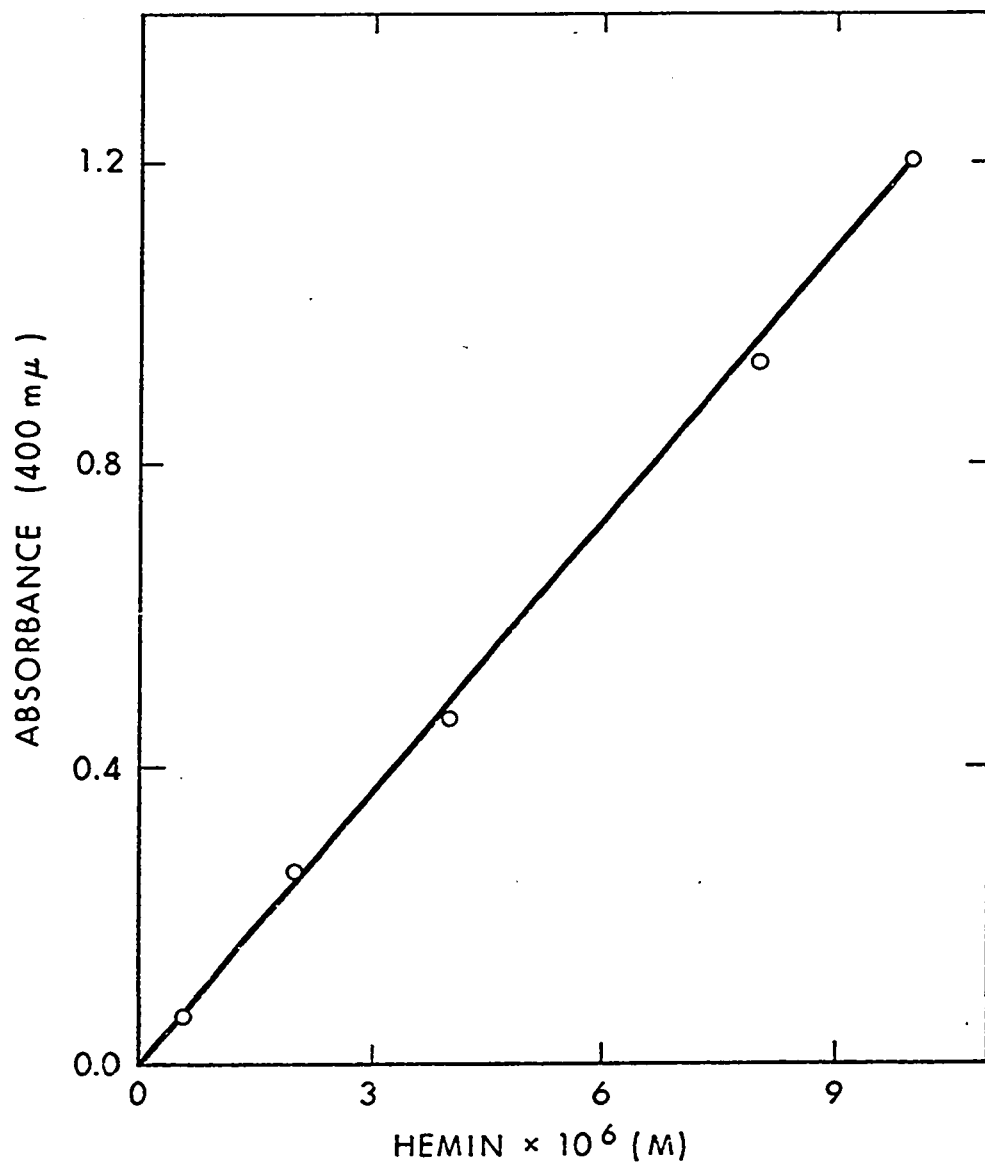
Figure 2. Plot of absorbance at 400 mμ vs concentration of hemin in 44.5 weight % ethanol at pH 7 showing that Beer's law is obeyed between hemin concentrations of 5 x 10^{-7} and 1 x 10^{-5} M.
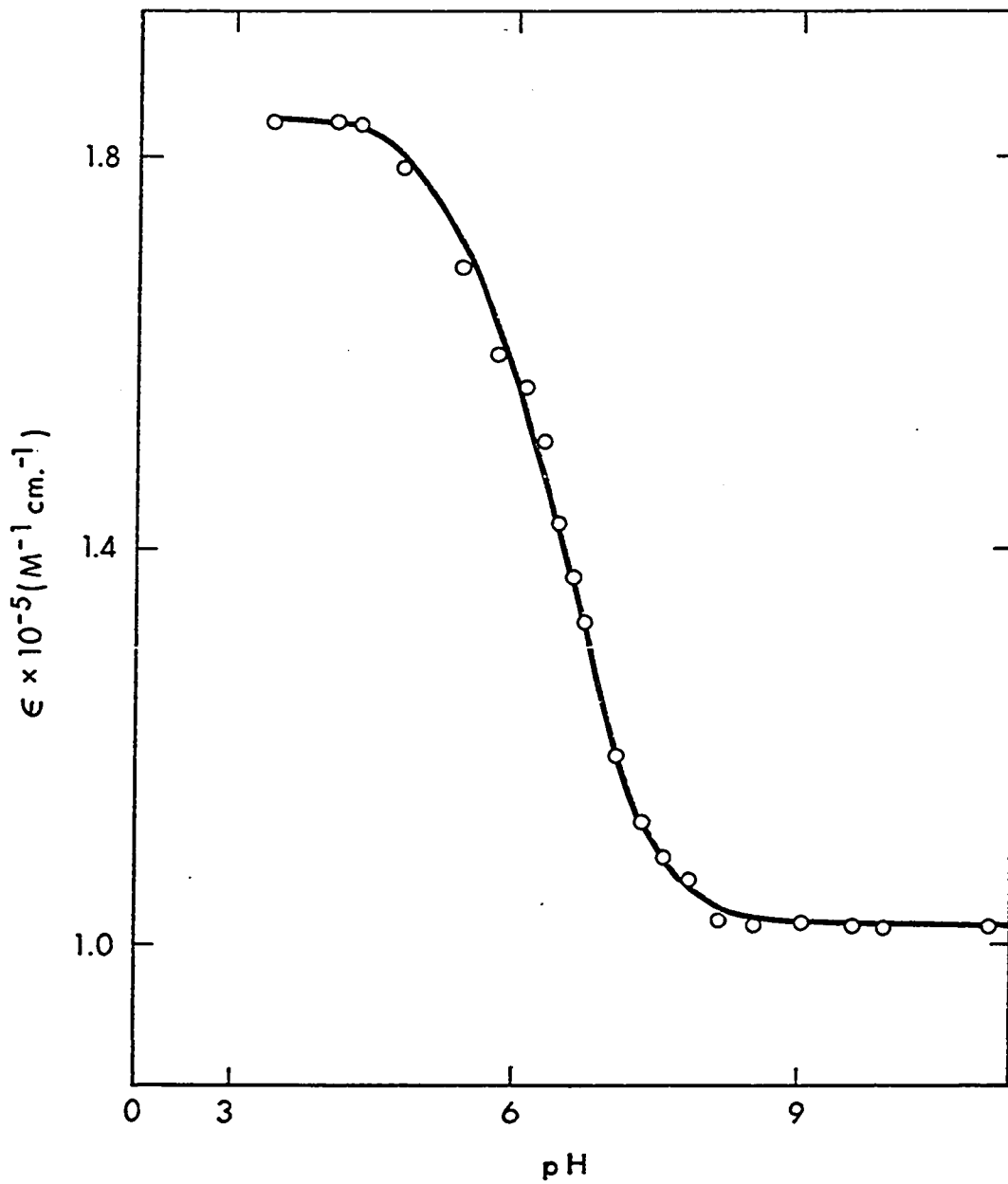
Figure 3. Influence of pH on the molar absorptivities, $\varepsilon(M^{-1}\ cm^{-1})$, of hemin at 400 mμ at 25° and μ = 0.11.
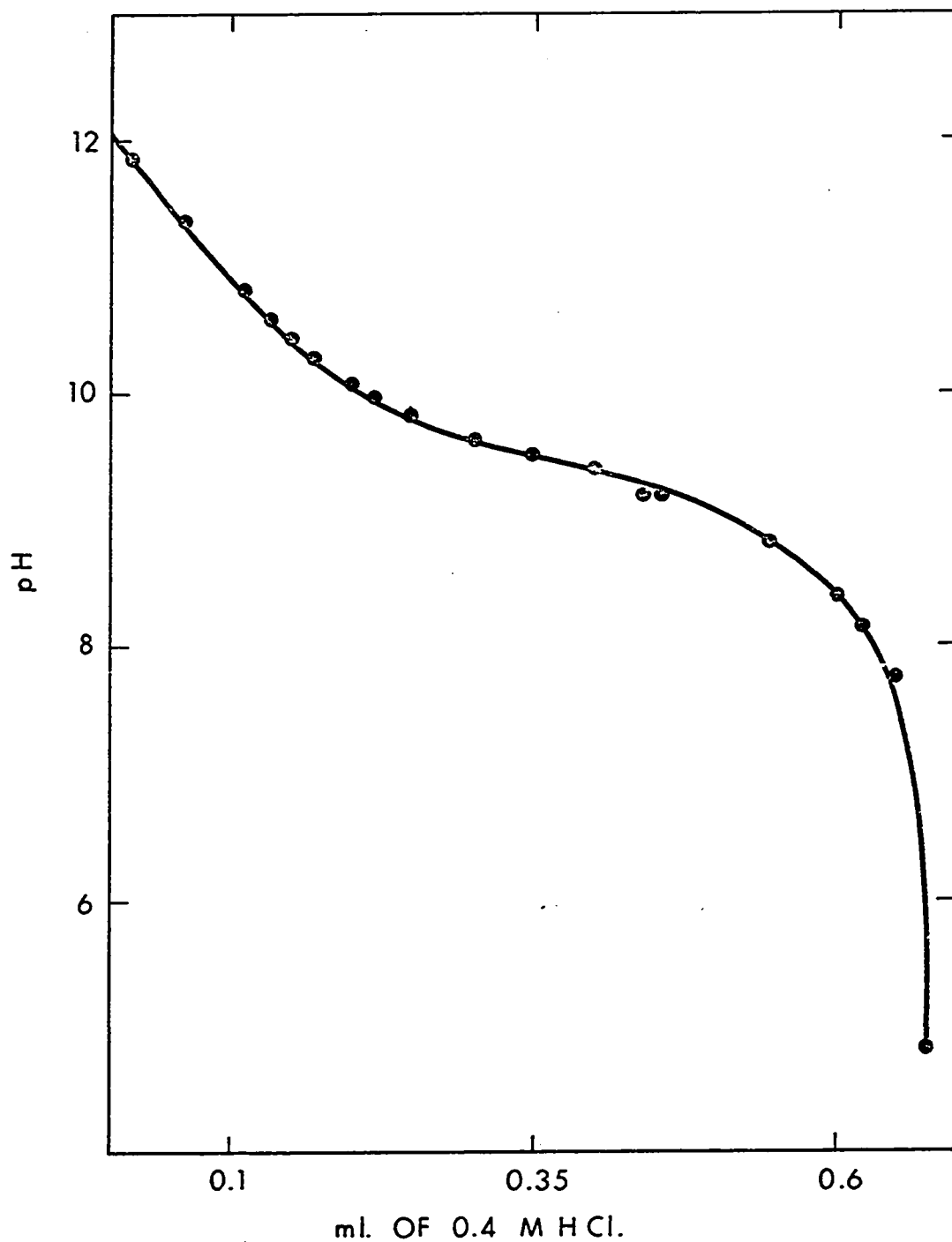
Figure 4. pH titration curve of 5×10^{-3} M KCN with 0.4 M HCl at 25° and $\mu = 0.11$.
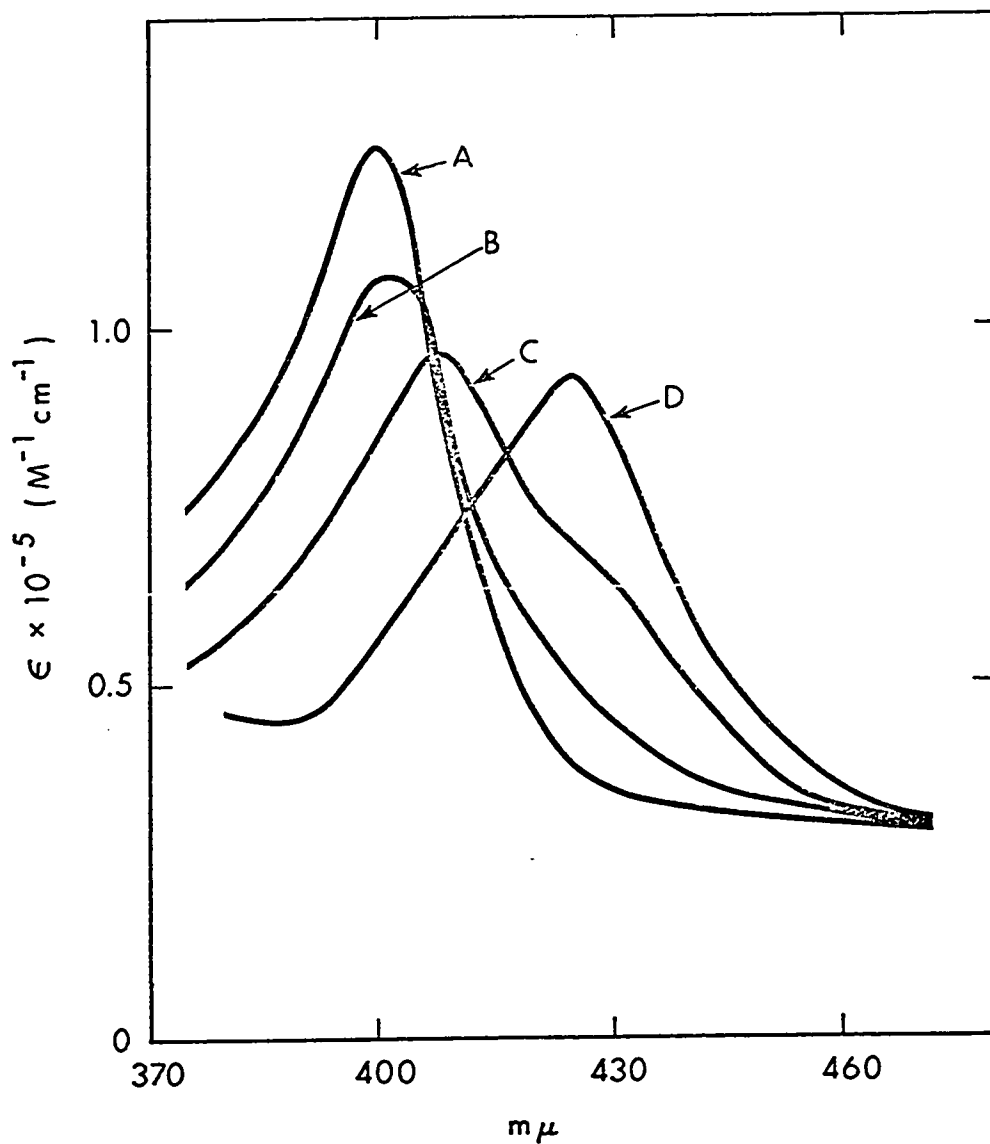
Figure 5. Plot of molar absorptivities, $\varepsilon(M^{-1}cm^{-1})$ vs wavelength. Concentration of hemin was 1.6×10^{-6} M and concentration of cyanide for curves A, B, C and D were 0, 1.6×10^{-3}, 6.5×10^{-3} and 0.2 M. The pH was 6.7 and ionic strength 0.11. Curve D is the spectrum of fully complexed dicyanohemin.
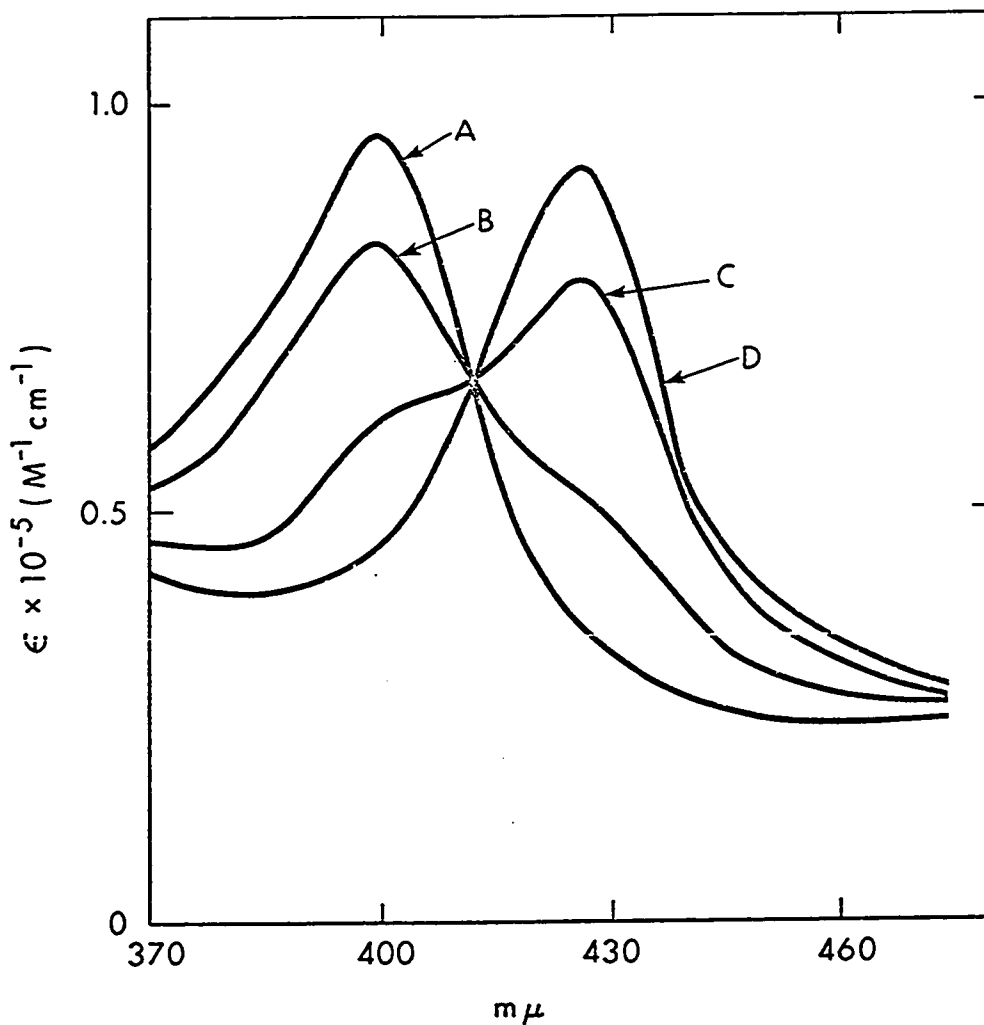
Figure 6. Plot of molar absorptivities $\varepsilon(M^{-1}cm^{-1})$ vs wavelength. Concentration of hemin was 4.0×10^{-6} M and concentration of cyanide for curves A, B, C and D were 0, 1.5 $\times 10^{-4}$, 8.0×10^{-4} and 5×10^{-2} M. The pH was 9.5 and ionic strength 0.11. Curve D is the spectrum of fully complexed dicyanohemin.

complex occurs at 426 mμ with a molar absorptivity of 9.2 x 10^4 M^{-1} cm^{-1}. In Figure 7 the effect of changing the pH of hemin-cyanide solutions, monitored at 400 mμ, is shown. The solution for each experiment contained 1.6 x 10^{-6} M hemin and the cyanide in each varied as follows: 1 x 10^{-4}, 1 x 10^{-3}, 1 x 10^{-2} and 0.14 M. At 1 x 10^{-3} M cyanide, three distinct though asymmetrical inflection points were obtained, corresponding roughly to pK's of 6.7, 8.5 and 10.5. The latter two inflection points disappear at higher cyanide concentration, with a shift of the remaining one to a lower value.

Titration curves of hemin with cyanide at pH's 7.0 and 9.5, shown in Figure 8, are somewhat asymmetrical about the single inflection point. If there were only two absorbing species in solution (see Appendix 1) then plots of

$$\frac{\Delta A}{[CN]_0^2} \quad vs \quad \Delta A \qquad \text{(VIII)}$$

should be linear with the slope giving the absolute value of the overall association constant. As shown in Figure 9, these plots are not linear except at high pH for high cyanide concentration where there is a tendency for linearity.

The equilibrium and kinetic behavior of the hemin-cyanide system at any given pH is consistent with three absorbing species in solution, as shown in the following two consecutive equations:
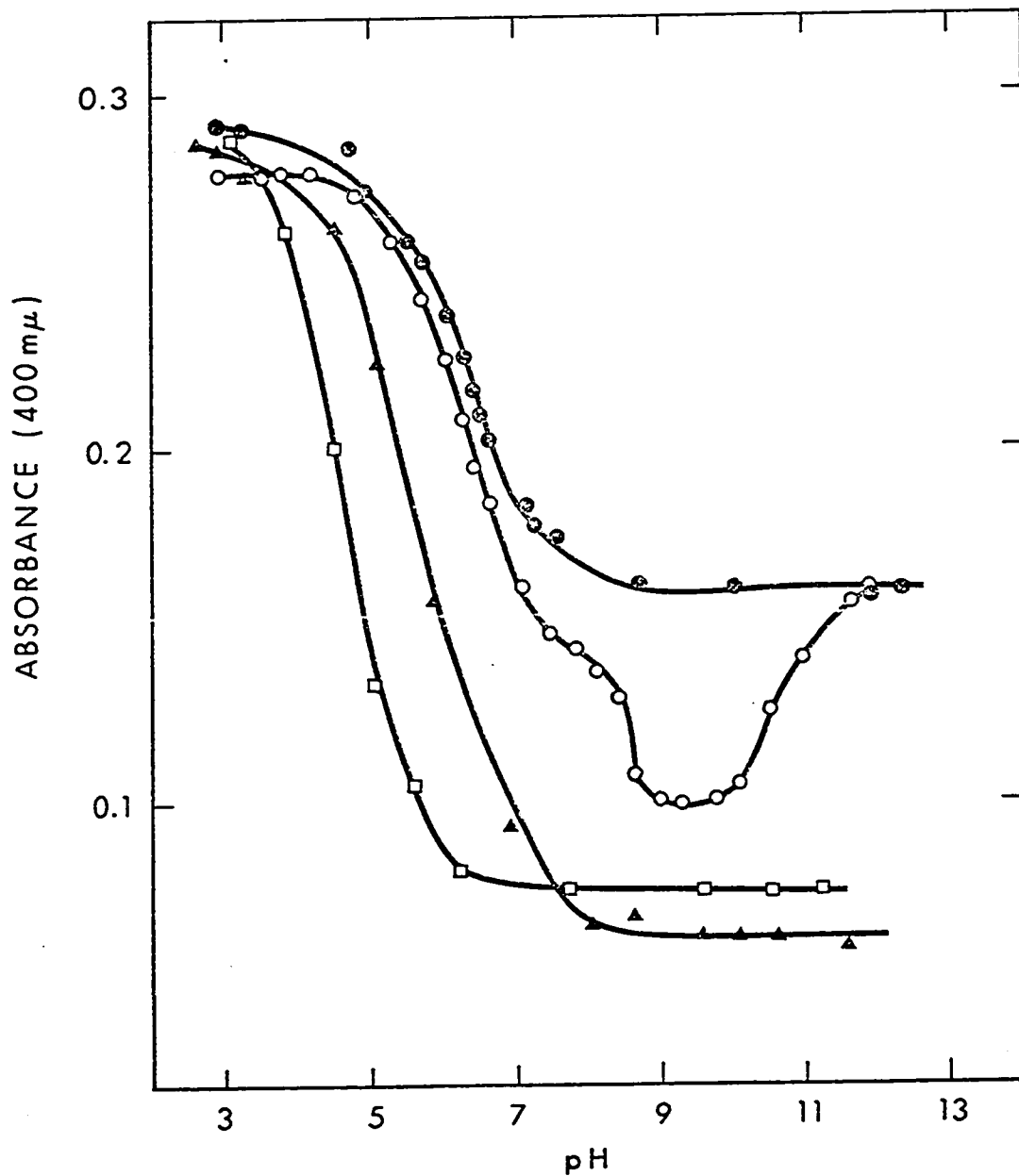
Figure 7. Plot of absorbance at 400 mμ vs pH for hemin-cyanide complex. The concentration of hemin was 1.6 x 10^{-6} M and concentration of cyanide for curves (●-●-●-●), (o-o-o-o), (▲-▲-▲-▲) and (□-□-□-□) were 1 x 10^{-4}, 1 x 10^{-3}, 1 x 10^{-2} and 0.14 M.
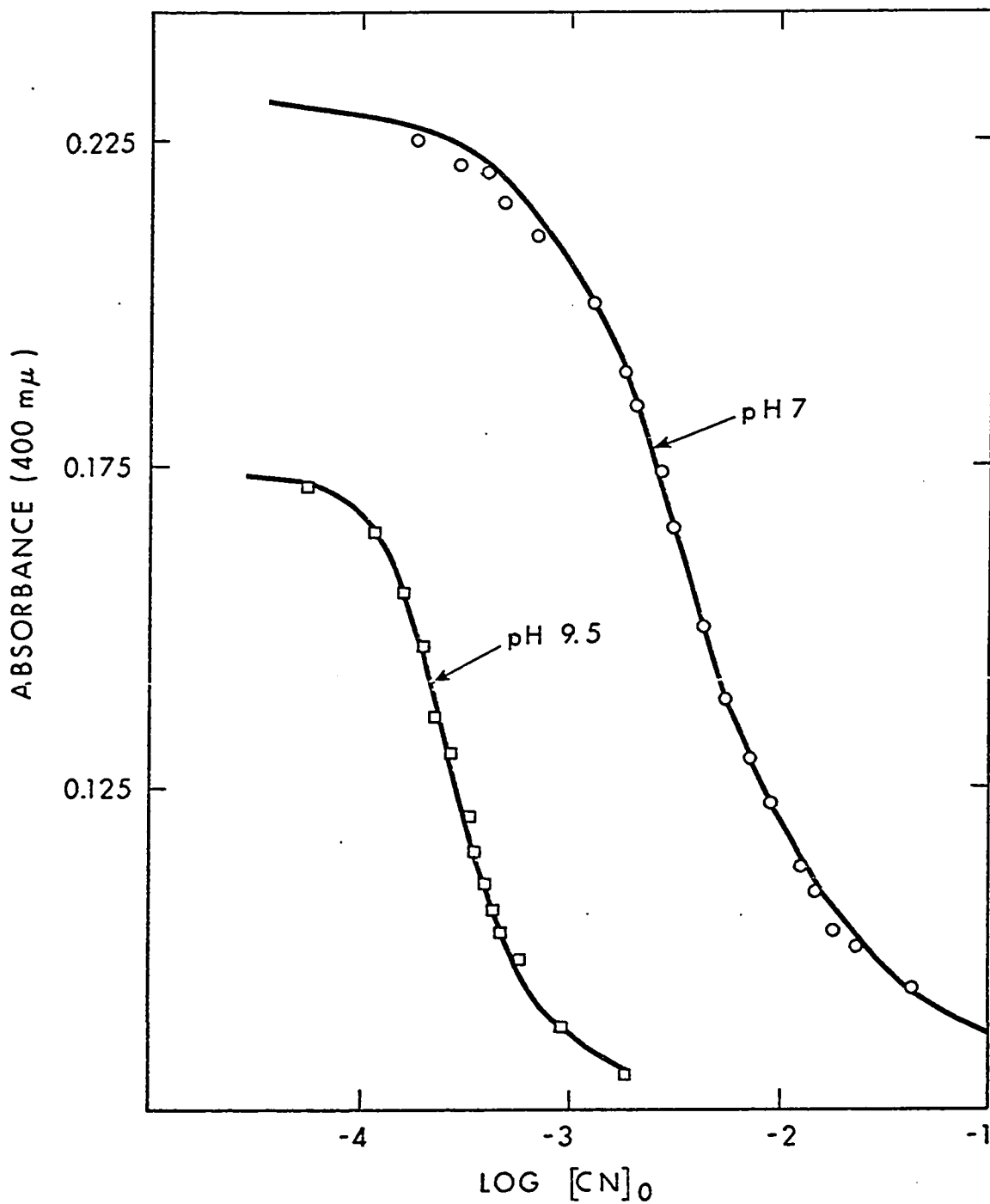
Figure 8. Typical titration curves of hemin with cyanide at 25° and μ = 0.11 at pH 7 and 9.5.
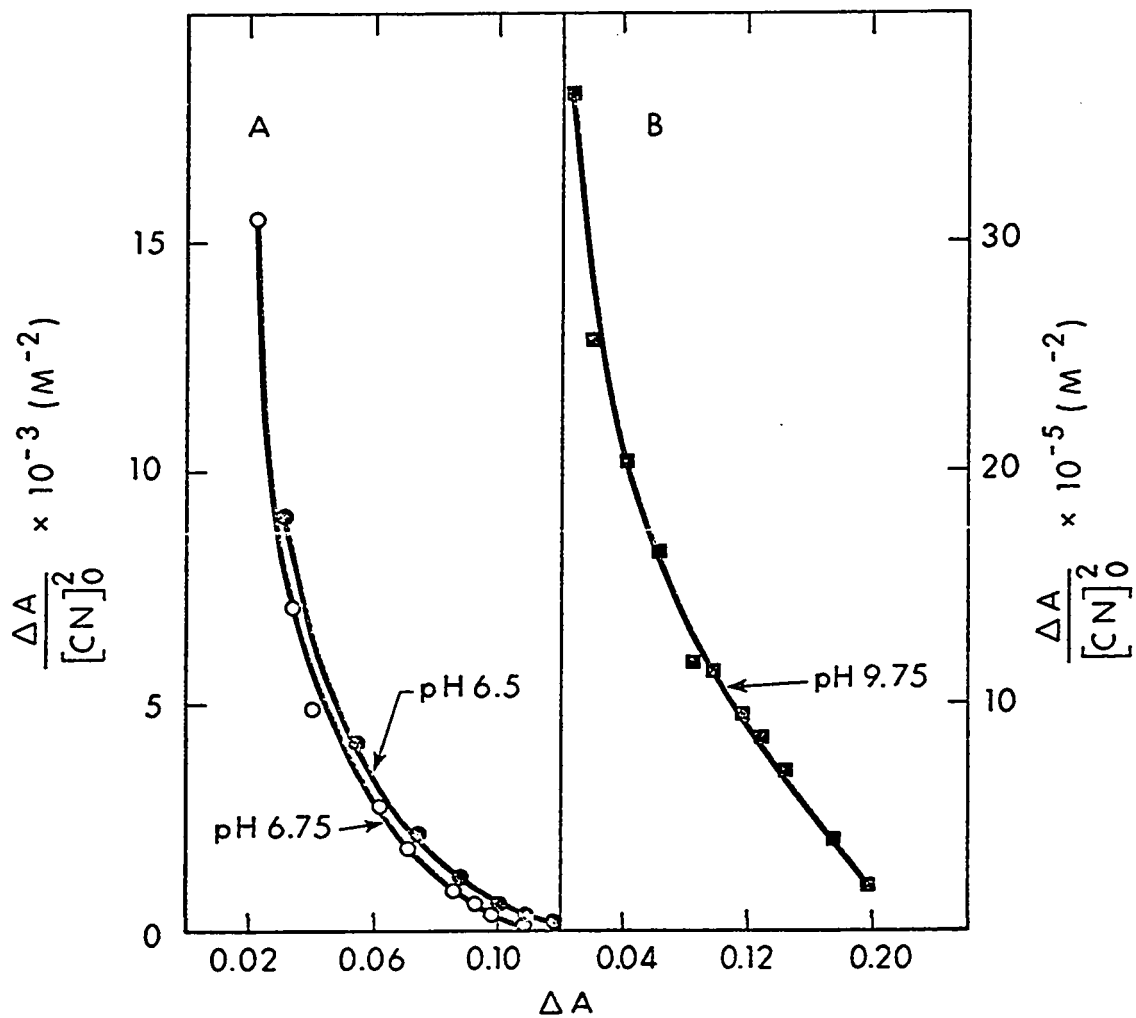
Figure 9. Test for the presence of two absorbing species in solution predicting a steady state process. If this test was valid then plots of $\Delta A/[CN]_0^2$ vs ΔA would be linear.

$$M + CN \underset{k_{-1app}}{\overset{k_{1app}}{\rightleftarrows}} MCN \qquad (1)$$

$$MCN + CN \underset{k_{-2app}}{\overset{k_{2app}}{\rightleftarrows}} MCN_2 \qquad (2)$$
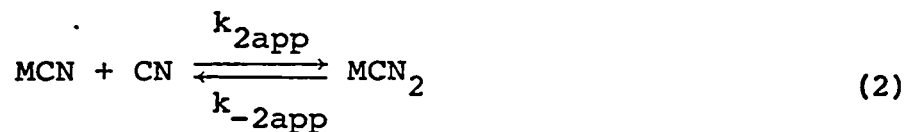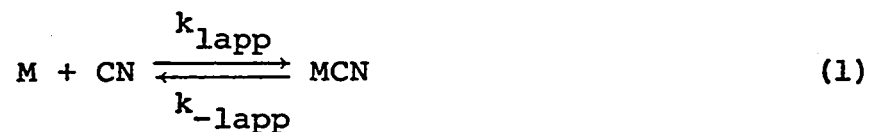
(where M, MCN, and MCN_2 represent all ionizable forms of free hemin, monocyanocomplex and dicyanocomplex and CN all forms of unbound cyanide; k_{1app} and k_{2app} are apparent second order association rate constants and k_{-1app} and k_{-2app} are apparent first order dissociation rate constants.) The dissociation constants for eq 1 and 2 are:

$$K_1 = \frac{[\overline{M}] [\overline{CN}]}{[\overline{MCN}]} \qquad (3)$$

$$K_2 = \frac{[\overline{MCN}] [\overline{CN}]}{[\overline{MCN_2}]} \qquad (4)$$

where the bars indicate equilibrium concentrations. The overall dissociation constant is:

$$K_\beta = K_1 K_2 = \frac{[\overline{M}] [\overline{CN}]^2}{[\overline{MCN_2}]} \qquad (5)$$

With the aid of a non-linear least squares program[11], best-fit values for K_1 and K_2 were obtained from the following eq (Appendix 2):

$$A = [M]_0 \times \left(\cfrac{1}{\cfrac{K_1}{[CN]} + \cfrac{[CN]}{K_2} + 1}\right) \times \left(\frac{\epsilon_1 K_1}{[CN]} + \epsilon_2 + \frac{\epsilon_3 [CN]}{K_2}\right) \quad \text{(XVI)}$$

(where A = absorbance of the hemin solution titrated with cyanide; $[M]_0$ = concentration of total hemin in solution; ϵ_1 is the extinction coefficient of hemin (M) at a given pH (Figure 3) and $\epsilon_3 = 9.2 \times 10^4$ M^{-1} cm^{-1}; ϵ_2 is unknown and used as an adjustable parameter.) Values for K_1 and K_2 were obtained from data at 426 mμ and 400 mμ, based on the assumption of both total cyanide[*] binding and cyanide ion binding to hemin. These values are given in Tables I and II. The values obtained for K_1 and K_2 at these two wave lengths do not correspond exactly, which is probably due to the uncertainty in obtaining dissociation constants with this method.

For the kinetic experiments between pH's 6.2 and 8.5, two consecutive reactions were observed as shown in Figure 10, which were considered consistent with eqs 1 and 2 respectively. These two reactions were considered essentially uncoupled as reaction one was very much faster than reaction two (Table 3). Since the concentration of cyanide was generally very much larger than hemin, both eqs 1 and 2 were considered to obey pseudo-first-order kinetics. Therefore, the simplified differential rate equation for eq 1 is

---

[*] Total cyanide means (CN^- + HCN)

TABLE I

Dissociation Constants Measured at 426 and 400 mμ for Total Cyanide Binding to Hemin in 44.5 Weight Percent Ethanol

	Measured at 426 mμ			Measured at 400 mμ		
pH	K_1 $\times 10^3$ M	K_2 $\times 10^3$ M	K_β $\times 10^5$ M^2	K_1 $\times 10^3$ M	K_2 $\times 10^3$ M	K_β $\times 10^5$ M^2
6.50				6.70	5.47	3.66
6.75	5.63	13.80	7.76	6.50	8.37	5.44
7.00	3.60	11.70	4.20	2.79	6.90	1.94
7.25	2.80	79.60	22.70	2.80	22.00	6.1
7.50	2.50	2.39	0.61	1.90	13.80	2.64
7.75	1.37	0.86	0.12	1.47	5.90	0.86
8.00	1.80	0.59	0.11	2.30	0.30	0.06
8.50	14.40	0.03	0.040			
9.25	2.58	0.18	0.050			
9.50	5.79	0.010	0.0057	1.65	0.040	0.0063
9.75	0.42	0.14	0.0060			
10.00	0.94	0.07	0.0070			

TABLE II

Dissociation Constants Measured at 426 mμ and 400 mμ for Cyanide Ion Binding to Hemin in 44.5 Weight Percent Ethanol

pH	Measured at 426 mμ			Measured at 400 mμ		
	K_1 × 10⁵ M	K_2 × 10⁵ M	K_β × 10⁸ M²	K_1 × 10⁵ M	K_2 × 10⁵ M	K_β × 10¹⁰ M²
7.00	1.78	4.50	0.08			
7.25	1.59	44.60	0.70	1.70	1.41	2.40
7.50	2.60	4.80	0.120	1.90	1.15	2.17
7.75	2.56	1.89	0.05	4.50	1.43	6.40
8.00	5.80	1.80	0.10	3.33	1.62	5.40
8.50	23.80	112.00	26.60			
9.25	98.40	6.79	6.66			
9.50	95.20	48.30	45.90	83.00	1.89	156.00
9.75	32.90	71.00	23.30			
10.00	56.00	6.15	3.44			
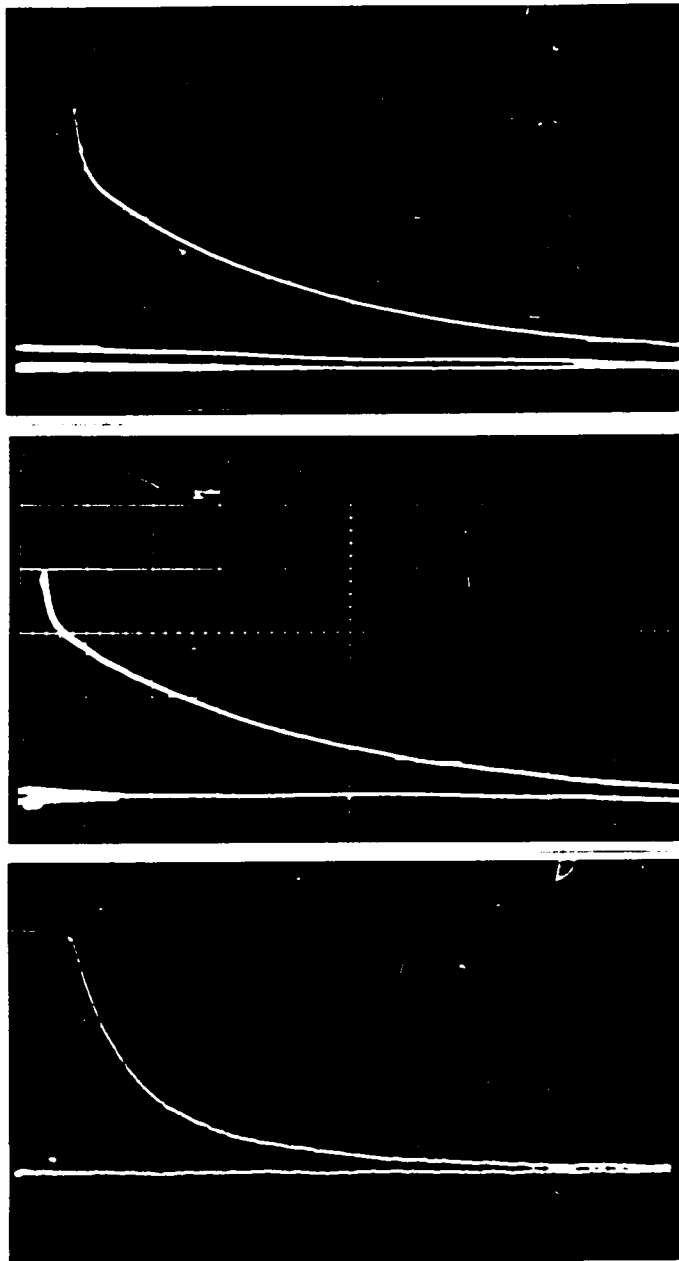
Figure 10. Typical oscilloscope traces of voltage vs time
for the reaction between hemin and cyanide in 44.5 weight %
ethanol. For each trace the horizontal scale is 2 sec/cm
and the vertical scale is 100 mV/cm. The monochromator set-
ting was 426 mμ. Top trace: pH 7.65; concentration of he-
min 1.6 x 10^{-6} M and of cyanide 8.0 x 10^{-4} M. Middle trace:
pH 7.9; concentration of hemin 1.6 x 10^{-6} M and of cyanide
8.0 x 10^{-4} M. Bottom trace: pH 8.5; concentration of he-
min 1.02 x 10^{-6} M and of cyanide 2.4 x 10^{-3} M.
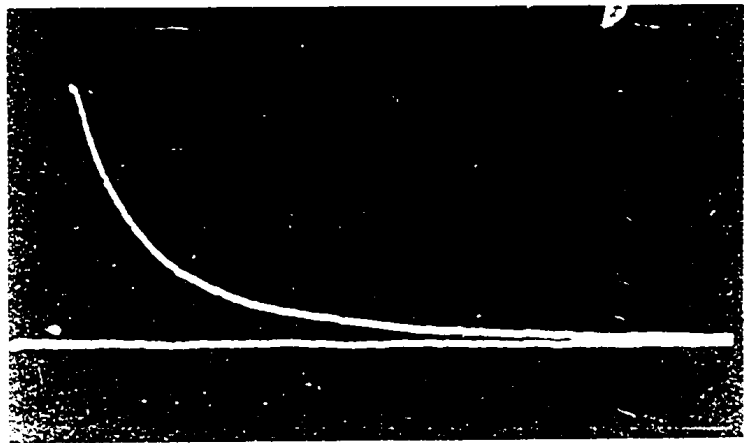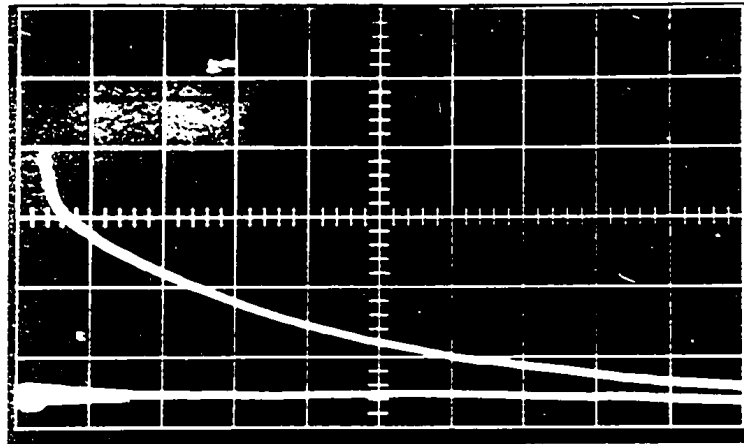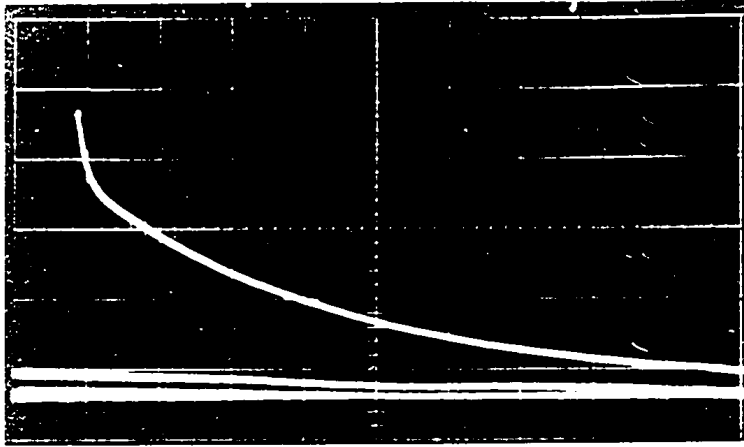
$$-\frac{d(M)}{dt} = k'_{1app}(M) - k_{-1app}(MCN) \tag{6}$$

where k'_{1app} (pseudo-first-order rate constant) $= k_{1app}[CN]_0$

This equation can be integrated to give

$$(V' - V'_\infty) = (V'_0 - V'_\infty) \, e^{-(k'_{1app} + k_{-1app}) \, t} \tag{7}$$

(where V' is the voltage proportional to the concentration

of MCN at any time t; V'_∞ is the voltage proportional to

the equilibrium concentration of MCN and V'_0 is proportional

to the concentration of hemin at time = 0.)

For eq 2 the differential equation is:

$$\frac{d(MCN_2)}{dt} = k'_{2app}(MCN) - k_{-2app}(MCN_2) \tag{8}$$

(where k'_{2app} is the pseudo-first-order rate constant

equal to $k_{2app}(CN)_0$.) Since eq 1 is considered to be in a

rapid equilibrium, eq 8 can be written as:

$$\frac{d(MCN_2)}{dt} = k'_{2app}(\overline{MCN}) - k_{-2app}(MCN_2) \tag{9}$$

By multiplying and dividing eq 9 by $\overline{M} + \overline{MCN}$ and dividing

by $\overline{MCN}$ the following equation is obtained:

$$\frac{d(MCN_2)}{dt} = \frac{k'_{2app}(\overline{M} + \overline{MCN})}{\dfrac{(\overline{M})}{(\overline{MCN})} + 1} - k_{-2app}(MCN_2) \tag{10}$$

By substituting eq 3 into 10 and rearranging eq 11 is obtained:

$$\frac{d(MCN_2)}{dt} = \frac{k'_{2app}(CN)_0(\overline{M} + \overline{MCN})}{(CN)_0 + K_1} - k_{-2app}(MCN_2) \tag{11}$$

From conservation relations

$$M_0 = \overline{M} + \overline{MCN} + MCN_2 \tag{12}$$

and by introducing eq 12 into 11 and rearranging eq 13 is obtained.

$$\frac{d(MCN_2)}{dt} = \frac{k'_{2app}(CN)_0 M_0}{(CN)_0 + K_1} - MCN_2\left(\frac{k'_{2app}(CN)_0}{(CN)_0 + K_1} + k_{-2app}\right) \tag{13}$$

Similarly to eq 6 this equation can be integrated to give

$$(V - V_\infty) = (V_0 - V_\infty)\, e^{-\left(\frac{k'_{2app}(CN)_0}{(CN)_0 + K_1} + k_{-2app}\right)t} \tag{14}$$

where V is proportional to the concentration of MCN_2 at any time t; V_∞ is the voltage proportional to the equilibrium concentration of MCN_2 and V_0 is proportional to the equilibrium concentration of MCN. Thus the two terms in brackets contained in exponents in eqs 7 and 14 are equivalent to apparent first order rate constants and can be considered analogous to the reciprocals of two relaxation times[12],

where $\frac{1}{\tau} = (k_{1app}(CN)_0 + k_{-1app}) \tag{15}$

$$\text{and } \frac{1}{\tau_2} = \frac{k_{2app}(CN)_0^2}{(CN)_0 + K_1} + k_{-2app} \tag{16}$$

In order to separate out the two relaxation times, plots of $\log\Delta V$ vs time were made where ΔV is equal to $(V - V_\infty)$. The slope of the line through the curve at long time[14,15] $(t\to\infty)$ is equal to $\frac{1}{\tau_2}$ (Appendix 3), and by extrapolating to zero time, ΔV_0 is subtracted from the initial part of the trace, corresponding to the first relaxation and the slope of this new time yields

$$\frac{1}{\tau_1} = (k_{1app}(CN)_0 + k_{-1app}) \tag{15}$$

τ_1 and τ_2 are the times taken for the concentration of reactant to be reduced to C_0/e, where C_0 is the concentration at time equal to zero, and $e = 2.718...$ The log plots and resolution into two straight lines are shown in Figure 11. The relaxation times so obtained are probably accurate to within 25%. In Table 3 the τ values obtained at 22 pH's are given.

By making plots of

$$\frac{1}{\tau_1} \text{ vs } (CN)_0 \tag{16}$$

and

$$\frac{1}{\tau_2} \text{ vs } \frac{(CN)_0^2}{(CN)_0 + K_1} \tag{17}$$

reasonably good straight lines were obtained (Figures 12 and 13). The slopes and intercepts of these two plots yield k_{1app}, k_{-1app}, k_{2app} and k_{-2app}. These values are listed in Table 4.

Between pH's 8.7 to 10.0, only a single relaxation time was observed, which can be considered due to the two relaxation times approaching each other. The evaluation of the eigenvalues for a two relaxation process[13] involves finally the solution of a quadratic equation:

$$\frac{1}{\tau} = 1/2 (p \pm q) \qquad (18)$$

where

$$p = [(k_{1app} + k_{2app})(CN)_0 + k_{-1app} + k_{-2app}] \qquad (19)$$

and

$$q = [(p^2 - 4(k_{1app}k_{2app}(CN)_0^2 + k_{1app}k_{-2app}(CN)_0 + \qquad (20)$$
$$k_{-1app}k_{-2app})]^{1/2}$$

Since only one τ value is obtainable and it is assumed that τ_1 is equal to τ_2, then it can be shown that $q = 0$ and therefore;

$$\frac{1}{\tau} = 1/2p \qquad (21)$$

By plotting $2/\tau$ vs $(CN)_0$, the slope and intercept yield $(k_{1app} + k_{2app})$ and $(k_{-1app} + k_{-2app})$ respectively, as

shown in Figure 14. These values are listed in Table IV. The dissociation constants obtained from kinetic data are listed in Table V.

If the single relaxation process observed from pH's 8.7 to 10.0 is due to a steady state in that $\overline{MCN}$ is vanishingly small, then

$$\frac{d(\overline{MCN})}{dt} = 0 \tag{22}$$

It can then be shown[7] that

$$\left(1 + \frac{(CN)_0^2}{K_\beta}\right)\tau = \frac{k_{2app}(CN)_0}{k_{-1app}\,k_{-2app}} + \frac{1}{k_{-2app}} \tag{23}$$

The K_β values are taken from Table 1 for total cyanide binding at 426 mμ. A plot of $\left(1 + \frac{(CN)_0^2}{K_\beta}\right)\tau$ vs $(CN)_0$ should give a straight line with a slope of $k_{2app}/k_{-1app}\,k_{-2app}$ and an intercept of $1/k_{-2app}$. From Figure 15 it is clear that a steady state assumption is not valid.
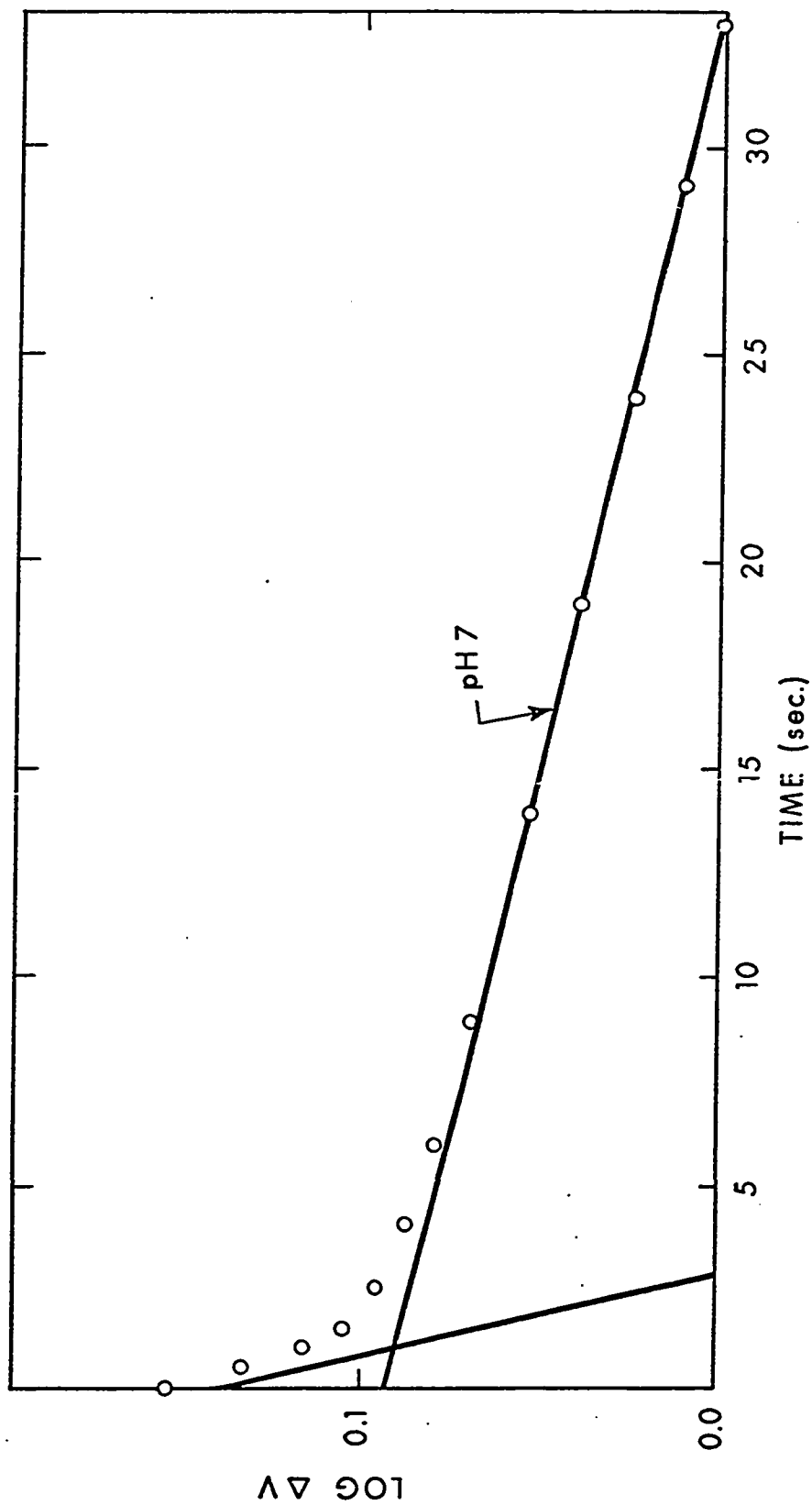
Figure 11. Plot of log ΔV vs time. A typical plot for the separation of two relaxation times. Concentration of hemin and cyanide for this plot at pH 7 were 1.6×10^{-6} and 1.6×10^{-3} M respectively. The slope of the line through the points at long time gives $1/\tau_2$ = 0.059 sec^{-1} and the slope of the second line gives $1/\tau_1$ = 1.12 sec^{-1}.
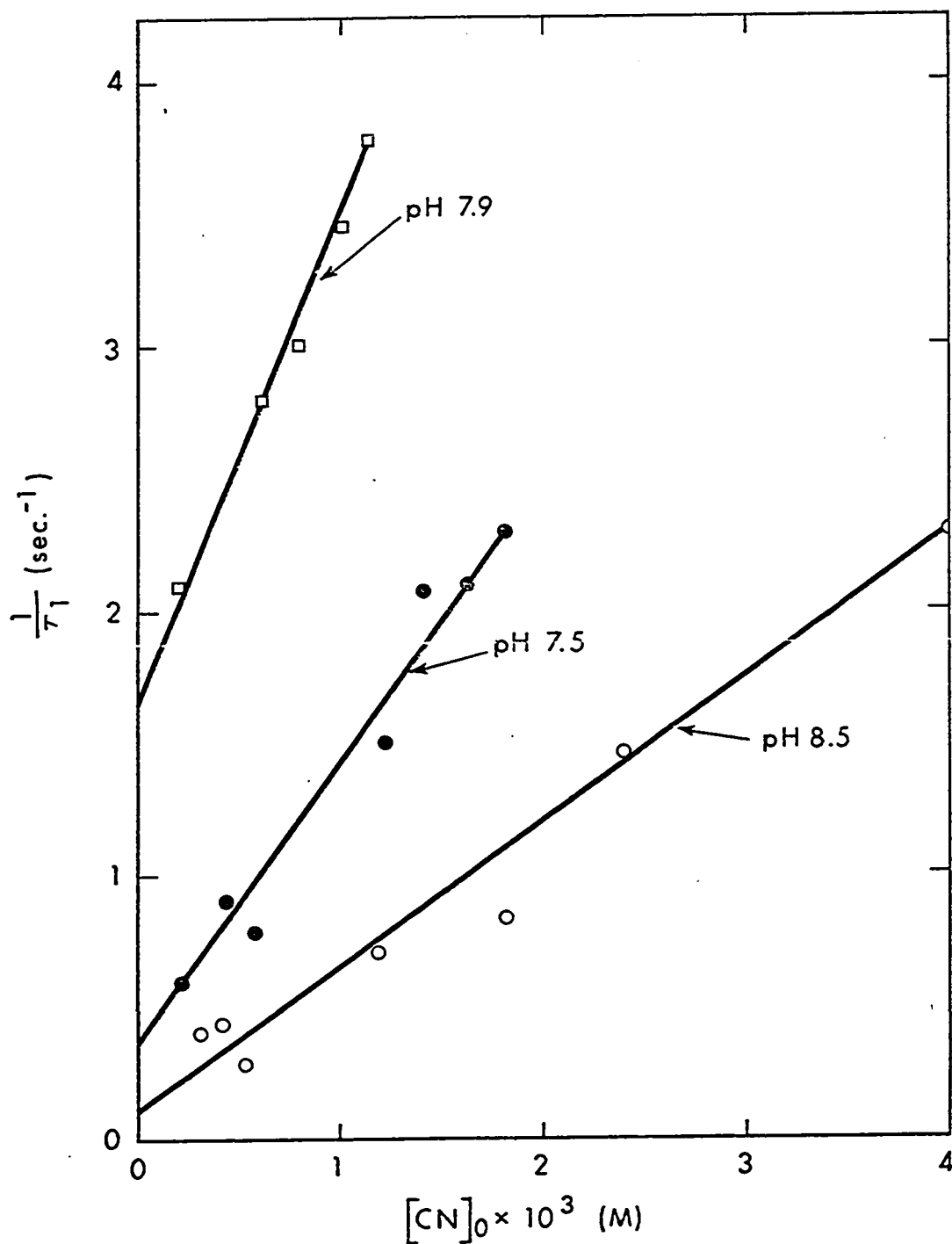
Figure 12.   Plot of reciprocal relaxation time, $1/\tau_1$, vs total cyanide concentration at various pH values.
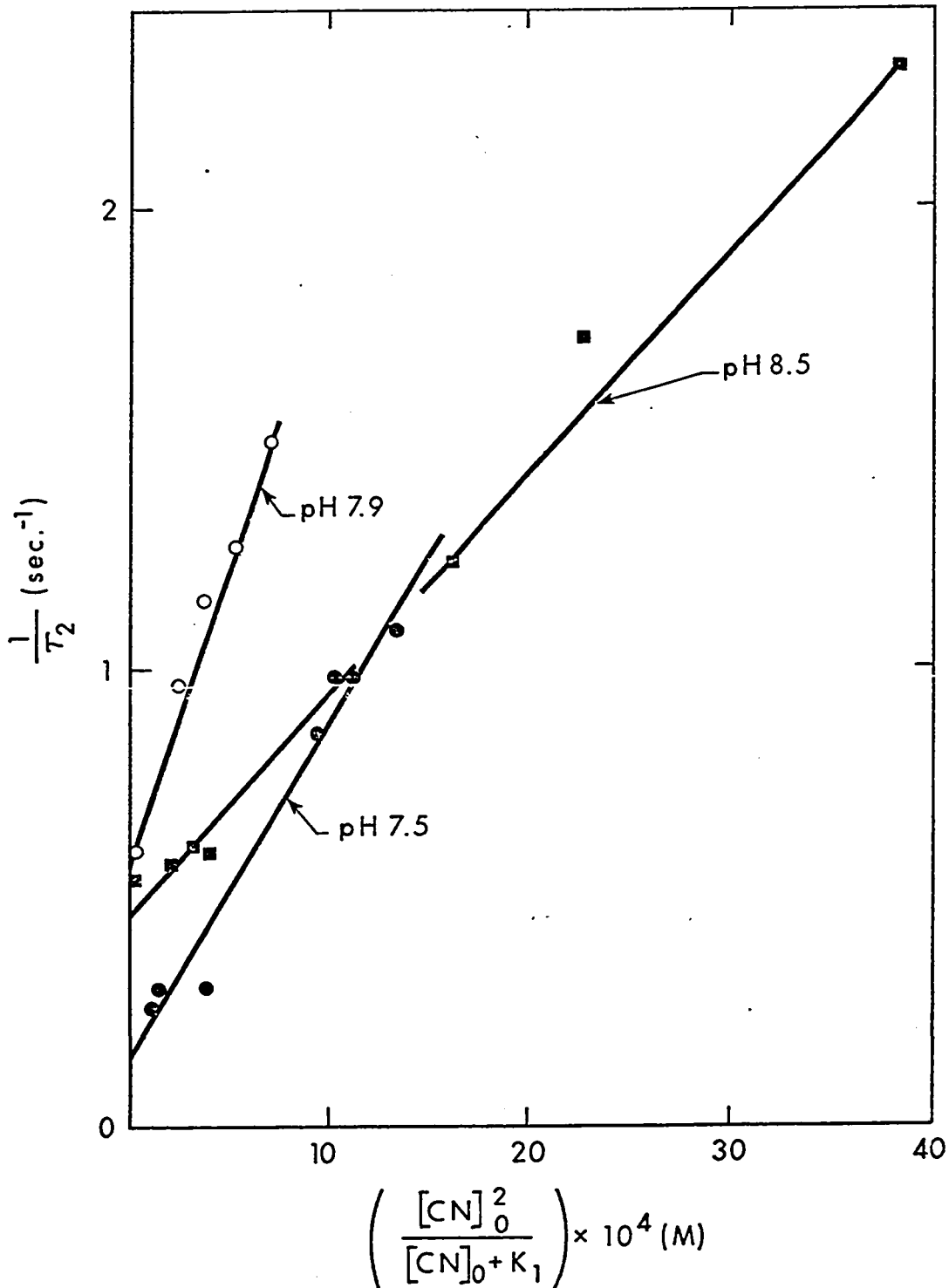
Figure 13. Plot of reciprocal relaxation time, $1/\tau_2$, vs $\dfrac{(CN)_0^2}{(CN)_0 + K_1} \times 10^4$ M at various pH values.
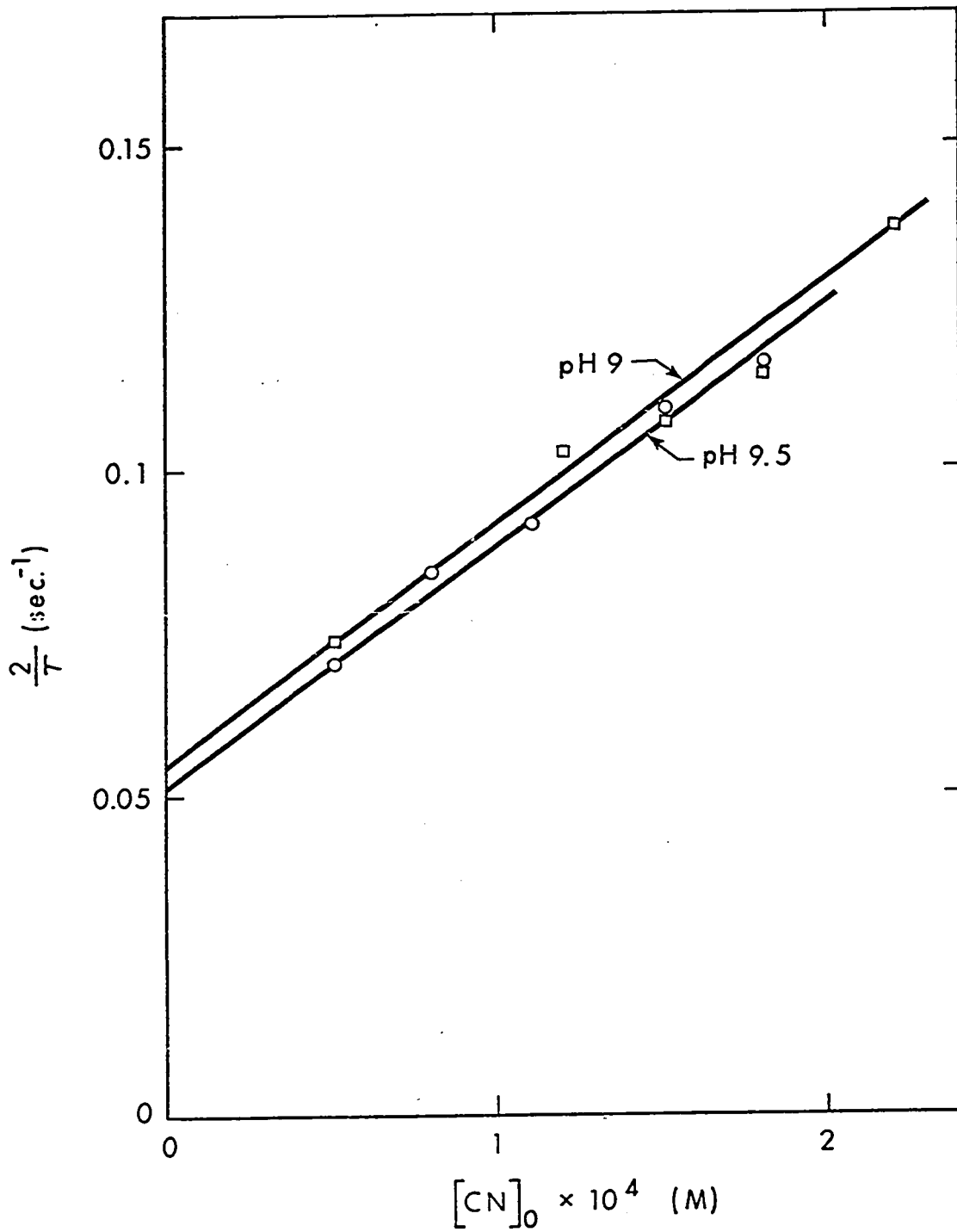
Figure 14. Plot of 2/τ against total cyanide concentration at high pH.
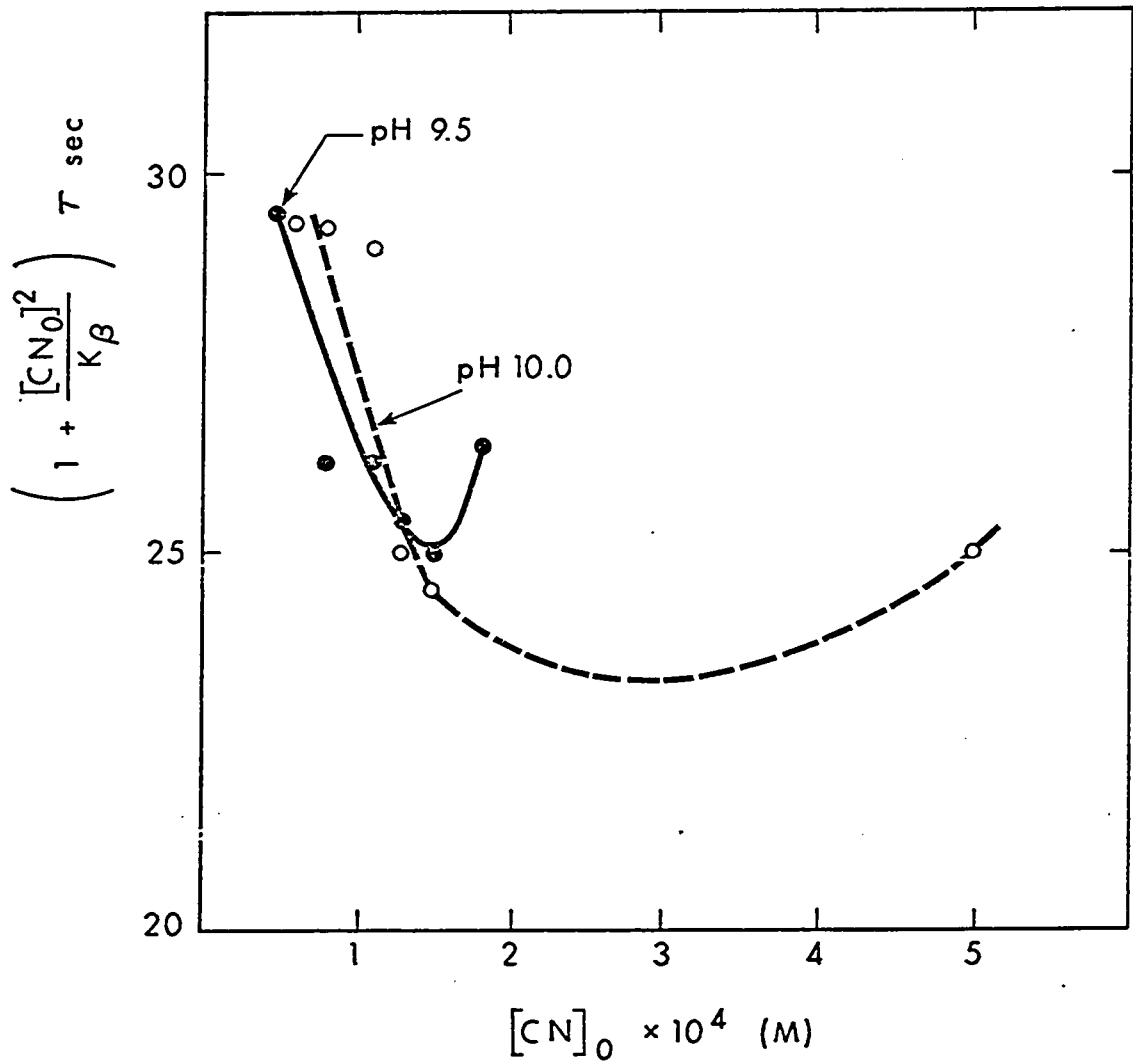
Figure 15. Test for a steady state mechanism for the single relaxation process observed at high pH, for cyanide binding to hemin. If this mechanism were valid then plots of $(1 + \frac{(CN)_0^2}{K_\beta})\tau$ vs $(CN)_0 \times 10^4$ M would be linear with a positive slope.

TABLE III

Mean Lives Obtained from Equations 16, 17 and 21 for the Binding of Cyanide by Hemin in 44.5 Weight Percent Ethanol

pH	τ_1 sec	τ_2 sec	Cyanide concentration $\times 10^3$ M	Hemin concentration $\times 10^6$ M
6.25	1.54	–	0.50	1.60
	0.81	–	2.00	"
	1.14	24.50	2.50	"
	0.86	18.05	3.00	"
	0.80	15.62	3.50	"
6.50	1.68	–	0.40	1.60
	1.57	–	0.60	"
	1.43	30.00	0.80	"
	1.11	27.80	1.00	"
	1.05	24.50	2.00	"
	0.80	15.40	3.00	"
	0.69	12.65	3.50	"
6.75	1.34	–	0.45	1.60
	0.87	26.00	1.00	"
	0.64	11.50	2.50	"
	0.61	10.80	3.00	"
	0.57	10.00	3.50	"
7.00	2.17	–	0.25	1.60
	1.35	34.80	0.50	"
	1.35	22.40	0.70	"

pH	τ_1 sec	τ_2 sec	Cyanide concentration $\times 10^3$ M	Hemin concentration $\times 10^6$ M
7.25	1.00	--	0.40	1.60
	0.91	26.00	0.60	"
	0.87	19.70	0.80	"
	0.74	17.32	1.00	"
	0.43	11.20	2.20	"
7.50	1.61	34.20	0.25	1.60
	1.10	33.30	0.45	"
	1.27	33.10	0.60	"
	0.67	11.45	1.20	"
	0.48	10.30	1.40	"
	0.43	10.65	1.80	"
	0.48	9.10	1.60	"
7.65	1.40	19.60	0.30	1.60
	1.00	14.10	0.50	"
	0.77	11.20	0.80	"
	0.54	10.20	1.25	"
	0.54	8.10	1.50	"
7.75	0.57	19.50	0.40	1.60
	0.45	18.00	0.50	"
	0.52	14.20	0.60	"

TABLE III (continued)

pH	τ_1 sec	τ_2 sec	Cyanide concentration x 10^3 M	Hemin concentration x 10^6 M
7.00	1.19	24.50	1.00	1.60
	0.89	17.00	1.60	"
	0.62	15.75	2.00	"
	0.51	11.84	2.30	"
7.85	1.11	36.20	0.20	1.60
	0.80	15.70	0.60	"
	0.62	13.20	0.80	"
	0.66	11.60	1.00	"
	0.42	10.30	1.23	"
	0.25	8.34	2.00	1.06
7.90	0.47	16.60	0.20	1.60
	0.36	10.30	0.60	"
	0.33	8.70	0.80	"
	0.29	7.90	1.00	"
	0.26	6.70	1.23	"
8.00	0.52	19.00	0.30	1.60
	0.40	17.30	0.40	"
	0.45	12.00	0.60	"
	0.44	11.00	0.70	"
	0.31	9.25	0.90	"
	0.28	6.50	1.20	"
8.00	0.89	23.00	0.30	1.60
	0.74	14.10	0.60	"
	0.57	12.50	0.80	"

pH	τ_1 sec	τ_2 sec	Cyanide concentration x 10^3 M	Hemin concentration x 10^6 M
7.75	0.40	13.00	0.70	1.60
	0.36	10.90	0.90	"
	0.32	12.20	1.05	"
	0.28	9.90	1.25	"
8.15	0.55	23.20	0.30	1.60
	0.41	17.20	0.60	"
	0.34	9.55	0.90	"
	0.24	7.15	1.20	"
	0.19	5.00	1.80	1.30
8.25	2.00	18.20	0.30	1.60
	1.50	11.80	0.60	"
	0.60	9.70	0.90	"
	0.62	7.55	1.20	"
	0.40	5.68	1.80	1.25
8.35	2.50	18.90	0.30	1.60
	1.79	20.00	0.60	"
	1.06	10.50	0.90	"
	0.72	8.80	1.20	"
	0.55	4.30	1.80	1.15
8.50	2.38	17.30	0.30	3.20
	2.33	16.60	0.40	3.20
	3.57	17.20	0.50	3.20

TABLE III (continued)

pH	T_1 sec	T_2 sec	Cyanide concentration x 10^3 M	Hemin concentration x 10^6 M
8.00	0.33	9.10	1.00	1.60
	0.27	8.40	1.20	"
	0.09	3.60	3.00	0.90
8.50	1.41	10.20	1.20	1.20
	1.19	8.10	1.80	1.06
	0.67	5.86	2.40	1.02
	0.44	4.36	4.00	0.97

pH	τ sec	Cyanide concentration x 10^3 M	Hemin concentration x 10^6 M
8.75	21.10	0.20	1.60
	16.90	0.30	"
	10.40	0.45	"
	9.00	0.62	"
	5.00	1.00	0.83
	2.67	2.00	0.72
9.00	27.10	0.05	3.20
	19.40	0.12	"
	18.70	0.15	"
	17.35	0.18	"
	16.00	0.20	"
	14.50	0.22	"
9.25	36.00	0.05	3.20
	19.70	0.10	"
	19.10	0.13	"
	17.70	0.15	"
	16.90	0.17	"
	15.60	0.20	"
9.50	28.50	0.05	3.20
	23.70	0.08	"
	21.80	0.11	"
	19.90	0.13	"
	18.20	0.15	"
	17.20	0.18	"
9.75	30.40	0.06	3.20
	22.60	0.08	"
	20.20	0.11	"
	20.00	0.13	"
	18.20	0.15	"
	0.80	1.50	0.62
10.00	28.10	0.06	3.20
	27.10	0.08	"
	25.00	0.11	"
	20.20	0.13	"
	18.50	0.15	"
	6.50	0.50	0.81

TABLE IV

Rate Constants for the Binding of Cyanide by Hemin in 44.5 Weight Percent Ethanol at 25°

pH	k_{1app} $\times 10^{-3}$ $M^{-1}sec^{-1}$	k_{-1app} sec^{-1}	k_{2app} $\times 10^{-2}$ $M^{-1}sec^{-1}$	k_{-2app} $\times 10^{2}$ sec^{-1}	$(k_{1app} + k_{2app})$ $\times 10^{-2}$ $M^{-1}sec^{-1}$	$(k_{-1app} + k_{-2app})$ $\times 10^{2}$ sec^{-1}
6.25	0.12	0.56				
6.50	0.22	0.57	0.25	2.10		
6.75	0.28	0.80	0.34	2.30		
7.00	0.44	0.43	0.37	2.20		
7.25	0.75	0.58	0.69	3.60		
7.50	1.08	0.34	1.38	3.60		
7.65	1.20	0.38	0.57	4.40		
7.75	1.87	1.20	1.00	3.40		
7.85	1.80	0.35	0.84	3.10		
7.90	1.92	1.65	1.15	5.90		
8.00	2.10	1.20	1.43	3.80		
8.00	3.50	0.40	0.97	1.00		

TABLE IV (continued)

pH	k_{1app} $\times 10^{-3}$ $M^{-1}sec^{-1}$	k_{-1app} sec^{-1}	k_{2app} $\times 10^{-2}$ $M^{-1}sec^{-1}$	k_{-2app} $\times 10^{2}$ sec^{-1}	$(k_{1app} + k_{2app})$ $\times 10^{-2}$ $M^{-1}sec^{-1}$	$(k_{-1app} + k_{-2app})$ $\times 10^{2}$ sec^{-1}
8.15	2.00	1.50	1.36	2.50		
8.25	1.45	0.05	0.85	3.20		
8.35	0.93	0.11	0.89	2.00		
8.50	0.53	0.10	0.47	4.70		
8.75					3.67	1.50
9.00					3.83	5.40
9.25					5.56	2.40
9.50					3.64	5.20
9.75					2.00	7.60
10.00					4.80	2.40

TABLE V

Dissociation Constants Obtained from Kinetic Data for the
Binding of Cyanide by Hemin in 44.5 Weight Percent Ethanol
at 25°

pH	K_1 $\dfrac{k_{-1app}}{k_{1app}}$ $\times 10^3$ M	K_2 $\dfrac{k_{-2app}}{k_{2app}}$ $\times 10^4$ M	K_β $\times 10^8$ M^2
6.25	4.67		
6.50	2.60	8.40	218.00
6.75	2.86	6.80	195.00
7.00	1.00	5.95	59.50
7.25	0.76	5.24	40.00
7.50	0.31	2.60	8.10
7.65	0.32	7.72	24.70
7.75	0.64	3.40	21.80
7.85	0.20	3.70	7.40
7.90	0.86	5.13	44.10
8.00	0.57	2.65	15.10
8.00	0.11	1.03	1.13
8.15	0.75	1.84	13.80
8.25	0.03	3.76	1.12
8.35	0.12	2.25	2.70
8.50	0.19	10.00	19.00

Discussion

As shown in Figure 5, the absence of isosbestic points at low pH must indicate the presence of more than two absorbing species in solution, which is contrary to the behavior of imidazole binding to hemin.[7] At high pH, from about 8.1, there is an isosbestic point at 412 mμ (Figure 6) indicating the presence of only two absorbing species. However the lack of linearity of plots of $\Delta A/[CN]^2$ vs ΔA, at low as well as high pH, indicate the presence of more than two absorbing species in solution. Above pH 8 the apparent isosbestic point may be caused by monocyano- and dicyano hemin having the same absorption spectrum. Thus there may be only two absorbing species in solution at pH 8 and above namely hematin and the cyano hemins. It has also been shown at these high pH's (Figure 15) that a steady state mechanism is not valid, ruling out the presence of two species in solution at low cyanide concentration. However, there appears to be a tendency for a steady state to develop at higher cyanide concentration probably due to the saturation of hemin with cyanide.

The best fit to the experimental data for the titration of hemin with cyanide was obtained for three species in solution over the entire pH region. Equivalent fits to the experimental data were obtained for both total cyanide and CN^- binding to hemin (Tables 1 and 2) except at pH 7 and

below for CN$^-$ binding based on measurements at 400 mμ. It appears that the K_β's obtained for both total cyanide and CN$^-$ binding are approximately equal and pH independent between pH 8.5 to 10. Below pH 8.5 there is an increase in the K_β's for total cyanide binding, whilst for CN$^-$ binding the K_β's are approximately invariant down to pH 7, though an order of magnitude lower than at high pH. Thus from the titration data it is unclear what the real trend in the K_β's are and what species of cyanide bind to hemin. The K_β's from kinetic data, Table V, generally have similar values to those obtained from the titration method between pH 8.5 and 10 which may indicate that the K_β's are really pH independent throughout the pH region. The differences shown for the K_β's obtained at 426 and 400 mμ for the same pH, are probably due to errors in the titration method. The dissociation constant of 1.6×10^{-3} obtained by Maehly[6] at pH 9.2 is close to the value of $K_1 = 2.6 \times 10^{-3}$ M for total cyanide binding at pH 9.25, Table I. Thus it appears that this value obtained by Maehly was for the binding of one cyanide to hemin.

In Table 3 it can be seen that the values of τ_1 are about 25 times larger than τ_2, but drop to about seven times between pH 8 and 8.5. If the differences between the τ values decrease further then τ_1 and τ_2 would be of the same order of magnitude making the separation of the relaxation times very difficult[16]. Between pH's 8.75 and 10 plots of

$log\Delta V$ vs time were linear with no indication of the presence of another relaxation time. Thus independent τ_1 and τ_2 values could only be obtained to pH 8.5 as shown in Figures 16 and 17.

In order to obtain a kinetic mechanism for the k_{1app} data ($k_{1app} = 1/\tau_1$) it was necessary to find constants by trial and error and keep them as non-adjustable parameters in the equations used. If this was not done then some constants in most of the mechanisms tried would come out negative in the process of finding best fits to the experimental points. This may have been due to the sharp decrease in k_{1app} values between pH's 8.0 and 8.5 and the absence of values above pH 8.5, so that the computer could not sense any trend in the data at higher pH except in a negative direction. By keeping some parameters constant as shown in Table VI a reasonable fit to the k_{1app} data could be obtained as discussed below.

The simplest mechanism that will provide a reasonable fit to the k_{1app} data involves three ionizable groups on hemin and can be written as mechanisms I_a and I_b.

$$
\begin{array}{c}
\quad M(OH_2)_2 \\
K_3 \quad \updownarrow \\
\quad M(OH_2)OH + CN^- \xrightarrow{\;k_1\;} M(OH)CN \\
K_4 \quad \updownarrow \\
\quad M(OH)_2 \\
K_5 \quad \updownarrow \\
\quad M^*(OH)_2
\end{array}
\qquad (I_a)
$$

$$
\begin{array}{l}
K_3 \quad
\begin{array}{c}
M(OH_2)_2 \\
\downarrow \uparrow
\end{array} \\[4pt]
K_4 \quad
\begin{array}{c}
M(OH_2)OH \\
\downarrow \uparrow
\end{array} \\[4pt]
\qquad M(OH)_2 + HCN \xrightarrow{\;k_2\;} M(OH)CN \qquad\qquad (I_b)\\[4pt]
K_5 \quad
\begin{array}{c}
\downarrow \uparrow \\
M*(OH)_2
\end{array}
\end{array}
$$
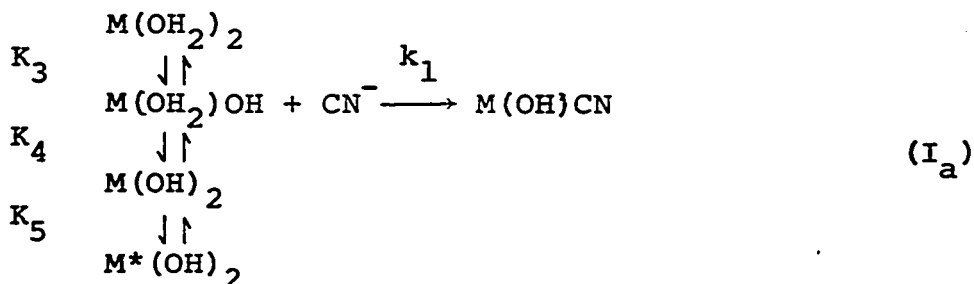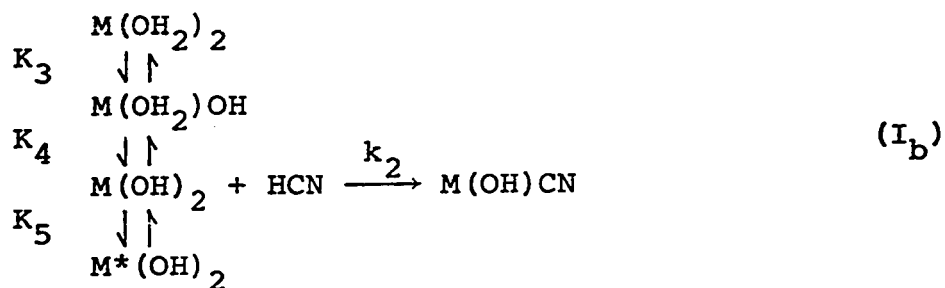
From mechanism I_a it can be shown that

$$
k_{1app} = \frac{k_1 \dfrac{K_3}{[H]}}{\left(1.00 + \dfrac{K_3}{[H]} + \dfrac{K_3 K_4}{[H]^2} + \dfrac{K_3 K_4 K_5}{[H]^3}\right)\left(1 + \dfrac{[H]}{K_L}\right)} \qquad (26)
$$

and from mechanism I_b it can be shown that

$$
k_{1app} = \frac{k_2 \dfrac{K_3 K_4}{[H]^2}}{\left(1.00 + \dfrac{K_3}{[H]} + \dfrac{K_3 K_4}{[H]^2} + \dfrac{K_3 K_4 K_5}{[H]^3}\right)\left(1 + \dfrac{K_L}{H}\right)} \qquad (27)
$$

where K_L is the dissociation constant of HCN. Mechanisms I_a and I_b will reproduce the forward rate data and will predict exactly the same values of k_{1app} at any given pH. The existence of two equivalent fits is due to the inability of the kinetic method to distinguish between reactions of the form:

$$
HM + CN^- \rightarrow
$$

and

$$
M + HCN \rightarrow
$$
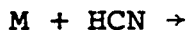
The best fit values for the rate and equilibrium constants for both mechanisms I_a and I_b using the non-linear least

squares program[11] are listed in Table VI. It should be noted that K_3, K_4 and K_L were used as non-adjustable parameters with values of 1.5×10^{-7}, 1.0×10^{-8} and 3.16×10^{-10} M. The fit of the k_{1app} values predicted by eqs 26 and 27 to the experimental data using any of the sets of constants in Table VI is shown in Figure 16 where the solid line gives the predicted values of k_{1app}. The pK's of the ionizable groups on hemin are 6.82, 8.0 and 7.9 of which only the latter value was obtained as an adjustable parameter from the computer fit. The latter two constants have essentially identical values which may have caused the narrow k_{1app} peak.

From a nuclear magnetic resonance study of solvent exchange on hemin[15] it appears that $M(OH_2)_2$ is an equilibrium mixture of diaquohemin and aquoethanol hemin, and $M(OH_2)OH$ a mixture of hydroxyaquo- and hydroxyethanol hemin. The pH titration curve of hemin, Figure 3, shows a single inflection point at about pH 6.7 which may correspond to a single dissociable group[7], most probably the equilibrium between $M(OH_2)_2$ and $M(OH_2)OH$. The forms of the other two ionizable groups are not known. However it may be speculated that the species represented by $M(OH)_2$ and $M^*(OH)_2$ are a dihydroxy- and ethoxyhydroxy hemin respectively. There may also be a conformational change in the shape of the hemin molecule affecting the binding of cyanide. That other species of hemin are present is strongly suggested by

TABLE VI

Rate and Equilibrium Constants of Mechanism I

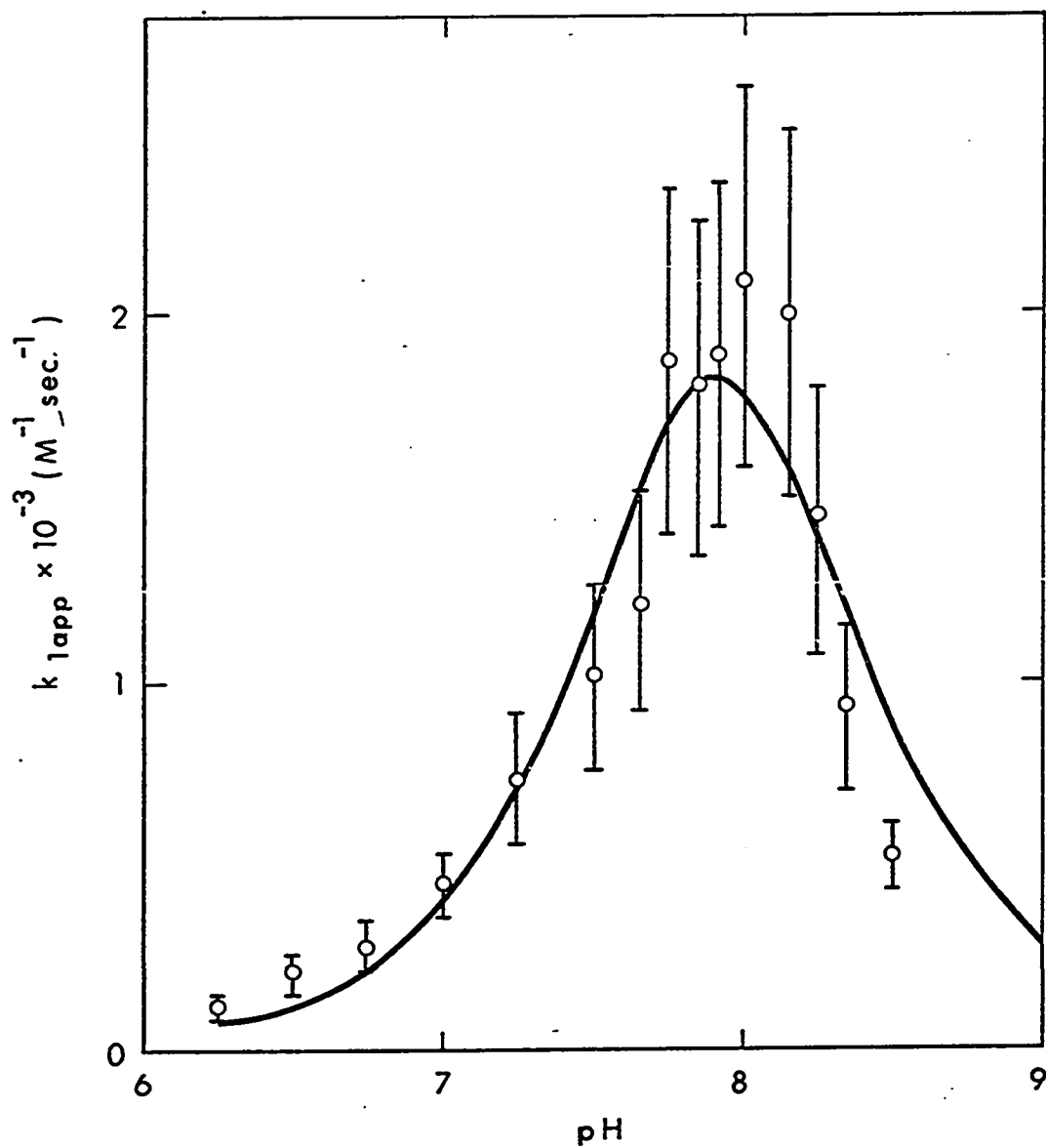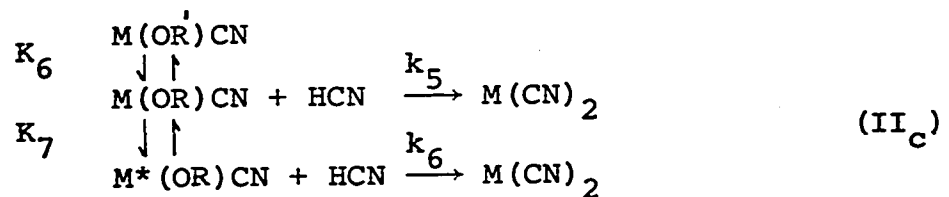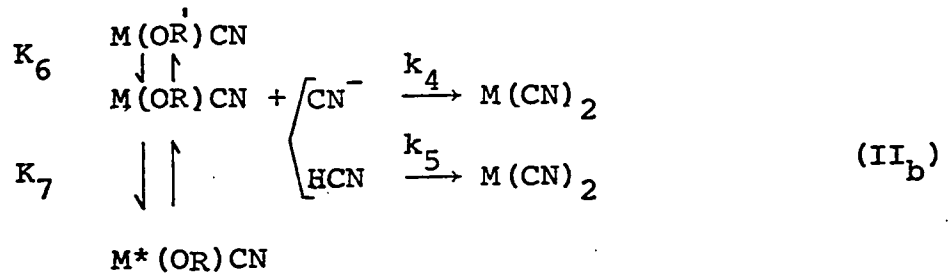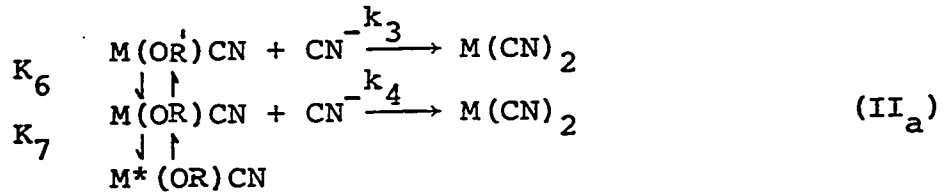| Constants	I_a	I_b
k_1	$(2.2 \pm 0.2) \times 10^5$	
k_2		$(6.8 \pm 0.7) \times 10^3$
K_3	1.5×10^{-7}	1.5×10^{-7}
K_4	1.0×10^{-8}	1.0×10^{-8}
K_5	$(1.6 \pm 0.4) \times 10^{-8}$	$(1.6 \pm 0.4) \times 10^{-8}$
K_L	3.16×10^{-10}	3.16×10^{-10}

Figure 16. Plot of k_{1app} vs pH for the binding of cyanide to hemin with error limits of ±25% shown for the k_{1app} values. The solid line is calculated using the best-fit parameters of mechanism I.

the asymmetry of the titration curve (Figure 3) about the
inflection point, at pH 6.7. The lack of other discrete
inflection points may be due to similar absorption spectra
of the species represented in mechanism I, and dissociation
constants which are possibly very close to each other.

The simplest mechanism that will explain the k_{2app}
data involves two dissociable groups on hemin and can be
written as mechanisms II_a to II_c:

$$
\begin{array}{ll}
K_6 & M(OR')CN + CN^- \xrightarrow{k_3} M(CN)_2 \\
 & \quad \downarrow \uparrow \\
K_7 & M(OR)CN + CN^- \xrightarrow{k_4} M(CN)_2 \\
 & \quad \downarrow \uparrow \\
 & M*(OR)CN
\end{array}
\qquad (II_a)
$$

$$
\begin{array}{ll}
K_6 & M(OR')CN \\
 & \quad \downarrow \uparrow \\
 & M(OR)CN + \begin{cases} CN^- \xrightarrow{k_4} M(CN)_2 \\ HCN \xrightarrow{k_5} M(CN)_2 \end{cases} \\
K_7 & \quad \downarrow \uparrow \\
 & M*(OR)CN
\end{array}
\qquad (II_b)
$$

$$
\begin{array}{ll}
K_6 & M(OR')CN \\
 & \quad \downarrow \uparrow \\
 & M(OR)CN + HCN \xrightarrow{k_5} M(CN)_2 \\
K_7 & \quad \downarrow \uparrow \\
 & M*(OR)CN + HCN \xrightarrow{k_6} M(CN)_2
\end{array}
\qquad (II_c)
$$

The symbols OR' and OR stand for OH^- and $OC_2H_5^-$, but we
have no way of identifying particular species. From mech-
anism II_a it can be shown that

$$
k_{2app} = \frac{k_3 + k_4 \dfrac{K_6}{[H]}}{\left(1 + \dfrac{K_6}{[H]} + \dfrac{K_6 K_7}{[H]^2}\right)\left(1 + \dfrac{[H]}{K_L}\right)}
\qquad (28)
$$

for mechanism II_b

$$k_{2app} = \cfrac{k_5 \cfrac{K_6}{[H]}}{(1 + \cfrac{K_6}{[H]} + \cfrac{K_6 K_7}{[H]^2})(1 + \cfrac{K_L}{[H]})} \qquad (29)$$

$$+ \cfrac{k_4 \cfrac{K_6}{[H]}}{(1 + \cfrac{K_6}{[H]} + \cfrac{K_6 K_7}{[H]^2})(1 + \cfrac{[H]}{K_L})}$$

and for mechanism II_c

$$k_{2app} = \cfrac{k_5 \cfrac{K_6}{[H]} + k_6 \cfrac{K_6 K_7}{[H]^2}}{(1.00 + \cfrac{K_6}{[H]} + \cfrac{K_6 K_7}{[H]^2})(1 + \cfrac{K_L}{H})} \qquad (30)$$

Mechanisms II_a to II_c will reproduce the forward rate data and predict exactly the same values of k_{2app} at any given pH, for the same reason as given above.

The best fit values for the rate and equilibrium constants for the mechanisms II_a to II_c using the non linear least squares program[11] are listed in Table VII. Only the pK of HCN of 9.5 was used as a non adjustable parameter. The fit of the k_{2app} values predicted by equation 28 to 30 to the experimental data using any of the sets of constants in Table VII is shown in Figure 17, where the solid line gives the predicted values of the k_{2app} data. The pK's of the ionizable groups are 7.33 and 8.2.

The pH titration of hemin cyanide complex (Figure 7)

TABLE VII

Rate and Equilibrium Constants of Mechanism II

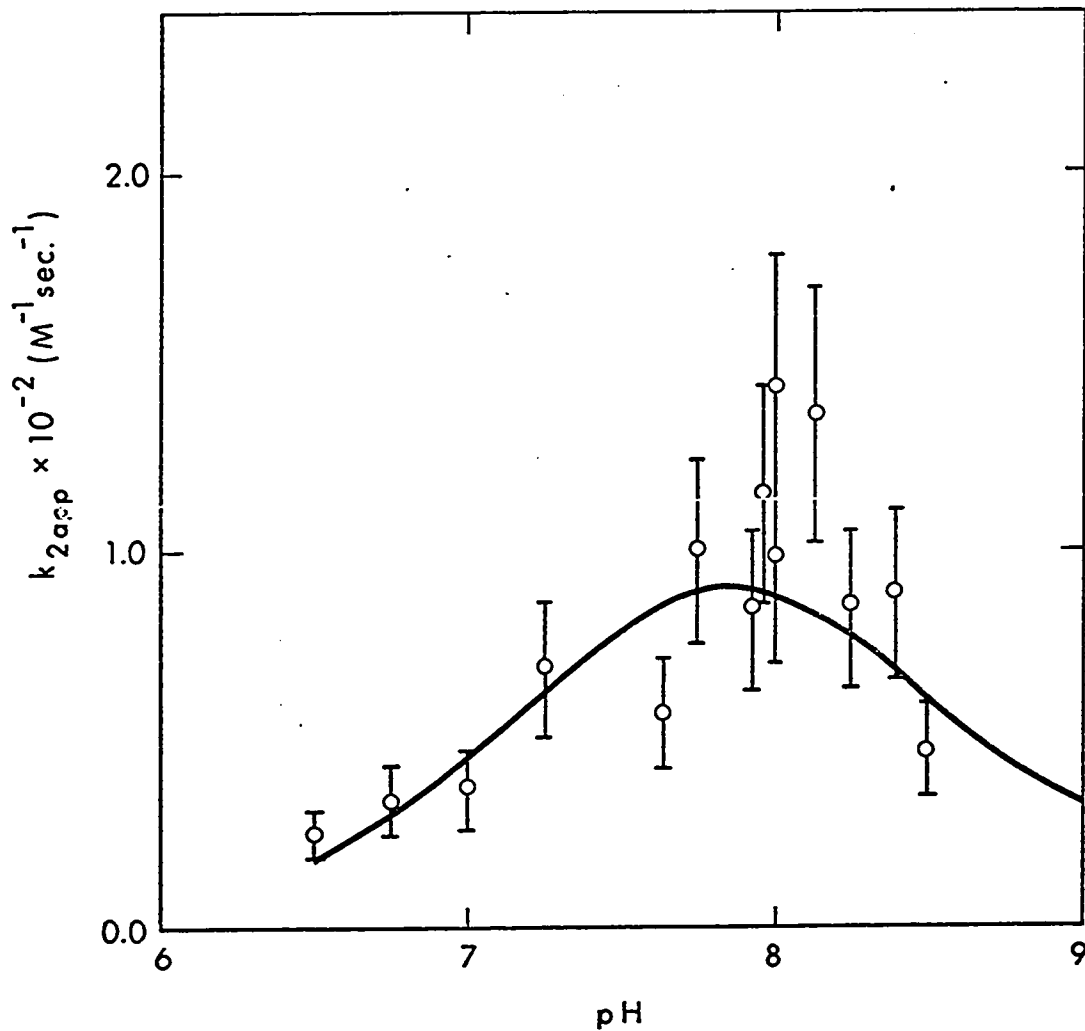| Constants	II_a	II_b	II_c
k_3	$(2.2\pm0.6)\times10^6$		
k_4	$(5 \pm8)\times10^2$	$(5 \pm8)\times10^2$	
k_5		$(1.5\pm0.6)\times10^2$	$(1.5\pm0.1)\times10^2$
k_6			$(2.7\pm0.8)\times10$
K_6	$(4.7\pm0.3)\times10^{-8}$	$(4.7\pm0.3)\times10^{-8}$	$(4.7\pm0.3)\times10^{-8}$
K_7	$(6 \pm7)\times10^{-9}$	$(6 \pm7)\times10^{-9}$	$(6 \pm7)\times10^{-9}$
K_L	3.16×10^{-10}	3.16×10^{-10}	3.16×10^{-10}

Figure 17. Plot of k_{2app} vs pH. The solid line is that predicted using the best-fit parameters of mechanism II. The circles are experimental points with error limits of 25%.

shows the presence of other dissociable groups at pH's above 6.7, with inflection points at about 8.5 and 10.5. The inflection point at pH 8.5 may represent an equilibrium between aquocyano hemin and hydroxycyano hemin, and at 10.5, between ethanolcyano and ethoxycyano hemin. The presence of the inflection point at about pH 8.5 gives added meaning to K_7 (Mechanisms II_a - II_c) since its value falls within the region of this inflection point. That an equivalent inflection point to K_6 is not observed may be due to overlapping of the titration curves between pH 6.7 and 8.5. The inflection point at pH 10.5 would not be expected to play a role since independent k_{1app} and k_{2app} data could not be obtained in this region. Mechanisms I_a and I_b show that $M(OH_2)_2$ does not bind to cyanide, and its presence is not necessary in Mechanisms II_a to II_c. This is possible for as shown in Figure 7 the inflection point of hemin at 6.7 appears to be unaffected by the presence of 1 x 10^{-3} M cyanide. In Table III it can be seen that generally the concentration of cyanide hardly exceeded 1 x 10^{-3} M. At higher cyanide concentrations the inflection points at 8.5 and 10.5 disappear indicating that the dissociable groups have been displaced by cyanide so that the absorption spectrum is no longer affected, forming one species, dicyanohemin. But at lower pH the inflection point initially at 6.7 begins to shift to lower pH. This probably means that dissociable groups on hemin have not been displaced by cyanide in this region. If CN^- is the binding

ligand at low pH then it is possible that protonation of the bound cyanide ligand is being monitored. The non adjustable parameters of K_3 in mechanism I and K_L in both mechanisms I and II where also obtained by the pH titration of hemin and cyanide (Figures 3 and 4) which give a further measure of credibility to the mechanisms obtained.

No attempt was made to analyze the k_{-1app} and k_{-2app} data due to the random nature of the experimental points.

The binding of cyanide to hemin is different to that of imidazole binding to hemin[7]. The difference could possibly be explained by simple electrostatic effects. If CN^- is the main form of cyanide that binds to hemin there would be a tendency for it to be repelled by the negatively charged hemin. Thus it would be expected that the rate of binding of the second CN^- ion would be even slower than the first, due to an increase in the negative charge on the monocyano hemin complex. There would be no tendency for repulsion of the imidazole ligand. If the imidazolium ion is the main form of imidazole that binds to hemin, there would be a strong electrostatic attraction to the negatively charged hemin with an increase in the rate of binding relative to that of CN^-. Once the first imidazolium ion has bound to hemin, the ligand in the trans position to it may become labilized resulting in the second imidazolium ion binding even faster, creating the steady state condition.

LITERATURE CITED

1. Falk, J. E., Porphyrins and Metalloporphyrins, Elsevier Publishing Company, Amsterdam- London- New York. 1964.

2. Morrison, M., Rombauts, W. A., and Schroeder, W. A., In Hemes and Hemoproteins. Edited by Chance B., Estabrook, R. W., and Yonetani, T., Academic Press, Inc., N.Y. 1966.

3. Hogness, T. R., Zscheile, Jr. F. P., Sidwell, Jr. A. E., and Barron, E. S. G., J. Biol. Chem. 118, 1, (1937).

4. Shack, J., and Clark, W. M., J. Biol. Chem. 171, 143, (1947).

5. Lemberg, R., and Legge, J. W., Hematin Compounds and Bile Pigments, Interscience, New York and London, 1949.

6. Maehly, A. C., and Akeson, A., Acta Chem. Scand. 12, 1259 - 1273, (1958).

7. Hasinoff, B. B., Dunford, H. B., and Horne, D. G., Can. J. Chem. 47, 3225·(1969).

8. Bates, R. G., Paabo, M., and Robinson, R. A., J. Phys. Chem. 67, 1833, (1963).

9. Ellis, W. D., and Dunford, H. B., Biochemistry 7, 2054, (1968).

10. Hasinoff, B. B., and Dunford, H. B., Biochemistry, submitted for publication.

11. IBM Share library, Program SDA 3094, modified for use on the University of Alberta IBM 360 computer.

12. Alberty, R. A., Yagil, G., Diven, W. F., and Takahashi, M., Acta Chem. Scand. 17, S 34, (1963).

13. Frost, A. A., and Pearson, R. G., "KINETICS AND MECHAN-ISM" 2nd Ed., John Wiley and Sons, N.Y., 1961, p 174.

14. Hammes, G. G., and Hubbard, C. D., J. Phys. Chem. 70, 1615-22, (1966).

15. Hammes, G. G., and French, C. T., unpublished work.

16. Eigen, M., and De Maeyer, L., In Techniques in Organic Chemistry, Friess, S. L., Lewis, E. S., and Weissberger, A., Editors. Vol. VIII. Part II. 2nd edition. Inter-science Publishers Inc., New York. 1963 p 915.

17. Angerman, N. S., Hasinoff, B. B., Dunford, H. B., and Jordan, R. B., Can. J. Chem. 47, 3217 (1969).

Appendix I

Equation for a steady state mechanism

If MCN in eq 1 is in vanishingly small quantities then a steady state mechanism is predicted where

$$\frac{d(MCN)}{dt} = 0 \qquad\qquad (I)$$

and the overall dissociation constant is

$$K_{DISS} = \frac{[\overline{M}]\,[\overline{CN}]^2}{[\overline{MCN_2}]} \qquad\qquad (II)$$

where the bars indicate equilibrium concentrations. From conservation relations

$$M = M_0 - MCN_2 \qquad\qquad (III)$$

where M_0 is the total concentration of hemin, and the total absorbance is

$$A = \varepsilon_0\overline{M} + \varepsilon_1\overline{MCN}_2 \qquad\qquad (IV)$$

where A = absorbance, ε_0 and ε_1 are extinction coefficients. By introducing eq (III) into (IV) and rearranging the following equation is obtained:

$$\overline{MCN}_2 = \frac{A-A_0}{\varepsilon_1 - \varepsilon_0} \qquad\qquad (V)$$

where A_0 is the absorbance due to hemin only. It is obvious that

$$M_0 = \frac{A_0}{\varepsilon_0} \qquad\qquad (VI)$$

Appendix I (continued)

and by introducing eqs (III), (V) and (VI) into eq (II) and rearranging the following equation is obtained:

$$K_{DISS}\left(\frac{A-A_0}{\varepsilon_1-\varepsilon_0}\right) = \left[\left(\frac{A_0}{\varepsilon_0}\right) - \left(\frac{A-A_0}{\varepsilon_1-\varepsilon_0}\right)\right][CN]^2 \qquad (VII)$$

$A-A_0$ can be designated ΔA, then equation (VII) can be rearranged to give:

$$\frac{\Delta A}{[CN]^2} = \frac{A_0}{K_{DISS}}\left(\frac{\varepsilon_1}{\varepsilon_0} - 1\right) - \frac{\Delta A}{K_{DISS}} \qquad (VIII)$$

if the steady state mechanism is valid then a plot of $\Delta A/[CN]^2$ vs ΔA should be linear with the slope giving the value of $1/K_{DISS}$ and the intercept $\frac{A_0}{K_{DISS}}\left(\frac{\varepsilon_1}{\varepsilon_0} - 1\right)$

Appendix II

Equation for the titration of hemin with cyanide

From eq 1 and 2 there are three absorbing species in solution such that:

$$A = \varepsilon_1 \overline{M} + \varepsilon_2 \overline{MCN} + \varepsilon_3 \overline{MCN}_2 \qquad (IX)$$

where bars indicate equilibrium concentrations of the three absorbing species in solutions, and ε_1, ε_2 and ε_3 extinction coefficients of the three respective species. From conservation relations

$$M_0 = \overline{M} + \overline{MCN} + \overline{MCN}_2 \qquad (X)$$

and M_0 is the total concentration of hemin.

f_1, f_2 and f_3 represent fractions of these three species such that

$$f_1 + f_2 + f_3 = 1 \qquad (XI)$$

By introducing eq (XI) into (IX) the following equation is obtained:

$$A = (\varepsilon_1 f_1 + \varepsilon_2 f_2 + \varepsilon_3 f_3) M_0 \qquad (XII)$$

From eqs 1 and 2 it can be shown that

$$K_1 = \frac{f_1}{f_2}[CN] \qquad (XIII)$$

$$\text{and} \quad K_2 = \frac{f_2}{f_3}[CN] \qquad (XIV)$$

Appendix II (continued)

and by introducing eqs (XIII) and (XIV) into (XII) the
following equation is obtained:

$$A = M_0 f_2 \left(\frac{\varepsilon_1 K_1}{[CN]} + \varepsilon_2 + \frac{\varepsilon_3 [CN]}{K_2} \right) \qquad \text{(XV)}$$

By dividing eq (XI) by f_2, rearranging, and then substitut-
ing into eq (XV) the following equation is obtained:

$$A = M_0 \left(\frac{1}{1 + \frac{K_1}{[CN]} + \frac{[CN]}{K_2}} \right) \left(\frac{\varepsilon_1 K_1}{[CN]} + \varepsilon_2 + \frac{\varepsilon_3 [CN]}{K_2} \right) \qquad \text{(XVI)}$$

This equation can be used with a non-linear least-squares
program to yield best fit values for K_1, K_2, ε_1, ε_2 and
ε_3.

Appendix III

A useful procedure for the separation of relaxation times[15]

The signal amplitude ΔV is given by

$$\Delta V = \sum_i^n \Delta V_{io} e^{-t/\tau i} \qquad \text{(XVII)}$$

where ΔV is the difference between signal at $t=t$ and $t=\infty$ and ΔV_{io} is the difference between signal at $t=0$ and $t=\infty$. A plot of $\log \Delta V$ vs t will be curved if $i>1$. At sufficiently long times all of the terms of the series except that characterized by the longest relaxation time, say the nth, will go to zero. Thus a straight line can be drawn through the curve at long time ($t\to\infty$) and the relaxation time and ΔV_{io} determined. This term can now be subtracted from the series, and the resultant series is

$$\Delta V = \sum_i^{n-1} \Delta V_{io} e^{-t/\tau i} \qquad \text{(XVIII)}$$

Repetition of this procedure will yield n relaxation times. In practice if the relaxation times do not differ by at least a factor of two, resolution of the relaxation spectrum is not possible.